THE Journal OF THE AMERICAN LEATHER CHEMISTS ASSOCIATION

October 2022 Vol. CXVII, No.10 *JALCA* 117(10), 405–452, 2022

117th Annual Convention

TO BE ANNOUNCED

For more information go to:
leatherchemists.org/annual_convention.asp

Contents

Distributed by
University of CINCINNATI
LIBRARY PUBLISHING SERVICES

An imprint of the University of Cincinnati Press

ISSN: 0002-9726

Communications for Journal Publication

Manuscripts, Technical Notes and Trade News Releases should contact:
Mr. Steven D. Lange, Journal Editor, 1314 50th Street, Suite 103, Lubbock, TX 79412, USA
E-mail: jalcaeditor@gmail.com Mobile phone: (814) 414-5689

Contributors should consult the Journal Publication Policy at:
http://www.leatherchemists.org/journal_publication_policy.asp

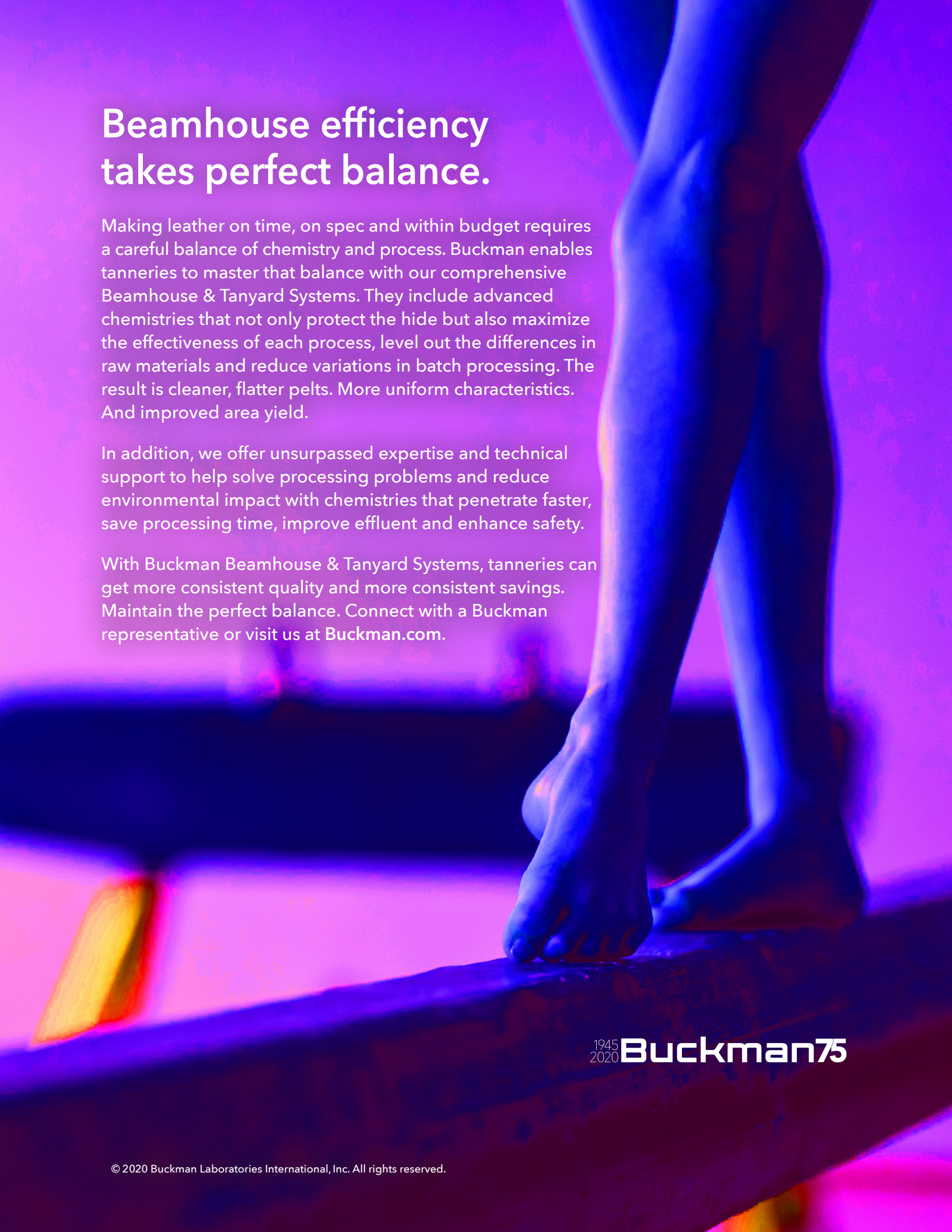

Beamhouse efficiency takes perfect balance.

Making leather on time, on spec and within budget requires a careful balance of chemistry and process. Buckman enables tanneries to master that balance with our comprehensive Beamhouse & Tanyard Systems. They include advanced chemistries that not only protect the hide but also maximize the effectiveness of each process, level out the differences in raw materials and reduce variations in batch processing. The result is cleaner, flatter pelts. More uniform characteristics. And improved area yield.

In addition, we offer unsurpassed expertise and technical support to help solve processing problems and reduce environmental impact with chemistries that penetrate faster, save processing time, improve effluent and enhance safety.

With Buckman Beamhouse & Tanyard Systems, tanneries can get more consistent quality and more consistent savings. Maintain the perfect balance. Connect with a Buckman representative or visit us at **Buckman.com**.

1945 2020 Buckman75

JOURNAL OF THE
AMERICAN LEATHER CHEMISTS ASSOCIATION

Proceedings, Reports, Notices, and News
of the
AMERICAN LEATHER CHEMISTS ASSOCIATION

THE JOURNAL OF THE AMERICAN LEATHER CHEMISTS ASSOCIATION (USPS #019-334) is published monthly by The American Leather Chemists Association, 1314 50th Street, Suite 103, Lubbock, Texas 79412. Telephone (806)744-1798 Fax (806)744-1785. Single copy price: $8.50 members, $17.00 non-member. Subscriptions: $185 for hard copy plus postage and handling of $60 for domestic subscribers and $70 for foreign subscribers; $185 for ezine only; and $205 for hard copy and ezine plus postage and handling of $60 for domestic subscribers and $70 for foreign subscribers.

Periodical Postage paid at Lubbock, Texas and additional mailing offices. Postmaster send change of addresses to The American Leather Chemists Association, 1314 50th Street, Suite 103, Lubbock, Texas 79412.

Website: www.leatherchemists.org E-mail: carol.adcock@ttu.edu

COLD
Milling

Smooth Leather
Milling

Erretre
Tannery Innovations

Erretre s.p.a. | Via Ferraretta,1 | Arzignano (VI) 36071 | tel. +39 0444 478312 | info@erretre.com

Physico-Insight on Sewability Properties of Crust Leathers Using Melamine Syntan and Synthetic Fatliquor

by

Jayakumar G.C.,[1,3] Niklesh C.,[1,3] Jeyas Kandhan S.,[1,3] Phebe Aaron K.[*2,3]and Krishnaraj K.[2,3]

[1]*Centre for Academic and Research Excellence (CARE)*

[2]*Shoe & Product Design Centre (SPDC)*

CSIR-Central Leather Research Institute, Adyar Chennai, India

[3]*Department of Leather Technology, Alagappa College of Technology*, Anna University, Chennai

Abstract

Leather being a natural material finds a most prominent position in the fashion field. Leather goods, garments and products symbolize luxury and comfort. Manufacturing of leather products requires meeting the physical and chemical norms stipulated by the international agencies depending on the end products. Among the various physical properties, sewability is very important in deciding the quality of manufactured products. The present research discusses about the effect of syntan and fatliquor on leather properties. Experiments have been designed with varied concentration of melamine syntan along with 10% fatliquor. Various physical characterizations such as sewability, tensile strength, grain crack and microscopic images have been studied to elucidate the effect of syntan and fatliquor on leather properties. The experimental results show that the presence of fatliquor is a critical component to achieve better sewability properties in leather. Similar effect has been observed in the case of grain crack and tensile strength of the crust leathers. Prosaically, the experimental data have shown that the usage of fatliquor shows better sewability property.

Introduction

Leather and leather products pose a permanent place in the luxury segment.[1] Among the various products, garments, gloves and shoes are widely used in the colder regions for protection. The breathability of leather makes it a unique material of choice for making garments.[2,3] Leather processing is classified into pre-tanning, tanning, post-tanning and finishing. Pre-tanning mainly focuses on cleaning the material and preparing it for the tanning process, which gives permanent stabilization against natural deterioration. The post-tanning process aids in the functional and performance properties of the leathers.[4] Depending on the end products, the process recipe is designed.

Re-tanning, dyeing and fatliquoring are carried out during the post-tanning process. Re-tanning employs a different class of syntans to provide performance properties such as grain tightness, selective filling, adding fullness, roundness, etc., properties to the leathers.[5] Phenolic, acrylic, melamine, malic styrene-based synthetic tanning agents are used in the re-tanning. Fatliquoring is another inevitable step in leather manufacture that provides lubrication to the fibers and reduces the friction between leather fibers, resulting in the softness of the leathers. Moreover, the essential properties required for garment leathers such as drape and breathability, are greatly influenced by choice of fatliquoring.[6] However, the usage of excess fatliquoring leads to its deposition on the surface, limiting the application of the leathers for various functionalities.[5] Dyeing is carried out to provide aesthetic colors to the leather. It can be stated that re-tanning and fatliquoring have significant contributions to leather performance properties. From our earlier studies, we have reported the impact of phenolic syntan on leather sewability properties.[6] In the present study, we have attempted to understand the sewability properties of the leather by varying the melamine syntan concentrations during the post-tanning. The experimental leathers have been evaluated for their sewability, grain crack, tensile strength and microscopic images.

Materials and Methods

Post-tanning chemicals for the process were of commercial grade. Wet blue goat leather was chosen as the tanned material for further post-tanning.

Experiments were designed with fixed fatliquor concentration accompanied by varying the syntan concentrations from 0-10% to understand the leather sewability as given in Table I.

*Corresponding author email: phebe@clri.res.in

Manuscript received February 28, 2022, accepted for publication March 30, 2022.

Table I
Experimental process

Process	Percentage	Durations
Neutralization		
Water	150%	60 min
Nutrigan	0.50%	(pH 5 to 5.5)
Drain & Wash		
Retanning		
Water	100%	
Syntan Base:	Melamine Base (FB6)	
Trial 1	0%	
Trial 2	2%	
Trial 3	4%	30 min (Each Trial)
Trial 4	6%	
Trial 5	8%	
Trial 6	10%	
Fatliquoring		
Fatliquor Base:	Anionic – Synthetic	
Sintoil EN	10%	30 min (Each Trial)
Fixing		
Formic Acid	0.50%	30 min (pH 4)
Drain & Wash		

Physical testing of the sample

Physical testing samples were prepared as per IULTCS methods.[7] The samples were conditioned (IUP 2, 2000) and were evaluated for the tensile strength (IUP 6, 2000) and grain crack testing (IUP 9, 1996).[8-9]

Sewability analysis

The testing sample (Crust leather) was taken in the dimension of 30 x 350 mm. This testing was carried out using the L&M Sewability Tester machine (penetration rate- 100/min, needle number-90, Needle System-34LR).[10] Good sewability range is generally considered to be in the range from 0-10%.[11]

Optical microscopic studies

Celestron Microscope was used to examine the grain surface and cross-sectional view of the experimental and the control leathers.

Results and Discussion

Leather manufacture is a complex process due to its three-dimensional matrix system.[12] To develop a new technique or address concerns and challenges of existing technologies, a fundamental understanding of leather science is inevitable. Post tanning process of leather is a critical step during leather manufacturing to obtain required physical properties. Since, most of the products require stitching, the sewability of the leather is the main parameter among the physical properties of the leather.[13-16] This holds very much in-line for garment and leather goods. In our earlier study, understanding the impact of phenolic syntan on leather has been reported.[6] Continuing with that, an insight on melamine syntan on sewability property has been studied. It is well known that leather's physical properties are not limited to individual performance chemicals. A combination of post tanning chemicals would contribute to the required properties concerning the leather product.

Nevertheless, understanding the influence of specific chemicals on leather properties would aid in developing the optimized process. In the present study, melamine syntan has been chosen to understand its impact on physical strength characteristics of the leathers. Melamine syntan belongs to the family of resin syntan, which is for its selective filling property during the post tanning process.[17] Leather being key material, the natural skin/hide characteristics significantly vary from region to region on the same material. To achieve the uniform filling characteristics, melamine syntan is the preferred choice of chemical. Therefore, melamine syntan would play significant role in achieving the specific physical property of leather.

To understand the influence of fatliquor on the leather, Experiments were carried out with 10% fatliquor (Table I). It can be observed from trials 5 and 6 that leathers with 8 and 10% melamine syntan and 10% fatliquor are found to exhibit better sewability. This study is in-line with our earlier studies with phenolic syntan.[6]

Table II
Sewability Measurements

Sample Description	Standard Threshold	Sewability (High)
TRIAL 1 – (10% Fatliquor; 0% Syntan)	500	78
TRIAL 2 – (10% Fatliquor; 2% Syntan)	525	81
TRIAL 3 – (10% Fatliquor; 4% Syntan)	475	15
TRIAL 4 – (10% Fatliquor; 6% Syntan)	500	41
TRIAL 5 – (10% Fatliquor; 8% Syntan)	550	4
TRIAL 6 – (10% Fatliquor; 10% Syntan)	500	5

Strength characteristics

Properties of grain crack strength of experimental leathers are given in Table III. It can be ascertained that leathers treated with the fatliquor and higher concentrations of syntan showed better grain strength properties.

The tensile strength of experiment leathers are given in Table IV, respectively. An increase in syntan concentration has also increased the tensile strength to certain extent with the combination of fatliquor. Thus, it is evident that retanning and fatliquoring processes influences the tensile strength of the leathers.

Morphological evaluation

Grain surface and cross-sectional view of the experimental leathers are visualized using an optical microscope.

Table III
Lastometer - Grain Crack

Sample Description	Measurement	Value
TRIAL 1	Load at Grain Crack (Kg)	39.8
(10% Fatliquor; 0% Syntan)	Distention at Grain Crack (mm)	9.8
TRIAL 2	Load at Grain Crack (Kg)	38.4
(10% Fatliquor; 2% Syntan)	Distention at Grain Crack (mm)	9.9
TRIAL 3	Load at Grain Crack (Kg)	37.5
(10% Fatliquor; 4% Syntan)	Distention at Grain Crack (mm)	10.1
TRIAL 4	Load at Grain Crack (Kg)	50.2
(10% Fatliquor; 6% Syntan)	Distention at Grain Crack (mm)	10.8
TRIAL 5	Load at Grain Crack (Kg)	42.6
(10% Fatliquor; 8% Syntan)	Distention at Grain Crack (mm)	9.8
TRIAL 6	Load at Grain Crack (Kg)	41.5
(10% Fatliquor; 10% Syntan)	Distention at Grain Crack (mm)	9.5

Table IV
Tensile Strength and Elongation Measurements

Sample Description	Direction	Tensile Strength [MPa]	Elongation at Break %
TRIAL 1	1	26	67.7
(10% Fatliquor; 0% Syntan)	2	44	41.5
TRIAL 2	1	18	57.3
(10% Fatliquor; 2% Syntan)	2	29	46.8
TRIAL 3	1	18.8	69.8
(10% Fatliquor; 4% Syntan)	2	33.6	42.2
TRIAL 4	1	29	70.3
(10% Fatliquor; 6% Syntan)	2	33.1	46.5
TRIAL 5	1	25.5	54.8
(10% Fatliquor; 8% Syntan)	2	25.7	36.8
TRIAL 6	1	28.2	70.5
(10% Fatliquor; 10% Syntan)	2	29.3	36.7

(a) (0% Syntan) Cross Section and Grain Surface

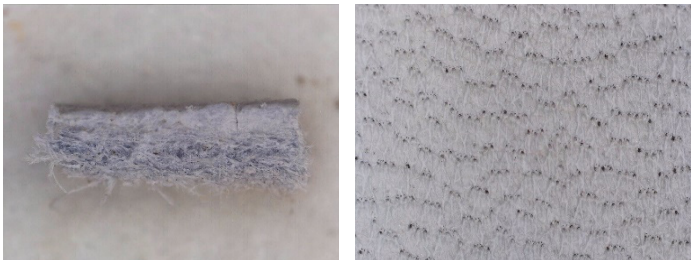

(b) (2% Syntan) Cross Section and Grain Surface

(c) (4% Syntan) Cross Section and Grain Surface

(d) (6% Syntan) Cross Section and Grain Surface

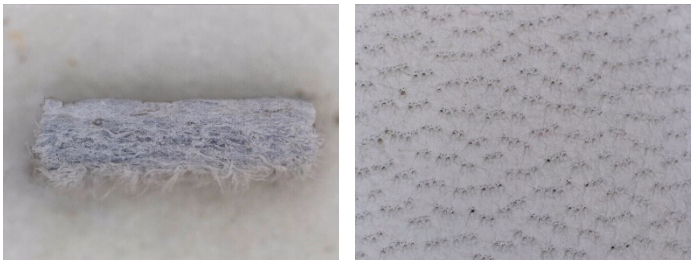

(e) (8% Syntan) Cross Section and Grain Surface

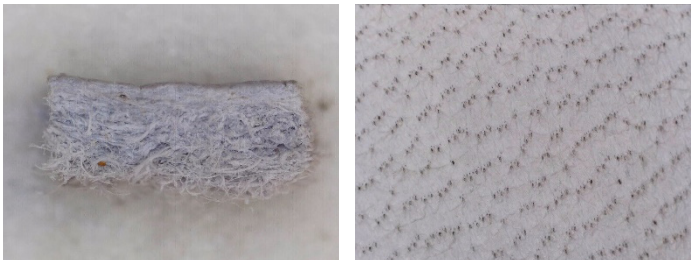

(f) (10% Syntan) Cross Section and Grain Surface

Figure 1. Optical images of leathers with 10% of fatliquor (cross section and grain surface)

Conclusion

The present study summarizes the effect of melamine syntan and synthetic fatliquor on the sewability properties of the leather. Post tanning processes have been designed to understand the impact of melamine syntan on leather with the offer of fatliquor. The leathers have been characterized for their physical strength properties such as sewability, tensile strength, grain crack and morphological evaluation. The present study confirms that melamine syntan is in accordance with the phenolic syntan sewability behavior reported earlier by our research group.[6] The results provide insight on the sewability property of melamine syntan leathers which provides a better understanding in formulating the process recipe for goods and garment leather manufacture.

Acknowledgement

Authors acknowledge the support for the testing of leathers at CATERS, CSIR-CLRI and Mr. Ashish Singh, Technical Assistant, SPDC, CSIR-CLRI for the help in measuring sewability. CSIR-CLRI communication number is 1687.

References

1. Alessandro, B.,Cecilia C.; The nature of luxury: a consumer perspective. *Int. J. Retail. Distrib.*, **41**, 823-847, 2013.
2. Krishnaraj, K., Thanikaivelan, P., Chandrasekaran, B.; Relation between drape and mechanical properties of goat suede garment leathers. *J. Soc. Lea. Tech. Chem*. **93**, 1-7, 2000.
3. Phebe, K., Chandrasekaran, B., Mandal, A.B.; Sewability of sheep nappa garment leather. *Res. J. Textile. Apparel*, **18** (2), 49-55, 2014.
4. Anthony D. Covington, William R. Wise; Current trends in leather science. *Journal of Leather Science and Engineering,* **2**:28, 2020.
5. Kallen Mulilo Nalyanya, Ronald K. Rop, Arthur Onyuka, Zephania Birech, Alvin Sasia; Effect of crusting operations on the physical properties of leather. *Leather and Footwear Journal*, **18**, 4, 2018.
6. Jayakumar GC, Phebe Aaron, K., Krishnaraj, K.; A comprehensive understanding on sewability of natural biomaterial: an insight on process optimization during leather manufacture. *JALCA*, **116**, 233-238, 2021.
7. IUP 2, Sampling. *J. Soc. Lea. Technol. Chem.*, **84**, 303, 2000.
8. IUP 6, Measurement of tensile strength and percentage elongation, *J. Soc. Lea. Technol. Chem.*, **84**, 317-321, 2000.
9. IUP 9, Measurement of distension and strength of grain by the ball burst test. Official methods of analysis, *J. Soc. Leather Tech. Chem.*, 1996.
10. Gararda, A.; Investigation of the seam performance of pet/nylon-elastane woven fabrics. *Textile Research J.*, **78** (21), 21-27, 2008.

11. Phebe, K., Krishnaraj, K., Chandrasekaran, B.; Evaluation of sewability of nappa leathers. *J. Fashion Technol. Textile Eng.*, **4**:2, 2016.
12. Procter, H. R.; The manufacture of leather. *Journal of the Society of Arts*, **47**, 851, 1898.
13. Phebe, K., Chandrasekaran, B.; Studies on influence of stitch density and the stitch type on seam properties of garment leather. *AATCC J. Res.*, **1** (6), 8-15, 2014.
14. Gurarda, A., Meric, B.; Sewing needle penetration forces and elastane fibre damage during the sewing of cotton/elastane woven fabrics. *Textile Res. J.*, **75** (8), 628-633, 2005.
15. Phebe, K., Chandrasekaran, B.; Performance of needles on sewability of garment leathers. *Leather footwear J.*, **11**, 2011.
16. Nilay, O. R. K., Mutlu Mehmet Mete, Yildiz Esra Zeynep, Pamuk Oktay; Sewability properties of garment leathers tanned with various tanning materials. Intern. Conf. Applied Res. Textile, 2010.
17. Balasubramanian, P., Azhar Zakir, M. J., Aravindhan, R., Sreeram, K. J.; Raghava Rao, J., Unni Nair, B.; Chrome-melamine Syntan: A Step Towards Developing Fuller Leather. *JALCA*, **110**, 2015.

Effects of Alkali and Acid on the Solubility and Molecular Weight of Collagen Hydrolysates Extracted from Bovine Hide

by

Lili Yan,[1,2] Sadaqat Ali Chattha,[1,2] Xu Zhang,[1,2] Mengchu Gao,[1,2] Chunxiao Zhang[1,2,3] and Biyu Peng[1,2,3]*

[1]*College of Biomass Science and Engineering, Sichuan University,* Chengdu, 610065, China

[2]*National Engineering Laboratory for Clean Technology of Leather Manufacture, Sichuan University*, Chengdu 610065, China

[3]*Key Laboratory of Leather Chemistry and Engineering of Ministry of Education, Sichuan University*, Chengdu 610065, China

Abstract

Preparation of collagen hydrolysates with high molecular weight to meet its industrial demand is a crucial step for resource utilization of solid waste of animal skins/hides. However, it is very difficult to achieve both higher molecular weight and solubility of collagen hydrolysates through the traditional methods. In this study, we attempted to prepare bovine hide collagen hydrolysates with high molecular weight and solubility through the application of NaOH or different types of acid. Influences of the concentration of alkali and acid, hydrolysis temperature and time on the molecular weight and solubility were studied, respectively. The results showed that NaOH has a strong hydrolysis effect on bovine collagen, making it a suitable candidate for the preparation of collagen hydrolysates with medium or low molecular weight. Under these optimized NaOH treatment conditions, i.e., NaOH concentration of 0.13 mol/L, hydrolysis temperature of 60 - 70°C and time of 5 h, we achieved 96% of solubility for hide pieces and the molecular weight of collagen hydrolysates were in the range of 25 - 30 kDa. By contrast, the molecular weight of the hydrolysates prepared through H_2SO_4 hydrolysis method was higher than that of NaOH hydrolysis method. Under the optimized H_2SO_4 treatment conditions, i.e. H_2SO_4 concentration of 0.5 mol/L, hydrolysis temperature of 50°C and time in the range of 5 - 7 h, the solubility of hide pieces reached up to 80 - 97%. Additionally, in the H_2SO_4 hydrolysates, the proportion of macromolecular components with molecular weight of about 100 kDa was 41 - 55% and that of medium molecular components with molecular weight of about 20 kDa was 45 - 59%. This study showed that high solubility and high molecular weight collagen products can be obtained by H_2SO_4 hydrolysis under specific conditions. Thus, this study provided a useful scientific method and process parameters to guide the controlling of molecular weight and the industrial application of collagen from waste on a bigger scale.

Introduction

The demand for meat and dairy products has been increasing day by day, and has promoted the growth of livestock. About 300 million pieces of bovine hide come from the meat and dairy industries every year, of which about 60% are used for tanning, and 40% (about 120 million) collagen sheets are discarded. Discarded collagen sheets generate 3 million tons of landfill waste and release 2.7 million tons of greenhouse gases.[1] In addition, 350 kg of solid leather waste is produced and discarded during one ton of leather manufacturing, which also causes serious environmental pollution.[2] Therefore, it is a dire need of our time to find some high-value utilization of the aforementioned produced solid waste.

Animal skin is mainly composed of water-insoluble connective tissue woven by collagen fibers. About 85 - 90% of collagen is found in the dermis. Soluble collagen can be mainly obtained by acid, alkali, enzymatic and heat treatment methods. In the course of its preparation, natural collagen is denatured and hydrolyzed to varying degrees. Therefore, the properties and suitable fields of application of collagen hydrolysates depend mainly on its preparation methods. For example, collagen with a complete triple helix structure can be obtained by the application of a low concentration of acid and pepsin. Its molecular weight is about 300 kDa, which has biological activity[3] and fibril formation properties.[4] It can be used in tissue engineering, bone substitution, ophthalmic surgeries, drug delivery vehicle, immunity localization effects and sponges for burns or wounds, etc.[5] Gelatin and hydrolyzed collagen are the denatured products of native collagen obtained through the application of strong acid, alkali, enzyme or heat. However, these denatured products generally don't have any biological activity.[3] Collagen hydrolysates obtained through different methods exhibit different molecular weights and properties, i.e., hygroscopicity property, water holding capacity, oil holding capacity, emulsifying properties, foaming properties and antioxidant activity.[6] Therefore, the collagen hydrolysates with divergent properties are suitable for different applications, such as food additives, protein dietary supplements edible films, coatings,[7] cosmetics,[8] wood adhesives,[9] leather retanning agents[10,11]and paper sizing agents.[12]

The field and scope of application of hydrolyzed collagen are closely related to its molecular weight. For example, collagen peptides with molecular weights below 3 - 6 kDa don't have gelling and fibril formation properties, but have water-holding, moisture absorption, and anti-aging properties.[13] Therefore, they are the

*Corresponding author email: pengbiyu@scu.edu.cn

Manuscript received February 26, 2022, accepted for publication April 3, 2022.

most suitable candidates for their application in cosmetics,[8,13] food additives,[7,13] and facial skin essence materials.[14] The molecular weight of UVB-induced anti-photo aging materials is about 1.0 kDa.[15] Hydrolyzed collagen with high molecular weight is generally used in the industrial field, such as photosensitive materials,[16] packaging materials, paper surface sizing agents,[17] etc. For example, enzymatic hydrolysates of waste collagen proteins from current industrial manufacture (leather, edible meat product casings, etc.) of mean molecular mass 20 - 30 kDa by a reaction with dialdehyde starch, produce hydrogels applicable as biodegradable (or even edible) packaging materials for food, cosmetic and pharmaceutical products.[17] Both physical, mechanical properties and water resistance of the corrugated paper coated by GDESA (GDESA was prepared by modifying collagen hydrolysate with Glycol diglycidyl ether, then grafted with Butyl acrylate and styrene) were significantly improved when the molecular weight of collagen hydrolysates was about 10 kDa, and its emulsion exhibited robust stability in long-standing time.[12] Collagen protein with medium molecular weight (10 - 30 kDa detected by SDS-PAGE) from chrome leather scraps has been used as retarding agent in gypsum application, which produced a positive retarding effect in the prolongation of setting time.[18]

As mentioned above, preparation methods for collagen hydrolysates mainly include acid, alkali, enzymatic hydrolysis and heat extraction. To get intact collagen with a complete triple-helix structure, 0.5 mol/L of acetic acid or pepsin at low temperatures is usually applied, however, the solubility of these methods was too low, generally less than 50%.[19-21] Heating can accelerate the hydrolysis of collagen by destroying the hydrophobic interaction and hydrogen bond in collagen, and promoting the dissolving of collagen. Therefore, thermal extraction method is adopted as the traditional preparation method of gelatin[22] though this method always brings high energy consumption. Therefore, collagen can be easily hydrolyzed into low molecular weight soluble products under strong action of acid, alkali or enzymes. In this preparation process, collagen products with high molecular weight can be obtained under weaker hydrolysis conditions though the solubility is very low. Strong hydrolysis conditions will have the opposite effect on the molecular weight and solubility which limits its application on commercial scale.

Bovine hide contains about 89% of collagen fiber.[23] The production of soluble collagen is another effective utilization of bovine hide except for leather making. The preparation of hydrolyzed collagen or gelatin from bovine hide has been widely investigated. For example, yak hides were hydrolyzed by trypsin to produce collagen hydrolysates with 98.79% of solubility and 1000 - 2236 Da of molecular weight.[24] Tannery and slaughterhouse bovine hides were hydrolyzed by acid or alkali to produce gelatin, and the solubilities of all of these methods are lower than 31%.[23] Delimed bovine pelts were hydrolyzed by acetic acid at 70°C for 6 h to produce gelatin, however, the yield is only 4.78 % and the molecular weight is in the range of 6 - 38 kDa.[25] Calf split was respectively treated by acetic acid, pepsin and alkali to produce completed Type I and Type III collagen.[26]

Although animal skins/hides can be used to produce undenatured collagen and used in the field of medicine, food and cosmetics with high values, however, the requirement for the quality of collagen products is very high and the demand is limited. Moreover, it is difficult to balance the molecular weight and solubility of collagen hydrolysates at the same time because of the difficult controllability of the molecular weight. Therefore, to solve the problem of resource utilization of collagen waste from animal skins, the most effective way is to develop the industrial application of collagen on a bigger scale. Hence, establishing preparation methods for soluble collagen with controllable molecular weight is required to fulfill the requirements of industry application.

As mentioned previously, the preparation of small molecule collagen is relatively simple, but the industrial application needs macromolecular collagen. Therefore, this study focuses on the effects of alkali and acid treatment conditions on the solubility of delimed bovine split and the molecular weight of collagen hydrolysates. We attempted to establish a method for preparing collagen hydrolysates with large molecular weight along with high solubility.

Materials and Methods

Materials

Delimed bovine hide substrate (1 cm × 1 cm) with moisture of 58.09% and freeze-dried hide powder with moisture of 5.31% was obtained from our laboratory. Standard protein samples of ovalbumin (45000Da), myoglobin (17000Da), aprotinin (6700Da), neurotensin (1700Da) and angiotensin II(1000Da) were purchased from Agilent Technologies Inc., USA. Gelatin (Number-average molecular weight (Mn) = 65997, Weight-average molecular weight (Mw) = 94749, Mw/Mn = 1.44) was purchased from Chengdu Chron Chemicals Co., Ltd. All the chemicals used for the reaction and analysis were of analytical grade.

Preparation of bovine hide hydrolysates through NaOH hydrolysis method

20.0 g of intact pieces of bovine hide was weighed and mixed with 80.0 mL of NaOH solution (the concentration is in the range of 0.0 - 1.0 mol/L). Then, the mixture was stirred at different temperatures (50 - 80°C) for different times (1 - 9 h) at 200 r/min. After the reaction, samples were cooled to room temperature and centrifuged for 20 min at 4°C, 9460 r/min, then, filtered with constant weight filter paper. The filtrate was collected to determine the content of hydroxyproline (Hypro) by Chloramine T method and the molecular weight by Gel Permeation Chromatography (GPC) method, respectively. In addition, the filter residues were collected, washed with distilled water thoroughly and dried for determining the solubility.

Preparation of bovine hide hydrolysates through acid hydrolysis method

Effect of acid type

10.0 g of bovine hide powder was mixed with different acid solutions. The mixture was stirred at 50°C for 3 h at 200 r/min. After the reaction, samples were centrifuged and filtered. The solubility, the content of Hypro in the filtrate and the molecular weight of the hydrolysates were determined as the methods described above.

Preparation of bovine hide hydrolysates through H_2SO_4 hydrolysis method

20.0 g of intact pieces of bovine hide were weighed and mixed with 80.0 mL of H_2SO_4 solution (the concentration is in the range of 0.0 - 1.2 mol/L). Then, the mixture was stirred at different temperatures (50 - 80°C) for different times (1 - 9 h) at 200 r/min. After the reaction, samples were centrifuged and filtered. The solubility, the concentration of Hypro in the filtrate and the molecular weight of the hydrolysates were determined as the methods described above.

Solubility of bovine hide

The collected residues from bovine hide hydrolysates after filtering were constantly weighted at 102 ± 2°C. Quantification of solubility is calculated according to the ratio of the dry weight of residues after hydrolysis (M_1) and the dry weight of bovine hide pieces or powder ($M_0 \times S$). The calculation formula is as follows:

$$Solubility = (1 - \frac{M_1}{M_0 \times S}) \times 100\%$$

In the equation, S is the solid content of untreated bovine hide pieces.

Determination of Hypro by Chloramine T method

The concentration of Hypro was determined according to the modified colorimetric method.[27,28] First, 2 mL of filtrate was mixed with 2 mL of HCl (12 mol/L) and hydrolyzed at 120°C for 4 h. A colored soluble product was obtained based on the reaction of Hypro with *p*-dimethylaminobenzaldehyde. The absorbance of the colored mixture was measured at 560 nm to determine the amount of Hypro.

Determination of molecular weight of bovine hide hydrolysates by GPC method

The molecular weight of the bovine hide hydrolysates was determined through GPC method. The HPLC system used was an Agilent 1260 Infinity II HPLC system with an SEC separation column (130A 2.7 µm particle size, 7.8mm×300mm) and a diode array detector (Agilent Technology Inc.).[29] The GPC conditions were as follows: flow rate, 1 mL/min; injection volume, 10 µL; column temperature 25°C; mobile phase 150 mmol/L of NaH_2PO_4-Na_2HPO_4 buffer (pH 7.0); Detection wavelength, 220 nm.

A standard curve was plotted from the logarithm of molecular weight (Mw) and retention time (T) of the standard protein samples (LogMw= 6.914-0.4223T, R^2 = 0.9904). The molecular weight of the samples was obtained by comparing the retention time of the sample with the standard curve. The relative content of each peptide fraction was expressed as a percentage of the chromatographic peak area.

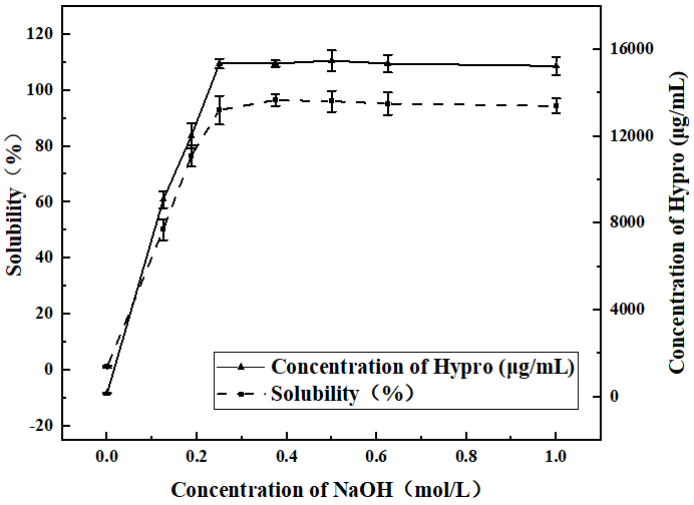

Figure 1. Effect of NaOH concentration on the solubility of bovine hide (50°C, 5 h)

Results and Discussion

Effect of NaOH hydrolysis conditions on the molecular weight of collagen hydrolysates

Effect of NaOH concentration

The results in Figure 1 showed that the solubility and concentration of Hypro in the reaction liquors were increased linearly with the increase of NaOH concentration in the range of 0.00 - 0.25 mol/L. The highest solubility of the bovine hide (about 93%) and the maximum content of Hypro in the hydrolysates (about 15000 µg/mL) were achieved at 0.25mol/L of NaOH at 50°C for 5 h. However, when the concentration of NaOH was higher than 0.25 mol/L, the solubility and content of Hypro have no significant increase.

The results in Figure 2 showed that the retention time of the hydrolysates was significantly shifted to the right along with the narrowing down of peak width with the increase of NaOH concentration, indicating the reduction in molecular weight and distribution of collagen hydrolysate. A linear negative correlation between the concentration of NaOH and the molecular weight of hydrolysates had been observed when the concentration of NaOH is no more than 0.25 mol/L. The most remarkable result to emerge from the data is that the M_W and the molecular weight distribution width (M_W/Mn) of the hydrolysates dropped off from 36 kDa to about 2.5 kDa and 3.64 to 1.69, respectively, as NaOH concentration increased from 0.13 mol/L to 1.00 mol/L. These results indicated that the proportion of low molecular weight components was increased with the increase of NaOH concentration and the preparation of low Mw collagen hydrolysates by the NaOH hydrolysis method is fairly simple.

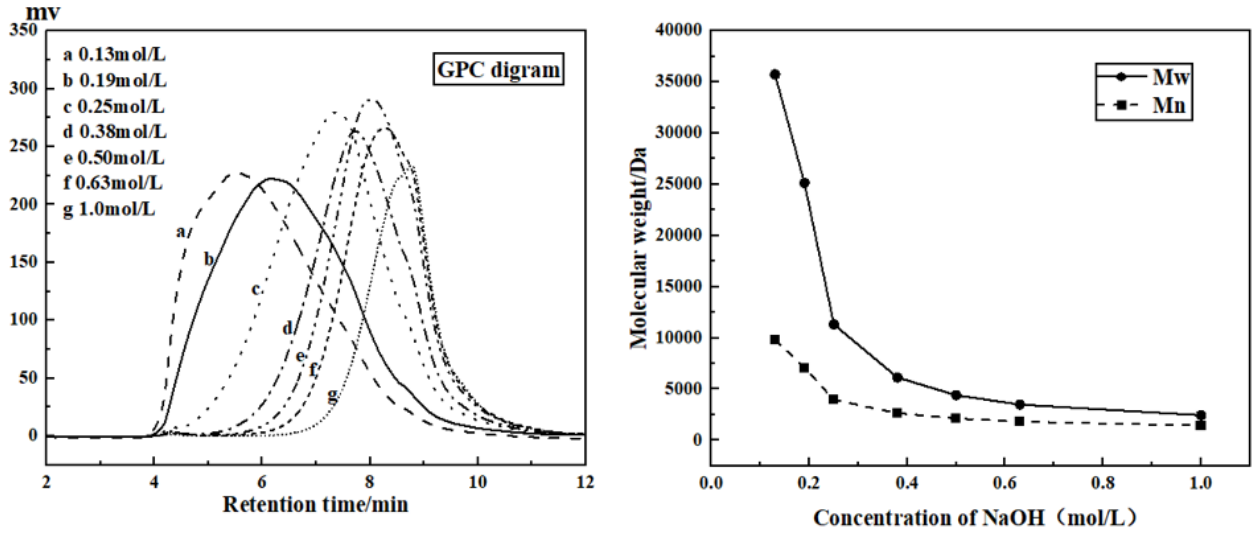

Figure 2. Effect of NaOH concentration on the molecular weight of collagen hydrolysates (50°C, 5 h)

In general, there is a negative correlation between the solubility of bovine hide and the molecular weight of the hydrolysates. When the concentration of NaOH is higher than 0.25 mol/L, more than 93% solubility of bovine hide had been observed, whereas, the molecular weight of the hydrolysates was lower than 12 kDa. Conversely, at a lower concentration of NaOH, i.e. 0.13mol/L, Mw of the hydrolysates was found to be higher than 30 kDa, however, the solubility of the bovine hide was only about 50%. These findings indicated that it is very difficult to prepare high molecular weight collagen hydrolysates along with high solubility from bovine hide. Therefore, from the perspective of preparing high molecular weight collagen hydrolysates, the effects of reaction time and temperature on the hydrolysis degree of bovine hide at low NaOH concentration were further investigated.

Effect of NaOH hydrolysis time

Results showed that the solubility of bovine hide was significantly increased with hydrolysis time and reached up to 50.2% ± 3.79% after reacting with 0.13 mol/L of NaOH at 50°C for 5 h. Then, with the consumption of NaOH, the hydrolysis of the bovine hide pieces gradually slowed down, and the solubility of the hide pieces was increased to 66.5% ± 2.34% at 9 h. The results in Figure 3 showed that the molecular weight of the collagen hydrolysates increased first and then decreased with hydrolysis time, which might be due to the heterogeneous reaction of the hydrolysis processes. In the early stage of hydrolysis (within 3 h), the hide pieces remained in a relatively intact state, and the solubility of low molecular hydrolysate components was faster than that of macromolecular components. The determined molecular weight of the collagen hydrolysates was about 36 kDa after 5 h of hydrolysis. Subsequently, the molecular weight of the hydrolysates was decreased to 32 - 36 kDa and the width of molecular weight distribution slightly increased (the M_W/Mn value is in the range of 3.62 - 4.23).

These results indicated that the high molecular weight hydrolysates (M_W > 30 kDa) can be prepared at low NaOH concentration and medium temperature. However, the solubility of the hide pieces was less than 70%, and it has little contribution to further improving the solubility by prolonging the hydrolysis time.

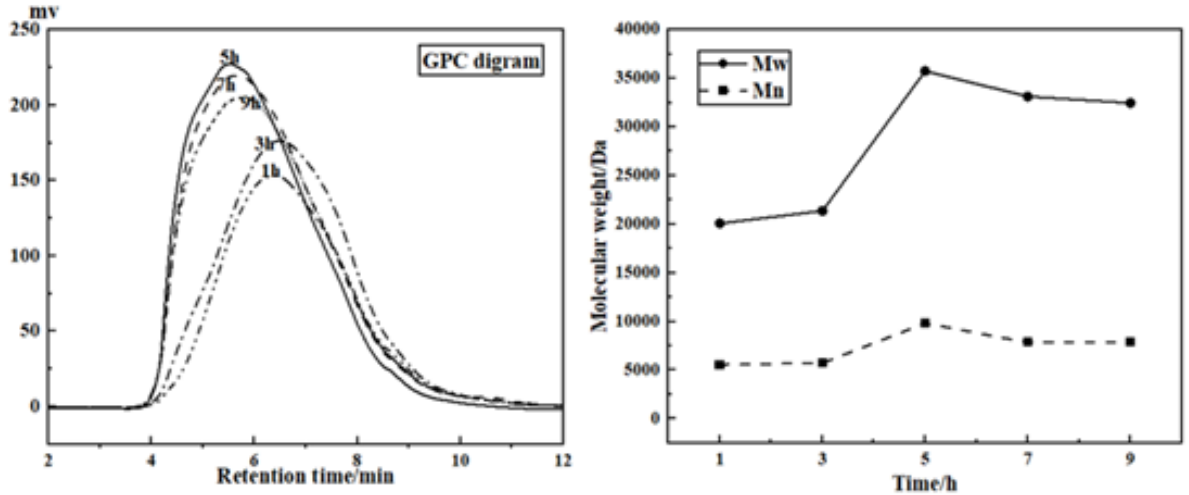

Figure 3. Effect of NaOH hydrolysis time on the molecular weight of collagen hydrolysates (C_{NaOH}=0.13 mol/L, 50°C)

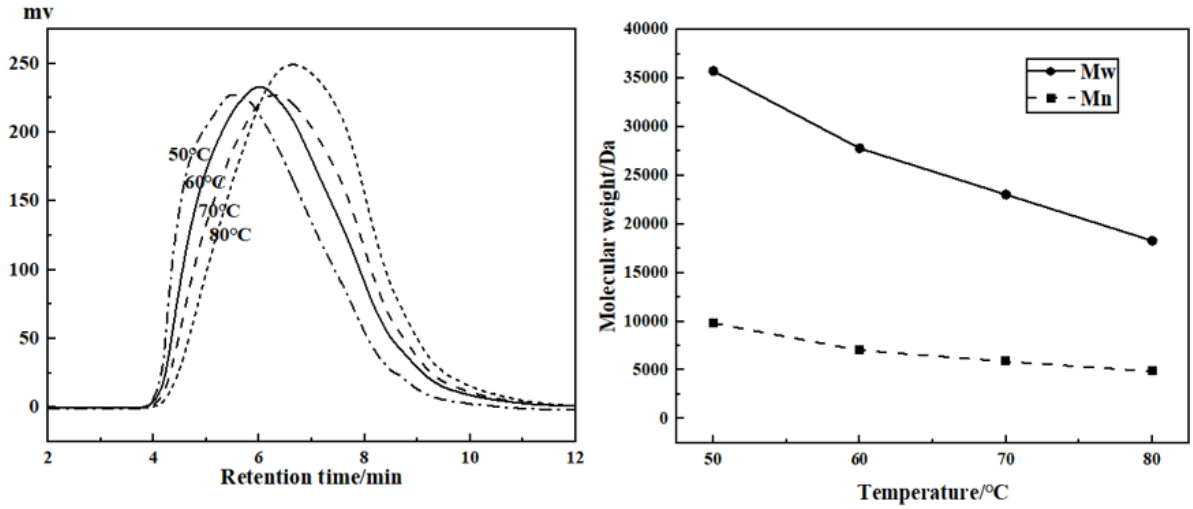

Figure 4. Effect of NaOH hydrolysis temperature on the molecular weight of collagen hydrolysates (C_{NaOH} =0.13 mol/L, 5 h)

Effect of NaOH hydrolysis temperature

In order to obtain high molecular weight hydrolysates with higher solubility, the effect of temperature on the hydrolysis of bovine hide at low NaOH concentration was further investigated. Results showed that the solubility of bovine hide was increased from 50.2% ± 3.79% to 96.6% ± 4.06% when the reaction temperature was increased from 50°C to 60°C at 0.13 mol/L of NaOH for 5 h. However, further increasing the reaction temperature just had a slight effect on the solubility of the bovine hide. The results in Figure 4 showed that the molecular weight of the collagen hydrolysates was decreased with the increase of hydrolysis temperature, e.g. the molecular weight of the hydrolysates was decreased to 18 kDa at 80°C from 36 kDa at 50°C. Additionally, hydrolysis temperature had little effect on the width of molecular weight distribution and the M_W/Mn value remained between 3.64 - 3.95.

In summary, NaOH solution has a strong hydrolysis effect on bovine hide, which is suitable for the preparation of collagen hydrolysates with low and medium molecular weight. The above results indicated that bovine hide pieces can be easily hydrolyzed into low molecular weight products (< 10 kDa) when the reaction conditions were reached or even higher than 0.25 mol/L of NaOH and 50°C. Oppositely, collagen hydrolysates with the molecular weight between 25 - 30 kDa can be produced when the concentration of NaOH is 0.13 mol/L and the hydrolysis temperature is in the range of 60 - 70°C for 5 h, and the solubility is reached up to 96%.

Effect of acid hydrolysis conditions on the molecular weight of collagen hydrolysates

Effect of acid type

Although the extraction of collagen hydrolysates from bovine hide pieces through NaOH method has higher solubility, the product has a lower molecular weight. Herein, the effect of acid hydrolysis on the molecular weight of the product was further studied.

Firstly, the effects of several typical acids on the solubility of bovine hide powder and the molecular weight of collagen hydrolysates were compared in a trial sample test to select optimal acids for further study (Table I). Results showed that, at a low concentration of acid (sulfuric acid 7.23 mmoL/g, other acids 14.46 mmoL/g, based on the dry weight of hide powder), the solubility of bovine hide powder by FA, AA, SA, MSA and NSA hydrolyzed at 50°C for 3 h were 29.18% ± 1.39%, 21.41% ± 1.18%, 74.8% ± 2.74%, 76.23% ± 2.18% and 74.99% ± 3.32%, respectively. The solubility of hide

Table I

Conditions of hydrolysis by different acids

Acid	Characterization	Liquor ratio	Content of acid (mmoL/g of hide powder)
Formic acid (FA)	Monoacid, Swelling acid	1:50	14.46
Acetic acid (AA)	Monoacid, Swelling acid	1:50	14.46
Sulfuric acid (SA)	Dibasic acid, Swelling acid	1:15	7.23
Methanesulfonic acid (MSA)	Monoacid, Swelling acid	1:15	14.46
2-Naphthalenesulfonic acid (NSA)	Monoacid, Non-swelling acid	1:15	14.46

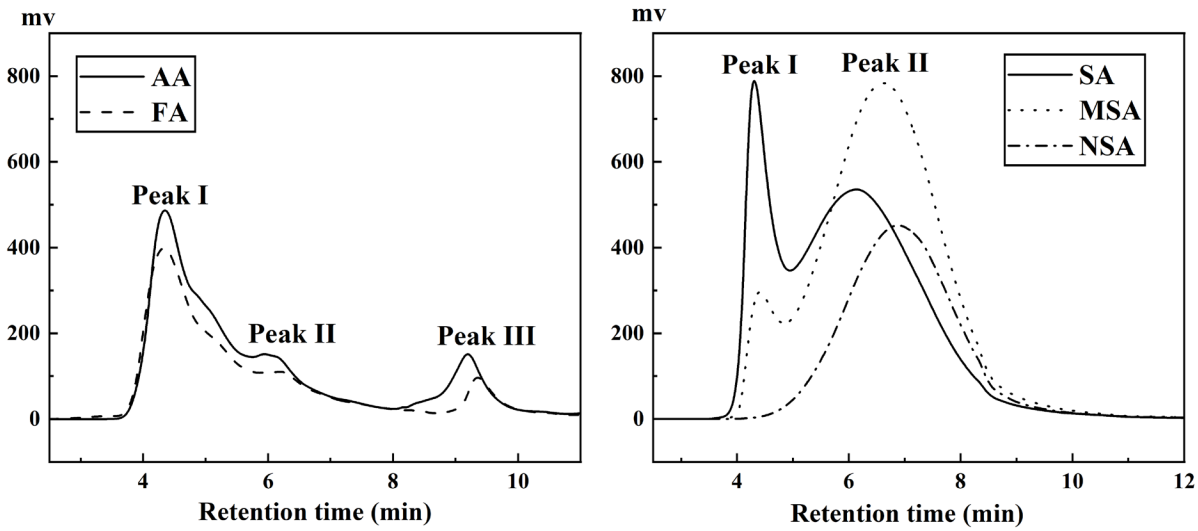

Figure 5. GPC diagrams of collagen hydrolysates by different acids
(AA: Acetic Acid, FA: Formic acid, SA: Sulfuric Acid, MSA: Methane Sulfonic Acid, NSA: 2-Naphthalene Sulfonic Acid)

Table II
Molecular weight of different acid hydrolyzed collagen hydrolysates

Acid	Peak	Mn (Da)	Mw (Da)	Mw/Mn	Peak area(%)
FA	I	75447	96196	1.28	73.28
	II	10543	14656	1.39	19.06
	III	<1000	<1000	-	7.66
AA	I	75826	92445	1.22	70.02
	II	15036	17994	1.20	17.85
	III	<1000	<1000	-	12.13
SA	I	104070	108339	1.04	26.93
	II	6994	21003	3.00	73.07
MSA	I	102481	104042	1.02	8.91
	II	6383	17071	2.67	91.09
NSA	II	5085	13666	2.47	100.00

powder was positively correlated with the strength of acids, e.g. weaker acid FA and AA with lower H^+ dissociation constant than strong acid SA, MSA and NSA, which produced lower strength of acid at the same theoretical acid concentration and result in low solubility. It is worth noting that compared with swelling acids, SA and MSA, there is no significant difference in the solubility of the bovine hide powder in non-swelling state when non-swelling acid NSA[30-31] was used.

The results in Figure 5 showed that the GPC chromatogram of the collagen hydrolysates produced by acid methods has obvious double-peak or multi-peak characteristics compared to NaOH hydrolysis method. For example, the collagen hydrolysates of FA and AA have triple peaks in a wide range, and the hydrolysates of SA, MSA and NSA have two peaks. Detailly, Peak I and II respectively represents the molecular weight of about 100 kDa and 15 - 20 kDa, and Peak III represent the molecular weight is lower than 1.0 kDa. The molecular weight of the Peak I component was larger than gelatin, indicating that the acid-soluble collagen might be in a complete structure. Table II showed that the proportion of Peak I in FA, AA, SA and MSA was 73.28%, 70.02%, 26.93% and 8.69%, respectively, indicating that weak organic acid is conducive to the dissolution of acid-soluble collagen in the bovine hide. Furthermore, there is no obvious Peak I component in the hydrolysates of the NSA treated sample, indicating that macromolecular acid-soluble collagen can be dissolved out at a non-swelling state of collagen fiber. To sum up, the treatment of hide powder by acids includes two stages at low concentrations of acid: the dissolution of macromolecular acid-soluble collagen and the hydrolysis of collagen; and the proportion of low molecular weight hydrolysates increased with the increase of acid strength.

Generally, the molecular weight of the collagen hydrolysates treated by H_2SO_4 is higher than 21 kDa, and the solubility is relatively high than other acids. Subsequently, the effect of H_2SO_4 concentration, hydrolysis temperature and time on the solubility of bovine hide and the molecular weight of hydrolysates were further investigated.

Table III

Molecular weight and distribution of collagen hydrolysates with varying H_2SO_4 concentrations

Concentration of H_2SO_4 (mol/L)	Content of H_2SO_4 per gram hide pieces (mmoL/g, dry weight)	Solubility (%)	Peak	Mn (Da)	Mw (Da)	Mw/Mn
0.3	2.86	67.33±2.52	I	117496	120620	1.03
			II	24008	29033	1.21
0.5	4.77	80.14±3.03	I	96146	108068	1.12
			II	11451	20430	1.78
0.7	6.68	93.60±2.40	I	97077	103546	1.07
			II	7770	18487	2.38
1.0	9.54	93.88±3.53	I	94024	99333	1.06
			II	6809	16384	2.41
1.2	11.45	92.88±2.42	I	94994	97673	1.03
			II	6169	10708	1.74

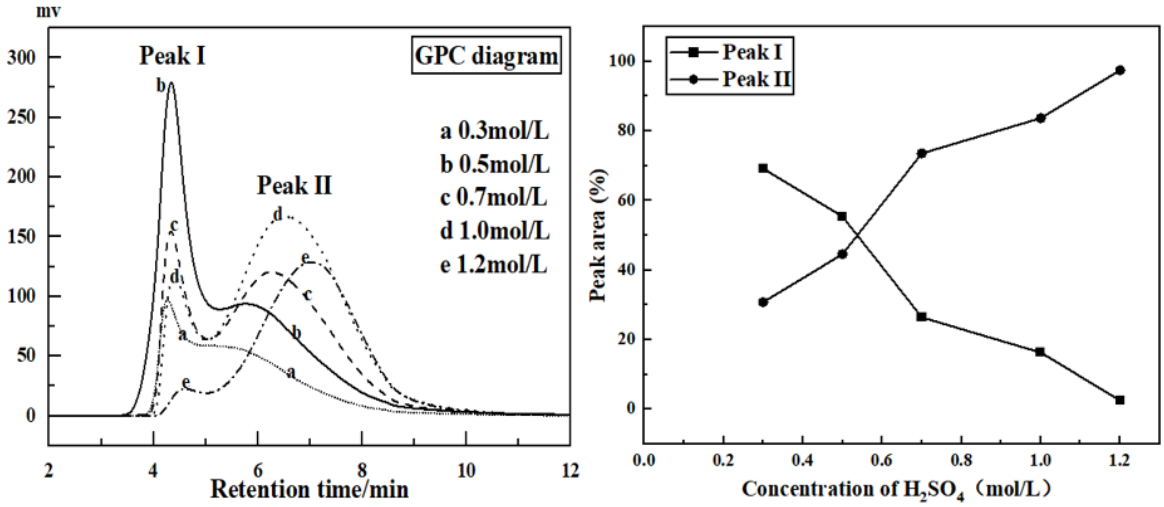

Figure 6. Analysis of GPC of collagen hydrolysates with varying H_2SO_4 concentrations (50°C, 5 h)

Effect of H_2SO_4 concentration

Bovine hide pieces were treated with different concentrations of H_2SO_4 at 50°C for 5 h. The results in Table III showed that when the concentration of H_2SO_4 was lower than 0.7 mol/L, the solubility of bovine hide increased obviously with the increase of acid concentration; When the concentration of H_2SO_4 reached up to 0.7 mol/L, the solubility of bovine hide tend to be the same at about 94%. At 0.7 mol/L of H_2SO_4, per gram of hide pieces (dry weight) had been hydrolyzed by 6.68 mmoL of H_2SO_4, which was close to 7.23 mmoL H_2SO_4 per gram of hide powder (dry weight) in the section of *Effect of acid type*. Therefore, the molecular weight and peak area ratio of collagen hydrolysates was very close to each other. However, the solubility at 7.23 mmoL of H_2SO_4 was lower than 6.68 mmoL of H_2SO_4 because of the shorter hydrolysis time.

The results in Table III and Figure 6 also showed that with the increase of H_2SO_4 concentration, the average molecular weight (Mn) of the macromolecular component (Peak I) changes little and the M_W is about 100 kDa; the Mn of the medium molecular component (Peak II) decreased obviously and the M_W is reduced from 30 kDa to 10 kDa. Besides, the area ratio of the two peaks changed apparently. With the increase of H_2SO_4 concentration from 0.3mol/L to 1.2mol/L, the area proportion of Peak I decreased from 69.21% to 2.51%, and the area proportion of Peak II increased from 30.79% to 97.49%. These results indicated that the hydrolysis degree of collagen products increased with the increase of H_2SO_4 concentration. Hence, the proportion of high molecular weight components in the product decreased, followed by the proportion of low and medium molecular weight components increased.

Compared with NaOH hydrolysis method, the molecular weight of the hydrolysates treated by H_2SO_4 method was obviously higher, and the molecular weight distribution was narrower, especially the M_W/Mn value of macromolecular compounds was about 1.0. When the bovine hide pieces were hydrolyzed by 0.3 mol/L of H_2SO_4 at 50°C, the proportion of macromolecular component (about 120 kDa) in the collagen hydrolysates was 69.21%, however, the solubility of the hide pieces was only about 67%. Although the molecular weight and the proportion of macromolecular components in the hydrolysates decreased when the concentration of H_2SO_4 solution increased to 0.5 mol/L, the solubility of the hide pieces was reached up to about 80%. Herein, the effects of hydrolysis time and temperature on the solubility and molecular weight of the hydrolysates were further investigated by using 0.5 mol/L of H_2SO_4.

Effect of H_2SO_4 hydrolysis temperature

The effects of temperature on the solubility of bovine hide and the molecular weight of collagen hydrolysates were investigated by using 0.5 mol/L of H_2SO_4 for 5 h, as shown in Figure 7 and Table IV.

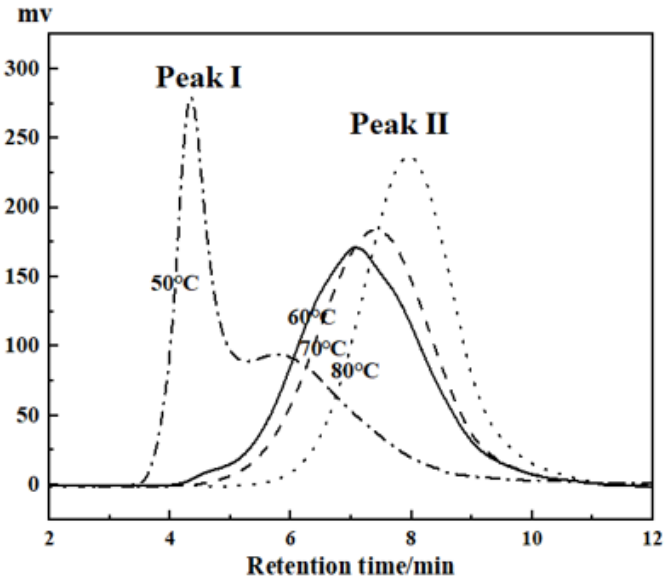

Figure 7. GPC diagrams of collagen hydrolysates by H_2SO_4 hydrolysis with varying temperatures (C_{H2SO4}= 0.5 mol/L, 5 h)

The results in Table IV showed that the solubility of bovine hide increased significantly with the increase of hydrolysis temperature and reached up to 96% when the temperature was 60°C. Further raising temperatures have no obvious effect on the solubility, oppositely, a significant reduction in the Mn of collagen hydrolysates and a considerable increase in the width of molecular weight distribution were presented. For example, the macromolecular component with M_W of about 100 kDa in the collagen hydrolysates was disappeared when the hydrolysis temperature was higher than 60°C, which has been further hydrolyzed into low molecular protein with M_W lower than 12 kDa. Results also showed that the major proportion of the collagen hydrolyzed into polypeptides with M_W less than 5 kDa at 80°C.

The above results indicated that the solubility of bovine hide and the molecular weight of the hydrolysates are inversely proportional to each other within a specific temperature range. For example, the solubility of bovine hide collagen was lower and the molecular weight of the hydrolysates was higher when the hydrolysis temperature was lower than 50°C; Although rising temperature could improve the solubility of collagen substrate, the molecular weight of the hydrolysates was significantly decreased. Furthermore, to overcome these limitations, the effects of H_2SO_4 hydrolysis time on the solubility of bovine hide and the molecular weight of hydrolysates were further investigated.

Effect of H_2SO_4 hydrolysis time

The effect of hydrolysis time on the solubility of bovine hides and the molecular weight of hydrolysate were investigated by using 0.5 mol/L of H_2SO_4 at 50°C, as shown in Figure 8 and Table V. The results in Table V showed that the solubility of bovine hide increased with the extension of hydrolysis time and reached up to about 97% at 7 h and then stabilized. The average molecular weight of both macromolecular and middle molecular components decreased slightly as time prolonged. The M_W of all the macromolecular components was more than 100 kDa, and the molecular weight distribution range was narrow (M_W/Mn value is about 1). The M_W of the middle molecular component was in the range of 20 - 26 kDa. On the other hand, by prolonging the hydrolysis time, it had been witnessed that the proportion of

Table IV

Molecular weight and distribution of collagen hydrolysates by H_2SO_4 hydrolysis with different H_2SO_4 hydrolysis temperatures (C_{H2SO4}=0.5 mol/L, 5 h)

Temperature (°C)	Solubility (%)	Peak	Mn (Da)	Mw (Da)	Mw/Mn	Peak area (%)
50	80.14 ± 3.03	I	96146	108068	1.12	55.41
		II	11451	20430	1.78	44.59
60	94.86 ± 2.39	I	4051	12114	2.99	100
70	93.98 ± 3.25	I	3568	9185	2.57	100
80	96.51 ± 2.34	I	2381	4727	1.99	100

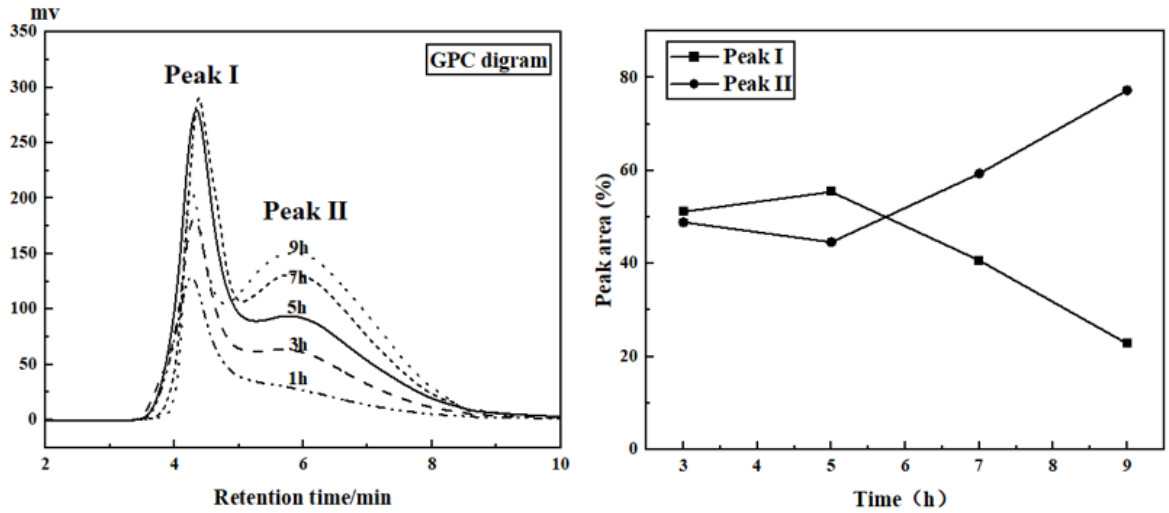

Figure 8. Analysis of GPC of collagen hydrolysates by H_2SO_4 hydrolysis with varying time (C_{H2SO4}= 0.5 mol/L, 50°C)

Table V

Molecular weight and distribution of collagen hydrolysates by H_2SO_4 hydrolysis with varying time (C_{H2SO4}=0.5 mol/L, 50°C)

Time (h)	Peak	Solubility (%)	Mn (Da)	Mw (Da)	Mw/Mn
3	I	49.77 ± 2.18	113586	122930	1.08
	II		14017	24637	1.76
5	I	80.14 ± 3.03	96146	108068	1.12
	II		11451	20430	1.78
7	I	97.12 ± 2.40	98295	105235	1.07
	II		10000	22587	2.26
9	I	96.36 ± 2.73	109947	114427	1.04
	II		10384	25791	2.48

macromolecular components decreased and the proportion of medium molecular components increased.

In the light of the above results, it may be assumed that the molecular weight of collagen hydrolysates prepared by H_2SO_4 hydrolysis method was significantly higher than that of NaOH hydrolysis method. The solubility of bovine hide could reach up to 80% - 97% after hydrolyzing at 50°C with 0.5 mol/L of H_2SO_4 for 5 - 7 h. The hydrolysates mainly had two molecular components, the proportion of macromolecular components with M_W of about 100 kDa was 55% - 41%, and the proportion of medium molecular components with M_W of about 20 kDa was 45% - 59%.

Conclusions

To prepare bovine hide collagen hydrolysates with high molecular weight and solubility, the effects of NaOH and acid treatment conditions on the solubility and molecular weight of collagen hydrolysates were studied. We have comprehensive results which show that NaOH is a suitable option for the preparation of low and medium molecular weight collagen hydrolysates owing to its strong hydrolysis effect. The bovine hide can be easily hydrolyzed into low molecular weight products (< 10 kDa) with 93% of solubility when the reaction conditions were reached or even higher than 0.25 mol/L of NaOH and 50°C. Oppositely, hydrolysates with the molecular weight between 25 - 30 kDa can be produced when the concentration of NaOH is 0.13 mol/L and the reaction temperature is in the range of 60 - 70°C, and the solubility is reached up to 96%. High molecular weight hydrolysates (M_W > 30 kDa) can only be prepared at low NaOH concentration and medium temperature (no more than 0.13 mol/L and 50°C), however, the solubility of the hide pieces was less than 70%.

Significantly, the hydrolysis effects of acid on bovine hide collagen were found to be weaker than that of alkali, and the molecular weight of collagen hydrolysates prepared by H_2SO_4 hydrolysis method was significantly higher than that of NaOH hydrolysis method. At lower acid concentrations, the hydrolysates had two main components: M_W about 100 kDa and 15 - 20 kDa. It is noteworthy to mention that with the increase in treatment intensity, a significant increase

in the hydrolysis degree of collagen was observed along with a considerable reduction in the proportion of macromolecular components. The solubility of bovine hide could reach up to 80% - 97% after hydrolyzing at 50°C with 0.5 mol/L of H_2SO_4 for 5 - 7 h, and the proportion of macromolecular components with M_W of about 100 kDa was 55% - 41%, the proportion of medium molecular components with M_W of about 20 kDa was 45% - 59%.

Acknowledgments

This work was financially supported by the National Natural Science Foundation of China (21908149) and the National Key R&D Program of China (2017YFB0308402).

References

1. https://chooserealleather.com/real-leather/sustainability-video/
2. Masilamani, D., Madhan, B., Shanmugam, G., et al.; Extraction of collagen from raw trimming wastes of tannery: a waste to wealth approach. *J Clean Prod* **113**, 338-344, 2016.
3. Li, G.Y., Fukunaga, S., Takenouchi, K., et al.; Comparative study of the physiological properties of collagen, gelatin and collagen hydrolysate as cosmetic materials. *Int J Cosmet Sci* **27**, 101-106, 2010.
4. Zhang, Z., Li, G.Y., Bi, H.I.; Physicochemical properties of collagen, gelatin and collagen hydrolysate derived from bovine limed split wastes. *JSLTC* **90**, 23-28, 2006.
5. Muthukumar, T., Sreekumar, G., Sastry, T.P.; Collagen as a potential biomaterial in biomedical applications. *Rev Adv Mater Sci* **53**, 29-39, 2018.
6. Xie Z.K., Wang X.G., Yu S.Y., et al.; Antioxidant and functional properties of bovine hide collagen peptides. *J Food Sci* **86**, 1802-1818, 2021.
7. Hashim, P., Ridzwan, M.M.S., Bakar, J., et al.; Collagen in food and beverage industries. *Int Food Res J* **22**, 1-8, 2015.
8. Sionkowska, A., Adamiak, K., Musia, K., et al.; Collagen based materials in cosmetic applications: A review. *Materials* **13**, 4217, 2020.
9. Islam, M.N., Rahman, F., Das, A.K., et al.; An overview of different types and potential of bio-based adhesives used for wood products. *Int J Adhes* **112**, 102992, 2022.
10. Liu, X., Yue, O., Wang, X., et al.; Preparation and application of a novel biomass-based amphoteric retanning agent with the function of reducing free formaldehyde in leather. *J Clean Prod* **265**, 121796, 2020.
11. Sathish, M., Madhan, B., Rao, J.R.; Leather solid waste: An eco-benign raw material for leather chemical preparation–A circular economy example. *Waste Manage* **87**, 357-367, 2019.
12. Wang, X., Chen, K., Li, W., et al.; A paper sizing agent based on leather collagen hydrolysates modified by glycol diglycidyl ether and its compound performance. *Int J Biol Macromol* **124**, 1205-1212, 2019.
13. León-López, A., Morales-Peñaloza, A., Martínez-Juárez, V.M., et al.; Hydrolyzed collagen—Sources and applications. *Molecules* **24**, 4031, 2019.
14. Chai, H.J., Li, J.H., Huang, H.N., et al.; Effects of sizes and conformations of fish-scale collagen peptides on facial skin qualities and transdermal penetration efficiency. *J Biomed Biotechnol* 757301, 2010.
15. Qin, X.Y., Xu, Y., Wei, Y., et al.; Effects of topical application of different molecular weight marine fish skin collagen oligopeptides on UVB-induced photoaging rat skin. *J Cosmet Dermatol* **01**, 1-10, 2021.
16. Calixto, S., Ganzherli, N., Gulyaev, S., et al.; Gelatin as a photosensitive material. *Molecules* **23**, 2064, 2018.
17. Langmaier, F., Mokrejs, P., Kolomaznik, K., et al.; Biodegradable packing materials from hydrolysates of collagen waste proteins. *Waste Manage* **28**, 549 - 556, 2008.
18. Ding, X., Shan, Z., Long, Z., et al.; Utilization of collagen protein extracted from chrome leather scraps as a set retarders in gypsum. *Constr Build Mater* **237**, 117584, 2020.
19. Nagai, T., Suzuki, N.; Preparation and partial characterization of collagen from paper nautilus (*Argonautaargo*, *Linnaeus*) outer skin. *Food Chem* **76**, 149-153, 2002.
20. Nagai, T., Araki, Y., Suzuki, N.; Collagen of the skin of ocellate puffer fish (*Takifugurubripes*). *Food chem* **78**, 173-177, 2002.
21. Wang, J., Pei, X., Liu, H., et al.; Extraction and characterization of acid-soluble and pepsin-soluble collagen from skin of loach (*Misgurnusanguillicaudatus*). *J Biol. Macromol* **106**, 544-550, 2018.
22. Alipal, J., Pu'ad, N.M., Lee, T. C., et al.; A review of gelatin: Properties, sources, process, applications, and commercialization. *Mater Today Proc* **42**, 240-250, 2021.
23. Nurhalimah, E.; Comparison of gelatine extraction process of bovine hide split by acid and base processes. IPB university, 2010.
24. Yang, H., Xue, Y., Liu, J., et al.; Hydrolysis process optimization and functional characterization of yak skin gelatin hydrolysates. *J Chem*, **3**, 1-11, 2019.
25. Talapphet, N., Prommajak, T., Raviyan, P.; Process optimization and properties of crude gelatin extracted from tannery bovine hide. *Food Appl. Biosci J* **5**, 132-148, 2017.
26. Li, G.Y., Fukunaga, S., Takenouchi, K., et al.; Physicochemical properties of collagen isolated from calf limed splits. *JALCA* **98**, 224-229, 2003.
27. Gao, M.C., Zhang, X., Tian, Y.X., et al.; Development and validation of a label-free method for measuring the collagen hydrolytic activity of protease. *Bioproc Biosyst Eng* **44**, 2525-2539, 2021.
28. Zhang, X., Gao, M.C., Chattha, S.A., et al.; Application of acidic protease in the pickling to simplify the pelt bating process. *J Leather Sci Eng* **3**, 27, 2021.
29. Zhang, X., Gao, M.C., Zhang, C.X., et al.; A rapid method for measuring elastin degradation and its application in leather manufacturing. *JALCA* **115**, 294-300, 2020.
30. Zhang, C.X., Lin, J., Jia, X.J., et al.; A salt-free and chromium discharge minimizing tanning technology: the novel cleaner integrated chrome tanning process. *J Clean Prod* **112**, 1055-1063, 2016.
31. Zhang, C.X., Xia, F.M., Long, J.J., et al.; An integrated technology to minimize the pollution of chromium in wet-end process of leather manufacture. *J Clean Prod* **154**, 276-283, 2017.

Superhydrophobic Modification of Collagen Fiber: A Potential Substitute for Tanning

by
Shuangfeng Xu,[1] Ya-nan Wang[1,2] and Bi Shi[1,2]*
[1]*College of Biomass Science and Engineering, Sichuan University,* Chengdu, 610065, China
[2]*National Engineering Laboratory for Clean Technology of Leather Manufacture, Sichuan University,* Chengdu 610065, China

Abstract

Tanning is considered to be the crosslinking reaction between collagen fibers and tanning agents, and a majority of tanning reactions result in suppressed water absorption and enhanced hydrophobicity of leather. However, extensive use of tanning agents may bring a burden to the environment. Herein, to facilitate a sustainable leather manufacturing industry, we propose a revolutionary strategy of "tanning" without tanning agents. Based on this strategy, superhydrophobic collagen fibers (FAS-CFs) were fabricated through dehydration, followed by superhydrophobic modification. Dehydration aimed to eliminate the "sticky" effect of water on collagen fiber to obtain a dispersed hierarchical structure. Superhydrophobic modification not only dispersed and stabilized the fiber structures, but also protected the fiber dispersity from water immersion. Compared with chrome-tanned collagen fibers (Cr-CFs) and glutaraldehyde-tanned collagen fibers (G-CFs), FAS-CFs showed higher hydrophobicity, lower water absorption, and superior mechanical properties. Meanwhile, FAS-CFs exhibited a high thermal denaturation temperature of 92.5°C and retained their original shape after being heated to 100°C. Therefore, our proposed strategy is expected to be a potential substitute for conventional tanning and might contribute to cleaner and sustainable leather manufacturing.

Introduction

For hundreds of years raw hides and skins have been converted into leather through physical and chemical processes[1]and tanning is an indispensable step in the conversion. Tanning agents demonstrate their tanning ability by forming intramolecular and intermolecular multi-point cross-links among the collagen fiber networks.[2-4] The effect of the cross-linking of most tanning agents on raw hides is manifested in the increase of hydrothermal stability, and the decrease of swelling capacity and water absorption.[5,6] Specifically, different types of tanning agents, such as glutaraldehyde and chromium salts, accurately capture amino groups and carboxyl groups on rawhide, respectively, to form new cross-linked bonds, and block the original hydrophilic sites of collagen, thereby reducing the water take-up and swelling capacity of leather. Contrary to this general trend, vegetable tanning enhances both the hydrophilicity and water absorption of leather due to the richness of hydrophilic phenolic hydroxyls of vegetable tannins. Vegetable tannins can generate cross-links among collagen fibers through multi-point hydrogen bond to increase the thermal stability of leather. Compared with chrome-tanned leather, the leather tanned by vegetable tannins has lower shrinkage temperature (75-85°C) with tighter character. This may relate to the fact that chrome tanning reduces the water absorption of leather and therefore remarkably improves the dispersity of collagen fibers.[7]

Water plays a crucial role in the geometrical and thermal properties of collagen fibers, since it is abundantly presented among the collagen fibers of the rawhide by forming stable hydrogen bonds with hydrophilic groups involving carboxyl, amino, and hydroxyl groups.[5,8] During the drying process of raw hides, the evaporation of water with high surface tension brings about fiber entanglement, cohesion, and compaction, severely ruining the dispersed structure of the collagen fiber. Other than fiber dispersity, the thermal stability of collagen is also closely related to water. The thermal stability temperature of anhydrous untanned collagen is high up to 200°C, whereas the fully water-filled collagen is only thermally stable at temperatures lower than 60°C[6]. Olle et al. developed a dehydration process for bovine/ovine hide with acetone to relieve the interference of water, and the dehydrated hides showed a porous fiber network and satisfactory organoleptic properties, similar to tanned leather.[9,10] Although the dehydrated hides are leather-like, in essence, they are not leathers because they are not waterproof.[6] Collagen fibers of the dehydrated hide will swell and recover to an adhesive state after water-absorbing, and the leather-like effect vanishes.

The most tanning methods, such as chrome tanning and aldehyde tanning, can weaken the hydration of collagen fibers and improve the thermal stability and mechanical properties of the leather. But the relation between these tanning methods and the surface wettability of leathers has seldom been investigated. We found that chrome-tanned leather with significant hydrophobicity presented superior thermal stability and mechanical properties compared with those of aldehyde-tanned leather and vegetable-tanned leather, leaving us contemplating the contribution of surficial wettability in leather properties. He et al.[11] reported that the hydrophobicity of chrome-tanned leather increased with the increase in chrome dosage, which may be attributed to the displacement of bound water by Cr (III) ions.[12] Zhu et al.[13] reported that the water contact angle (WCA)

*Corresponding author email: shibi@scu.edu.cn
Manuscript received February 12,2022, accepted for publication April 12, 2022.

of leather tanned with 2% chrome tanning agent was 108.1°. The outstanding comprehensive properties of chrome-tanned leather may stem from the excellent ability of Cr (III) to weaken hydration and improve hydrophobicity. To date, chrome tanning still occupies the predominant position in tanning technology due to the superior comprehensive properties of chrome-tanned leather.[14,15] However, potential chrome pollution restricts the sustainable development of the leather industry.[16] Hence, it is of significance and urgency to propose a novel and sustainable process for leather tanning.

Based on the aforementioned analyses, we proposed a novel strategy for leather manufacturing without the use of conventional tanning agents. From the perspective of water removal and hydrophobicity construction, the 'tanning agent-free strategy' was designed to manufacture leather by eliminating hydration and stabilizing fiber dispersity. Focusing on the two characteristics, "tanning" is supposed to be replaced by dehydration followed by superhydrophobic modification of a pelt. In this study, collagen fibers were used as the model of pelt to explore the feasibility of this strategy so as to prevent the influence of penetration of hydrophobic material in pelt hide on this theoretical exploration. Ethanol was used to remove the water among collagen fibers to gain hierarchical structures. Superhydrophobic modification further strengthened the dispersibility and stability of the fiber and protected the porous and dispersed hierarchical structure from water interference. The hydrophobic properties, fiber dispersity, thermal stability, and mechanical properties of the superhydrophobic collagen fiber were evaluated, and conventional tanned collagen fibers were used for comparison.

Experimental

Materials

Pickled pelt of cow hide was provided by a local tannery in China. 1H, 1H, 2H, 2H-perfluorodecyltriethoxysilane (FAS, 96 wt%) was purchased from Aladdin Co., Ltd. (Shanghai, China). Ethanol (95 wt%), isopropanol (99.7 wt%), glutaraldehyde (50 wt%), $Cr_2(SO_4)_3{\cdot}6H_2O$, $NaHCO_3$, HCOOH, and all of the other chemicals were purchased from Kelong Co., Ltd. (Chengdu, China).

Fabrication of collagen fibers (CFs)

The pickled cow hide pelt was deacidified and fully washed. Then, a piece of pelt was soaked into 150 wt% ethanol and stirred for 120 min. This operation was repeated for sixfold to remove water. The dehydrated pelt was dried at 35°C and crushed and sieved with a super centrifugal grinder (Retsch, zm200) to obtain collagen fibers (CFs) of 40 mesh.

Fabrication of superhydrophobic collagen fibers (FAS-CFs)

FAS-CFs were prepared by immersing 5 g of CFs into 50 mL of FAS/isopropanol solution (1:100, 3:100, 5:100, 7:100, w/v) for 24 h, followed by filtering, heating at 105°C for 4 h, ethanol washing, and drying at 105°C for 2 h.

Fabrication of Cr (III) cross-linked collagen fibers (Cr-CFs)

Five grams of CFs were immersed in 50 mL deionized water for 12 h. Subsequently, 50 mL of chromium sulfate solution (containing 0.5 g of Cr_2O_3) was added, and the pH was adjusted to 3.0 with 10 wt% formic acid. The solution was stirred at 25°C for 4 h. Then, the crosslinking system was stirred for 14 h at 40°C and stopped for 4 h at 25°C after basification to pH 4.0 with 10 wt% $NaHCO_3$ solution. The cross-linked CFs were washed with deionized water for three times, and dried at 50°C for 12 h to obtain Cr-CFs.

Fabrication of glutaraldehyde cross-linked collagen fibers (G-CFs)

Five grams of CFs were soaked into 0.4 wt% glutaraldehyde solution. The crosslinking reaction was first carried out at 25°C for 4 h and heated to 35°C for 4 h after the pH was adjusted to 7.0 with 10 wt% $NaHCO_3$ solution. The products were washed with deionized water for three times, and dried at 50°C for 12 h to obtain G-CFs.

Characterization of CFs and FAS-CFs

The surface structures of CFs and FAS-CFs were detected by using a field-emission scanning electron microscope (FESEM, Nova Nano SEM 450, FEI, USA) with an acceleration voltage of 15 kV. The element composition of FAS-CFs was obtained with a coupled energy dispersive X-ray spectrometer (EDS, Ultim Max, Oxford Instruments, U.K.). Fourier transform infrared spectrometer (FT-IR, NICOLET iS10, Thermo Fisher Scientific, USA) was used to confirm the functional groups of CFs and FAS-CFs. X-ray photoelectron spectroscopy (XPS, Thermo Scientific, Escalab250Xi, USA) was used to further identify the chemical composition of CFs and FAS-CFs.

Measurements of surface wettability of CFs, G-CFs, Cr-CFs, and FAS-CFs

Surface wettability of CFs, G-CFs, Cr-CFs, and FAS-CFs was measured by a contact angle goniometer (Krüss, DSA30, Germany) with a deionized water droplet of 5μL under ambient condition. The fiber samples (0.1 g) were glued on the glass slide with a double-sided adhesive, and then the fiber samples were compacted by a weight of 100 g to ensure that the fibers were evenly distributed on the surface of the glass slide to facilitate the observation of WCA. The WCA result was the average of data from five different points on each sample surface. Besides, the distribution of water droplets on the surface of FAS-CFs was also observed under the Super Depth of Field 3D Microscope System (VHX-5000, KEYENCE, Japan).

Measurements of hydrophobic durability of FAS-CFs

One group of FAS-CFs were immersed in water for 24 h and then dried at 50°C. One group of FAS-CFs were immersed in water for 24 h without drying. One group of FAS-CFs were irradiated by UV light for 6, 12, 24 and 48 h. One group of FAS-CFs were immersed in the water with different pH values (2, 4, 6, 8, 10, 12) for 12 h and then dried at 50°C. The other two groups were immersed in ethanol and isopropanol for 1, 6, 12 and 24 h, respectively. Then WCA measurements were carried out as described above.

Measurements of water absorption of CFs, G-CFs, Cr-CFs, and FAS-CFs

Two grams of CFs, G-CFs, Cr-CFs, and FAS-CFs were immersed in 20 mL of deionized water for 24 h, separately. The water absorption rate of the samples was calculated by determining the mass change before and after the water immersion. Measurements were conducted in triplicate. In addition, the samples after water immersion were dried at 50°C for 5 h, and their microstructures were observed by FESEM under 15 kV accelerating voltage.

Measurements of the thermal stability

CFs, G-CFs, Cr-CFs, and FAS-CFs were first kept under 65% RH for 48 h at 30°C. Then, the thermal stability of which was determined using a differential scanning calorimetry (DSC, PerkinElmer, DSC8000, USA) from 30°C to 200°C with a heating rate of 5°C/min under nitrogen atmosphere. In addition, shrinkage behaviors of CFs, G-CFs, Cr-CFs, and FAS-CFs were measured. A single fiber bundle with a length of 2.5–3.5 mm was placed in the recess of a single-concave slide, covered with a cover glass, and heated from 20°C to 200°C with a heating rate of 1°C/min on a benchtop temperature controller (Shanghai Weitu Instrument Technology Development Co., Ltd.). The changes in fiber morphology and length were monitored and recorded by a stereomicroscope (Leica, M205 C, Germany) with a frequency of 10°C interval.

Measurements of the mechanical properties

The length and diameter of single fiber bundles (CFs, G-CFs, Cr-CFs, and FAS-CFs) were recorded with a stereomicroscope to calculate the mechanical properties. Then, two ends of the single fiber bundle were attached to a piece of paper by epoxy resin. The tensile strength of the single fiber bundle was determined with an electronic single fiber strength tester (Model LLY-06B, Laizhou Electronic Instrument Co., Ltd., Laizhou, China, 0.02% of sensitivity) in accordance with the standard method (GB/T 14337). The test was carried out at 25°C and 65% RH with 21 replicate measurements for each sample. The clamping gap was set to 30 mm, and the stretching speed was 5 mm/min.

Results and Discussion

"Tanning agent-free strategy" for leather manufacturing

Collagen fibers are hydrophilic in nature, and water can bind with functional groups on the polypeptide chains through hydrogen bonds and even form hydrogen-bond networks (Figure 1, left panel). However, the swelling behavior of CFs disappeared after ethanol dehydration, and they presented the porous and dispersed structures (Figure 1, middle panel) after drying, laying the foundation for superhydrophobic modification. Superhydrophobic modification aimed at manufacturing leather without tanning agents through eliminating water absorption, stabilizing, and protecting the hierarchical structure of collagen fibers. FAS with low surface energy was supposed to be hydrolyzed by the remaining moisture of CFs to form free silanol groups (–SiOH)[17]and covalently bonds with hydroxyl groups on CFs under heating,[18,19] depleting the remained water and blocking the hydrophilic sites. The low surface energy fluorine-containing long chain at the other end could endow FAS-CFs with superhydrophobicity to resist water infiltration (Figure 1, right panel).

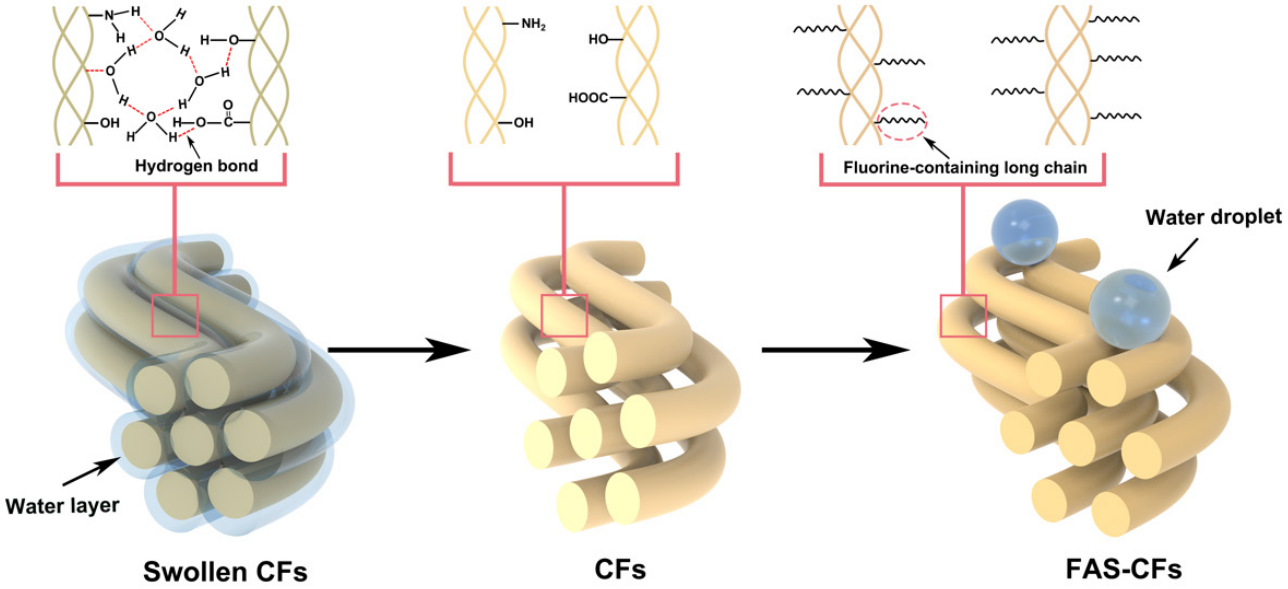

Figure 1. Schematic illustration of the fabrication of FAS-CFs

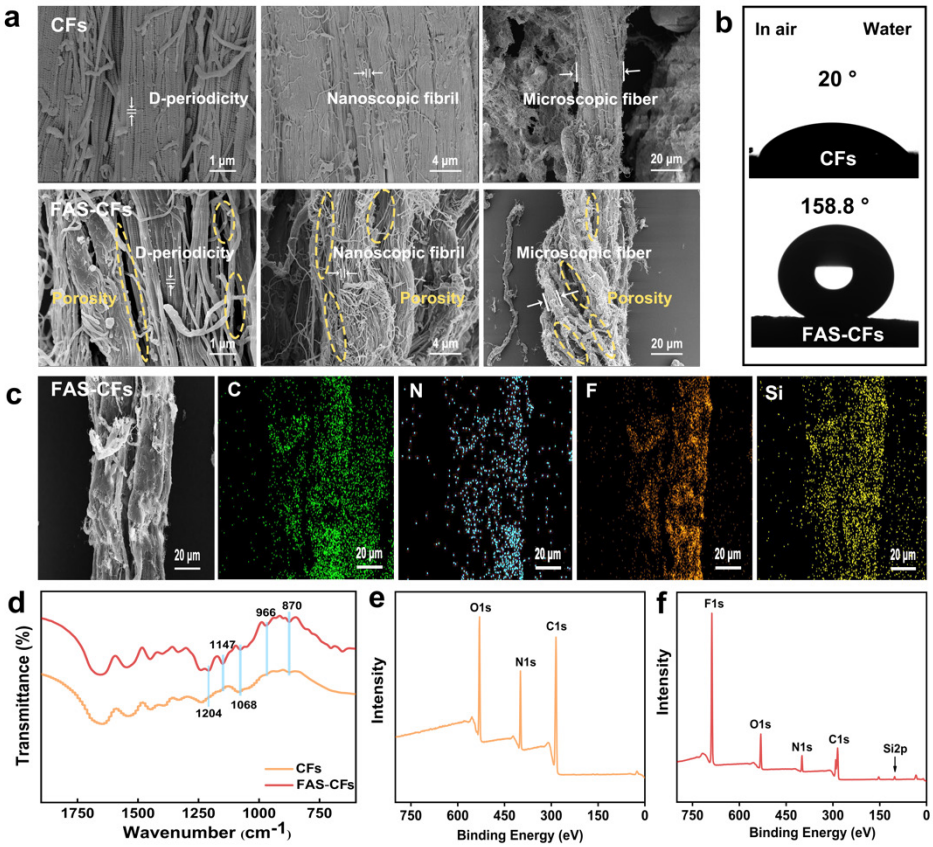

Figure 2. SEM images of CFs and FAS-CFs **(a)**, WCA of CFs and FAS-CFs in the air **(b)**, EDS mapping of FAS-CFs **(c)**, FT-IR spectra of CFs and FAS-CFs **(d)**, and XPS survey of CFs **(e)** and FAS-CFs **(f)**.

Characterization of CFs and FAS-CFs

After ethanol dehydration for six times, CFs with a water content of 3.86% maintained a hierarchical fibrous structure from nanofiber to microfiber and intertwined fiber bundles[20] (Figure 2a). The nanofibrils that are composed of parallel and staggered type I collagen molecules showed a distinct axial D-periodicity of approximate 67 nm.[21] The hierarchically self-assembled micro/nanostructure of CFs contributes to supplying natural and essential roughness for superhydrophobic modification.[22] After treatment by FAS, the hierarchical fibrous structures (Figure 2a) of FAS-CFs remained intact, including D-periodicity, nanofiber, microfiber, and fiber bundles. Significantly different from the CFs, more prominent porosity with different sizes appeared among nanofibers, microfibers, and fiber bundles, indicating that superhydrophobic modification facilitates fiber dispersity. From the water contact angle measurement result (Figure 2b), the instantaneous WCA of CFs surface was approximate 20°, indicating hydrophilicity of CFs. FAS-CFs was functionalized as superhydrophobic material because its WCA reached up to 158.8°.[23,24] To prove that CFs were successfully modified by FAS, EDS and FT-IR analyses of FAS-CFs were then performed to give evidence. As shown in Figure 2c, F and Si are evenly distributed on the fiber surfaces of FAS-CFs and display the same trend as those of C and N, proving the successful loading of FAS. Compared with the XPS spectrum of CFs (Figure 2e), F and Si peaks appear in the full spectrum of FAS-CFs,[24,25] and the F peak is significantly higher than the C, N, and O peaks (Figure 2f), indicating that FAS has formed a dense low-surficial-energy film on the surface of fibers, which could resist the water association with collagen fibers. The FT-IR spectra of FAS-CFs and CFs were illustrated in Figure 2d. As compared to CFs, FAS-CFs exhibits new peaks at 870, 966, and 1068 cm^{-1}, which could be assigned to the stretching vibrations of Si–C, Si–O–Si, and Si–O–C,[26,27] respectively. This result suggested that the silanol groups have reacted with the hydroxyl groups on CFs and converted into Si–O–C covalent bonds. The peaks at 1204 and 1147 $cm^{-1}$are ascribed to the stretching vibration of C–F,[24,28] which belongs to FAS. The above-mentioned results indicated that CFs are successfully chemically modified by FAS, and the superhydrophobic modification contributes to excellent fiber dispersity.

Effect of fluorine content on hydrophobicity of FAS-CFs

Figure 3a shows that the WCAs of FAS-CFs increased from 142.4° to 154.7° with the increase of FAS content from 1% to 7%, indicating enhanced hydrophobicity. The water absorption of FAS-CFs sharply decreased from 219% to 75.7% (Figure 3b), suggesting that increasing hydrophobicity resulted in significant reduction in water absorption. To further explore the hydrophobicity of FAS-CFs, the distribution of water droplets on the surface of FAS-CFs was also observed. The water droplets distributed on the fiber surface changed from a flat shape to a more pronounced spherical shape as the FAS content

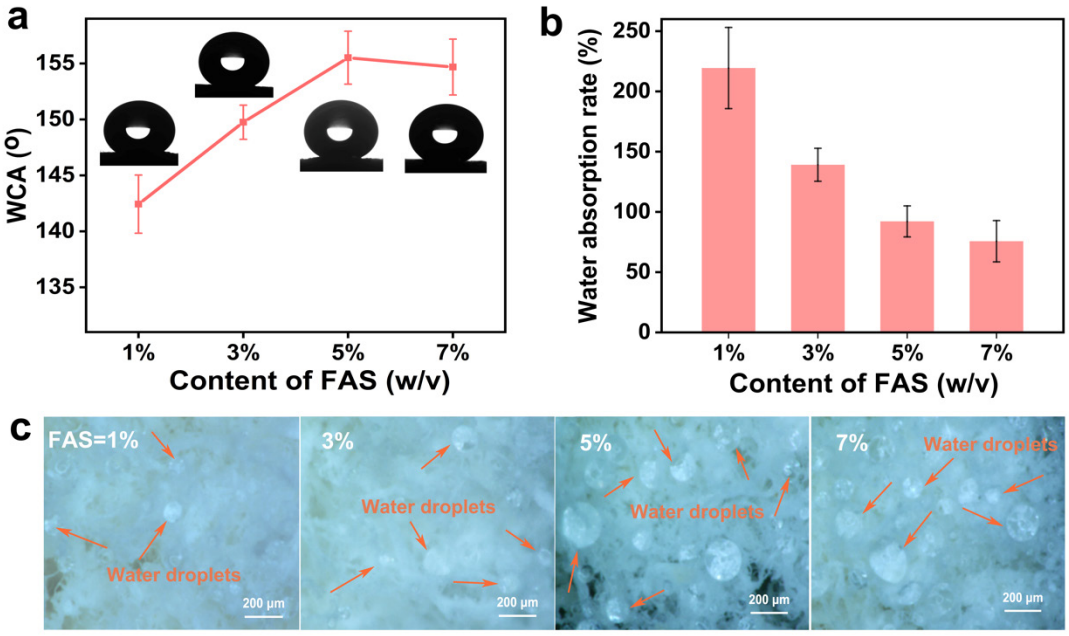

Figure 3. The influence of FAS content on WCA **(a)** and water absorption rate **(b)** of FAS-CFs

increased (Figure 3c). All the results above demonstrated that the increase in FAS content led to the enhancement of hydrophobicity. However, when FAS content was higher than 5%, the hydrophobicity of FAS-CFs was no longer enhanced greatly. In general, FAS-CFs fabricated by 5% of FAS exhibited outstanding superhydrophobicity (WCA >150°) and low water absorption.

Hydrophobic durability of FAS-CFs

Based on the results above, FAS-CFs fabricated with 5% FAS were selected for further investigation. The hydrophobic durability of FAS-CFs after treatment in different environments was investigated. WCAs of FAS-CFs showed a slight decrease to 150.1° under UV irradiation for 48 h (Figure 4a). As shown in Figure 4b, FAS-CFs still maintained outstanding superhydrophobic properties after immersion in the water with a wide pH range from 4 to 12 (Figure 4b). When FAS-CFs were soaked into ethanol and isopropanol for 24 h, the value of WCA decreased but still remained higher than 145° (Figure 4c and 4d). The above-mentioned results suggested that the hydrophobicity was stable enough to protect FAS-CFs against harsh environments.

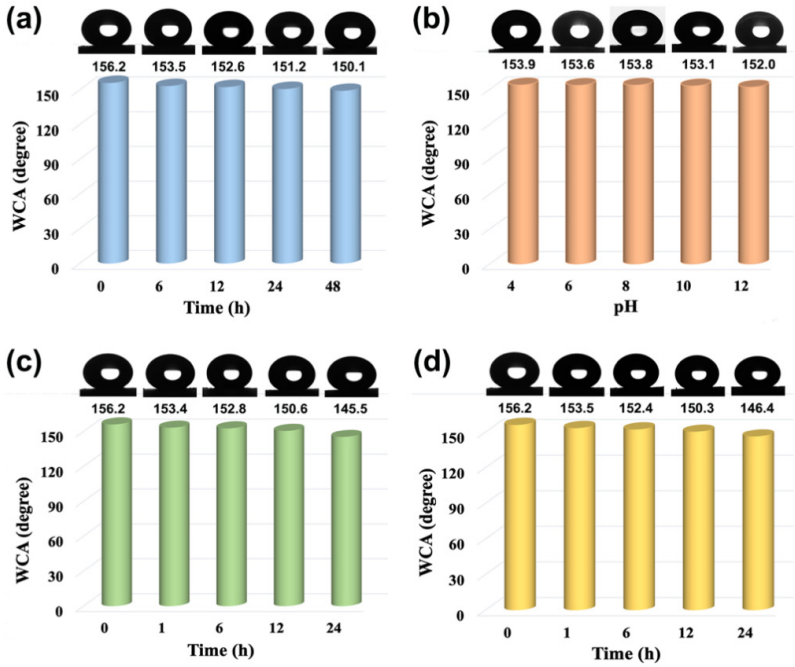

Figure 4. WCAs of FAS-CFs after treatment in different environments: **(a)** after irradiation by UV light, **(b)** after immersion in water with different pH values for 12 h, **(c)** after immersion in ethanol, **(d)** after immersion in isopropanol.

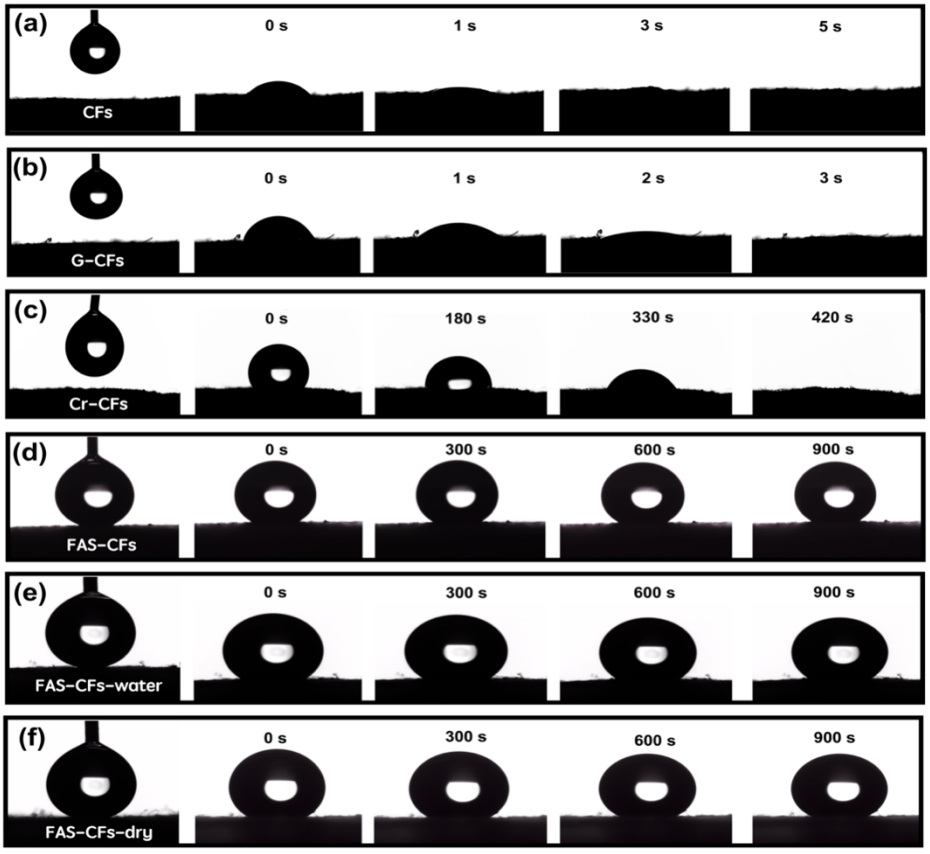

Figure 5. Shapes of a water droplet (5μL) on CFs **(a)**, G-CFs **(b)**, Cr-CFs **(c)**, FAS-CFs **(d)**, FAS-CFs after water immersion for 24 h **(e)**, and FAS-CFs after water immersion for 24 h and then dryingat 50°C for 5 h **(f)** at different testing moments.

Hydrophobicity of CFs, G-CFs, Cr-CFs, and FAS-CFs

The surface wettability of water on CFs, G-CFs, Cr-CFs, and FAS-CFs was evaluated by recording WCAs at different testing moments. As shown in Figure 5a–b, the water droplet rapidly spread out on the surface of CFs and G-CFs within 5 s and 3 s, respectively, revealing their hydrophilicity and poor water resistance. CFs exhibited poor hydrophobicity due to the fact that it contains a lot of hydrophilic groups. For G-CFs, glutaraldehyde only reacted with amino groups of CFs, and a lot of hydroxyl and carboxyl groups still remained. Therefore, G-CFs maintained hydrophilicity to some extent. Compared with CFs and G-CFs, Cr-CFs showed better hydrophobicity. It took 420 s for water droplets to penetrate into Cr-CFs (Figure 5c), which was consistent with the results stated in the previous report.[13] The hydrophobicity of chrome-tanned leather should be attributed to the strong coordination reaction of Cr (III) with carboxyl groups while having reactivity with amino and hydroxyl groups, which effectively reduced the number of hydrophilic functional groups. Unsurprisingly, WCA on the surface of FAS-CFs could be stabilized at around 155° for at least 900 s (Figure 5d). After immersion in water for 24 h, FAS-CFs still showed satisfactory hydrophobicity with the WCA of 149° within 900 s (Figure 5e). The WCA restored to 154° (Figure 5f) after the water immersed FAS-CFs were dried again. In addition, the water absorption rates of FAS-CFs and Cr-CFs were lower than that of CFs and G-CFs. Among them, the superhydrophobic FAS-CFs exhibited the lowest water absorption rate (92%) (Figure 6). These results suggested higher superhydrophobicity of FAS-CFs compared to CFs, G-CFs and Cr-CFs.

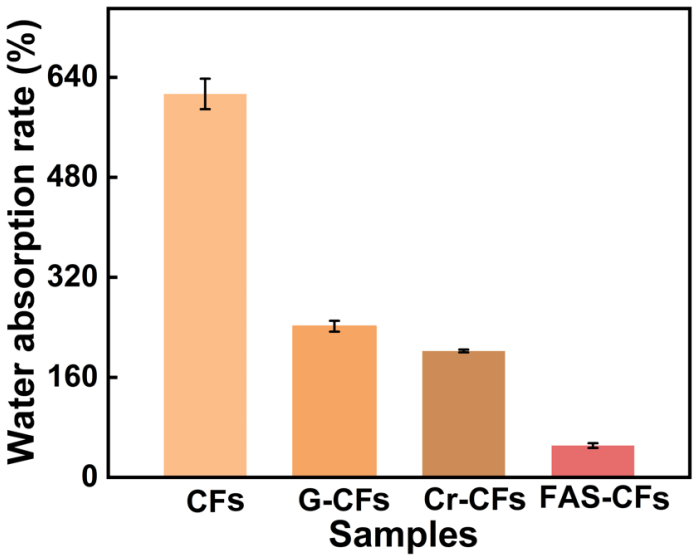

Figure 6. Water absorption rate of CFs, G-CFs, Cr-CFs, and FAS-CFs

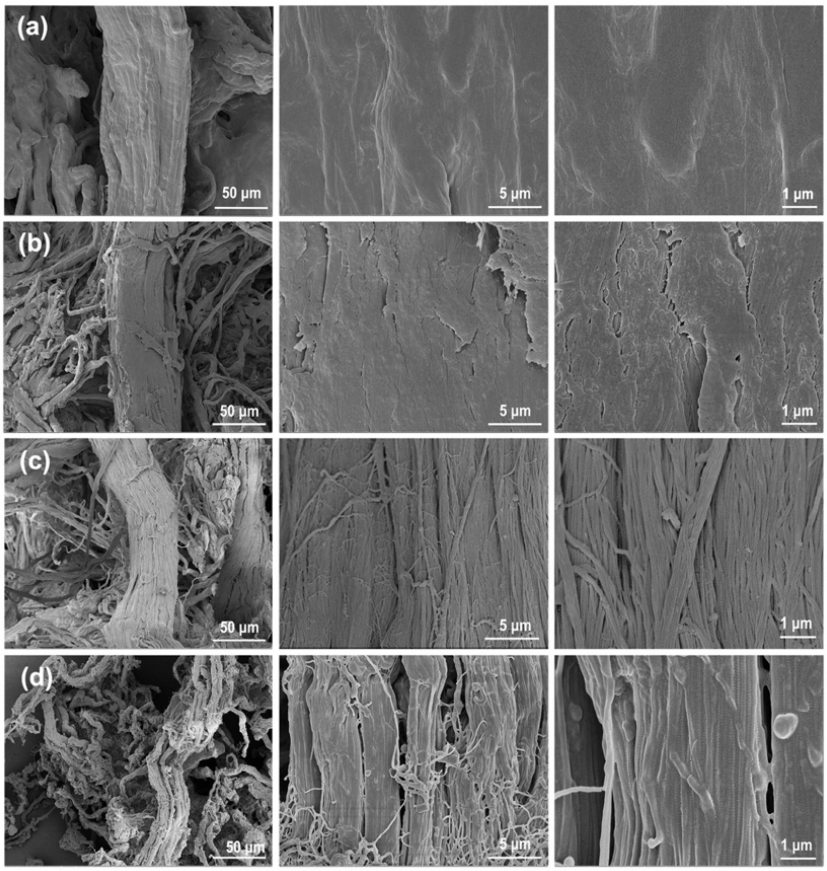

Figure 7. The SEM images of CFs **(a)**, G-CFs **(b)**, Cr-CFs **(c)**, and FAS-CFs **(d)** after soaking in water for 24 h and then drying.

Afterward, the morphology of CFs, G-CFs, Cr-CFs, and FAS-CFs following water immersion and drying was analyzed to evaluate the durability of fiber dispersion. After soaking in water for 24 h and then drying, the initially dispersed multilayer structures of CFs and G-CFs were completely eliminated. During the drying process, the evaporation of water with high surface tension brought about the cohesion of collagen fibers, resulting in fiber entanglement and a smooth surface without hierarchical structures. Specifically, the D-period on the fibrils vanished, and nanofibers and microfibers cohered into a flat and smooth plane (Figure 7a and b). The destruction of the dispersed structures of CFs and G-CFs after water immersion may be attributed to their poor hydrophobicity. On the contrary, the porous and dispersed hierarchical structure of FAS-CFs was fully retained after water immersion and drying (Figure 7d), which is similar to Cr-CFs (Figure 7c). These phenomena confirmed that superhydrophobic modification can effectively stabilize and protect the fiber dispersibility of FAS-CFs. The significant difference in the morphology of FAS-CFs was closely related to its low surface energy. The covalent bonding of FAS with collagen fibers reduced the interfacial energy of FAS-CFs, resulting in a decreased surface affinity with water, so that the hierarchical fibrous structure of FAS-CFs remained intact. In a word, superhydrophobic modification of collagen fibers brings about nearly the same effect as conventional tanning in terms of weakening the hydration of collagen fibers and improving fiber dispersity. The performance of superhydrophobic modification is superior to glutaraldehyde tanning and comparable to chrome tanning.

Thermal stability and mechanical properties of CFs, G-CFs, Cr-CFs, and FAS-CFs

The thermal stability and mechanical properties of FAS-CFs were investigated in comparison with conventional tanned collagen fibers (G-CFs, Cr-CFs). As shown in DSC plots (Figure 8a), the onset and peak denaturation temperatures of FAS-CFs were remarkably higher than those of CFs and G-CFs and only slightly lower than Cr-CFs. Compared with CFs and G-CFs, the endothermic peak area of FAS-CFs was enlarged, suggesting that the enthalpy change of FAS-CFs denaturation increased. To further evaluate the heat resistance of FAS-CFs, their shrinkage behaviors were investigated. Specifically, a stereomicroscope was used to capture the changes in the length of fiber with increasing temperature (Figure 8b). The length of FAS-CFs remained unchanged at 100°C, while CFs, G-CFs, and Cr-CFs showed a slight shrinkage to 98.3%–99.1%. In Figure 8c–f, a significant plateau was found in the initial stage of the shrinkage curve of FAS-CFs, which was much broader than those of CFs, G-CFs, and Cr-CFs, indicating the outstanding thermal stability

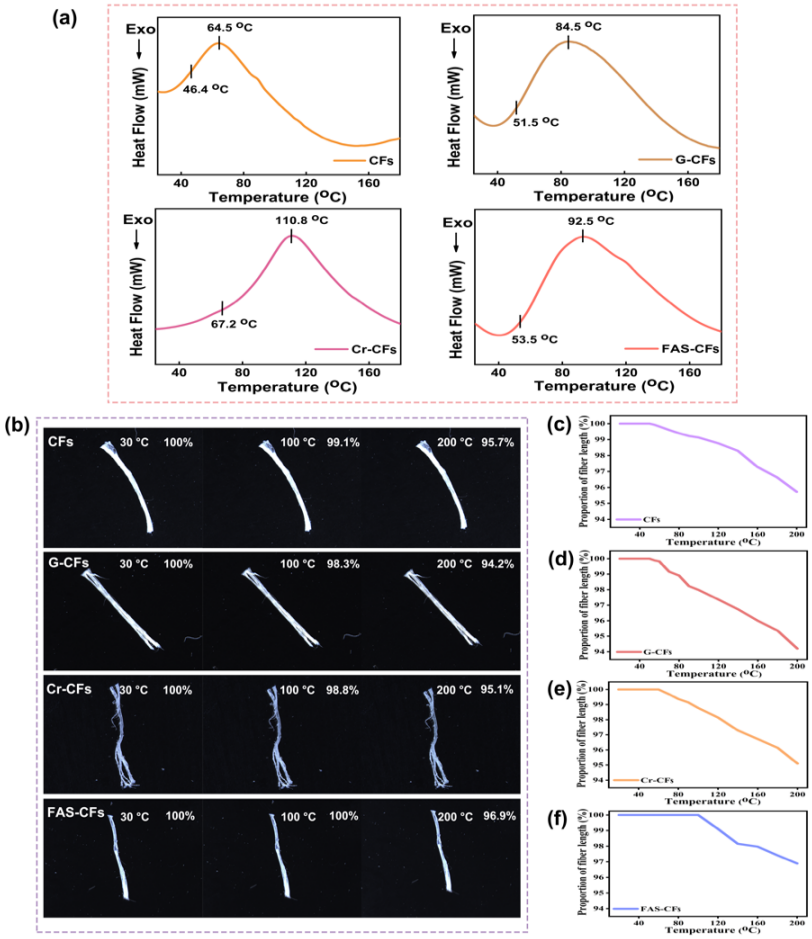

Figure 8. DSC curves of CFs, G-CFs, Cr-CFs, and FAS-CFs (**a**), stereomicrographs showing the shrinkage of CFs, G-CFs, Cr-CFs, and FAS-CFs (**b**) with rising temperature, shrinkage curve of CFs (**c**), G-CFs (**d**), Cr-CFs (**e**), and FAS-CFs (**f**) with rising temperature.

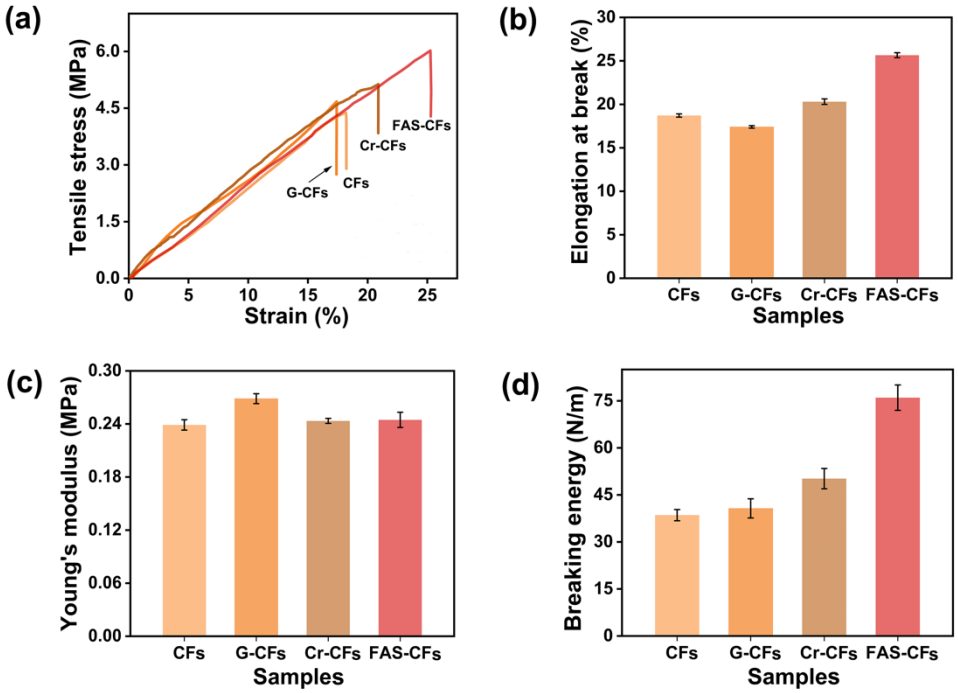

Figure 9. Stress-strain curves (**a**), elongation at break (**b**), Young's modulus (**c**), and breaking energy (**d**) of different collagen fibers.

of FAS-CFs. FAS was covalently bonded with the hydroxyl groups on the surface of CFs. The introduction of Si–O bonds with high cracking energy and C–F bonds with stable bond energy effectively protected the structural stability of FAS-CFs, thereby improving the thermal stability of FAS-CFs. In comparison, FAS-CFs possessed better heat resistance than conventional tanned collagen fibers, such as G-CFs and Cr-CFs.

Among four tested samples, CFs demonstrated the poorest flexibility because of their low tensile strength (Figure 9a) and breaking energy (Figure 9d). After conventional tanning, the tensile strength and breaking energy of G-CFs and Cr-CFs were improved. However, the higher Young's modulus (Figure 9c) and lower elongation at break (Figure 9b) of G-CFs showed that G-CFs were more fragile than Cr-CFs. In comparison, the tensile strength (Figure 9a), elongation at break (Figure 9b), and breaking energy (Figure 9d) of FAS-CFs were significantly higher than those of CFs, G-CFs, and Cr-CFs. Besides, Young's modulus of FAS-CFs was almost equivalent to that of Cr-CFs and CFs (Figure 9c). The above results indicated that FAS-CFs exhibited better strength flexibility than conventional tanned collagen fibers. The satisfactory mechanical properties of FAS-CFs may be attributed to the reduced hydration of collagen fibers and improved fiber dispersity brought by the superhydrophobic modification.[29, 30] In addition, the increased strength was likely due to the lubricating effect of the long hydrophobic chain of FAS, so that FAS-CFs can slide and reorient to adapt to the strain.[31] In short, FAS-CFs performed better mechanical properties than G-CFs and Cr-CFs, suggesting the feasibility of the established strategy based on dehydration followed by superhydrophobic modification without tanning.

Conclusions

We developed a "tanning agent-free" strategy for leather manufacturing. The core of this novel strategy aimed to manufacture leather by eliminating hydration and stabilizing fiber dispersity via dehydration and superhydrophobic modification. Superhydrophobic modification inhibited water infiltration and absorption and promoted porous and dispersed fibrous structures. The modified collagen fibers, FAS-CFs, showed durable water resistance against harsh environments, such as UV irradiation, immersion in water with a wide pH range, and soaking in organic solvents. FAS-CFs exhibited a high thermal denaturation temperature and a lower shrinkage change within 200°C compared to Cr-CFs. Besides, the mechanical properties of FAS-CFs far exceeded those of G-CFs and Cr-CFs. This "tanning agent-free" strategy is expected to be an alternative to conventional tanning and open up a new theory for greener and sustainable leather manufacturing.

In this research, perfluorodecyltriethoxysilane was chosen as hydrophobic agent for CFs modification since it can conveniently endow CFs with excellent hydrophobicity. But perfluorinated compounds may be toxic. Therefore, in consideration of practical application, we should screen environmentally friendly materials, such as organosilicon compounds, as hydrophobic modifier. This work is undertaking in our laboratory.

Acknowledgement

This work is financially supported by the National Natural Science Foundation of China (No.21978176).

References

1. Jia, L., Zeng, S., Ding, H., Smith, A. T., Lachance, A. M., et al.; Leather-based multi-stimuli responsive chromisms. *Adv. Funct. Mater.*, **31**, 2104427, 2021.
2. Hu, Y., Liu, L., Gu, Z., Dan, W., Dan, N., et al.; Modification of collagen with a natural derived cross-linker, alginate dialdehyde. *Carbohydr. Polym.*, **102**, 324-332, 2014.
3. Kanth, S. V., Rao, J. R. and Nair, B. U.; Tanning with natural polymeric materials. Part II: Efficiency of dialdehyde sodium alginate as a bi-functional cross-linking agent. *J. Soc. Leather Technol. Chem.,* **92**, 65-70, 2008.
4. Ding, W., Zhou, J., Zeng, Y., Wang, Y. N. and Shi, B.; Preparation of oxidized sodium alginate with different molecular weights and its application for crosslinking collagen fiber. *Carbohydr. Polym.*, **157**, 1650-1656, 2017.
5. Molinier, C. E, Happillon, T., Bouland, N., et al.; Investigating the relationship between changes in collagen fiber orientation during skin aging and collagen/water interactions by polarized-FTIR microimaging. *Analyst*, **140**, 6260-6268, 2015.
6. Reich, G., Taeger, T.;From collagen to leather-the theoretical background.*World Leather*, **20**, 40, 2008.
7. He, X., Wang, Y. N., Zhou, J., Wang, H., Ding, W., et al.; Suitability of Pore Measurement Methods for Characterizing the Hierarchical Pore Structure of Leather. *JALCA,* **114**, 41-47, 2019.
8. Covington, T.; Tanning Chemistry - The Science of Leather. 2009.
9. Olle, L., Sorolla, S., Casas, C. and Bacardit, A.; Developing of a dehydration process for bovine leather to obtain a new collagenous material. *J. Clean. Prod.,* **51**, 177-183, 2013.
10. Olle, L., Sorolla, S., Casas, C. and Bacardit, A.; Design of a prototype to produce a new collagen material by dehydration. *J. Soc. Leather Technol. Chem.,* **97**, 244-250, 2013.
11. He, L., Cai, S., Wu, B., Mu, C., Zhang, G., et al.; Trivalent chromium and aluminum affect the thermostability and conformation of collagen very differently. *J. Inorg. Biochem.*, **117**, 124-130, 2012.
12. Rose, G. D., Wolfenden, R.; Hydrogen Bonding, Hydrophobicity, Packing, and Protein Folding. *Annu. Rev. Biophys. Biomol. Struct.*, **22**, 381-415, 1993.
13. Zhu, R., Yang, C., Li, K., Yu, R., Liu, G., et al.; A smart high chrome exhaustion and chrome-less tanning system based on chromium (III)-loaded nanoparticles for cleaner leather processing. *J. Clean. Prod.,* **277**, 123278, 2020.

14. Zhang, X., Xu, S., Shen, L. and Li, G.; Factors affecting thermal stability of collagen from the aspects of extraction, processing and modification. *J. Leather Sci. Eng.*, **2**, 19, 2020.
15. Zhang, Y., Buchanan, J. K., Holmes, G., Mansel, B. W. and Prabakar, S.; Collagen. structure changes during chrome tanning in propylene carbonate. *J. Leather Sci. Eng.*, **1**, 2019.
16. Krishnamoorthy, G., Sadulla, S., Sehgal, P. K. and Mandal, A. B.; Greener approach to leather tanning process: d-Lysine aldehyde as novel tanning agent for chrome-free tanning. *J. Clean. Prod.*,**42**, 277-286, 2013.
17. Xue, L., Tabil, L. G. and Panigrahi, S.; Chemical Treatments of Natural Fiber for Use in Natural Fiber-Reinforced Composites: A Review. *J. Polym. Environ.,* **15**, 25-33, 2007.
18. Lung, C. and Matinlinna, J. P.; Aspects of silane coupling agents and surface conditioning in dentistry: An overview. *Dent. Mater.*, **28**, 467-477, 2012.
19. Xie, Y., Hill, C., Xiao, Z., Militz, H. and Mai, C.; Silane coupling agents used for natural fiber/polymer composites: A review. *Compos. Part Appl. Sci. Manuf.*,**41**, 806-819, 2010.
20. Huang, X., Kong, X., Cui, Y., Ye, X. Wang, X. and Shi, B.; Durable superhydrophobic materials enabled by abrasion-triggered roughness regeneration. *Chem. Eng. J.*, **336**, 633-639, 2018.
21. Shoulders, M. and Raines, R. T.; Collagen structure and stability. *Annu. Rev. Biochem*, **78**, 929-958, 2010.
22. Ye, X., Wang, Y., Ke, L., Cui, Y., Luo, W., et al.; Competitive adsorption for simultaneous removal of emulsified water and surfactants from mixed surfactant-stabilized emulsions with high flux. *J. Mater. Chem. A*,**6**, 14058-14064, 2018.
23. Hou, K., Zeng, Y., Zhou, C., Chen, J. and Pi, P.; Facile generation of robust POSS-based superhydrophobic fabrics via thiol-ene click chemistry. *Chem. Eng. J.*, **332**, 150-159, 2017.
24. Zhu, K., Zhang, J., Hao, Z., Tan, H., Zhang, W., et al.; Fabrication of durable superhydrophobic coatings based on a novel branched fluorinated epoxy. *Chem. Eng. J.*, **351**, 569-578, 2018.
25. Wang, J., He, J., Ma, L., Zhang, Y., Shen, L., et al.; Multifunctional conductive cellulose fabric with flexibility, superamphiphobicity and flame-retardancy for all-weather wearable smart electronic textiles and high-temperature warning device. *Chem. Eng. J.*, **390**, 124508, 2020.
26. Periolatto, M., Ferrero, F., Montarsolo, A. and Mossotti, R.; Hydrorepellent finishing of cotton fabrics by chemically modified TEOS based nanosol. *Cellulose*, **20**, 355-364, 2013.
27. Przybylak, M., Maciejewski, H., Dutkiewicz, A., DaBek, I. and Nowicki, M.; Fabrication of superhydrophobic cotton fabrics by a simple chemical modification. *Cellulose*, **23**, 2185-2197, 2016.
28. Das, I. and De, G.; Zirconia based superhydrophobic coatings on cotton fabrics exhibiting excellent durability for versatile use. *SCI REP-UK*, **5**, 18503, 2015.
29. He, X., Ding, W., Zeng, Y., Yu, Y. and Shi, B.; Insight into the Correlations Between Fiber Dispersion and Physical Properties of Chrome Tanned Leather. *JALCA,* **115**, 23-29, 2020.
30. Ding, W., Pang, X., Ding, Z., Tsang, D. C. W., Jiang, Z., et al.; Constructing a robust chrome-free leather tanned by biomass-derived polyaldehyde via crosslinking with chitosan derivatives. *J. Hazard. Mater.*, **396**, 122771, 2020.
31. Du, J., Peng, B., Huang, C.; Influence of Hydrophobic Side Chain Structure on the Performance of Amphiphilic Acrylate Copolymers in Leather-making. *J Soc Leath Tech Ch*., **100**, 67-72, 2016.

Structure and Function of Wool Keratin Polypeptide Extracted by Superheated Water

by

Ting Wu,[a, b] Min He,[a, b] Wenhua Yang,[a, b] Zhihua Shan,[a, b] Hui Chen[a, b,*]

[a]*College of Biomass Science and Engineering, Sichuan University,* Chengdu, 610065, China

[b]*The Key Laboratory of Leather Chemistry and Engineering (Sichuan University), Ministry of Education,* Chengdu, 610065, China

Abstract

Pyrohydrolytic wool keratin polypeptides (PWKPs) were successfully extracted by hydrolyzing waste sheep wool from a tannery with superheated water. The results revealed that the properties of PWKPs varied significantly under different hydrolysis temperatures. At 170°C, the weight average molecular weight and the polydispersion index of the product PWKP-170 were determined to be 1080 ± 71 Da and 1.55 ± 0.04, respectively, which displayed a distribution trend for "equilong chain segments". Furthermore, the extraction yield and the repeated water solubility reached 93.5 ± 1.7% and 99.8 ± 0.2%, respectively, and no α-helical structure was found to exist in PWKP-170. Organic element and amino acid analyses for the PWKPs showed that the decrease in sulfur and cysteine content was related to the fracture of disulfide bonds during the hydrolysis process of keratin. Specificity studies indicated that PWKP-170 exhibited a new ultraviolet absorption characteristic at 309 nm, with an antibacterial titer of 11.24 AU/mg against Staphylococcus aureus at a concentration of 1×10^6 CFU/mL, reflecting its potential application value as a keratin polypeptide functional material.

Introduction

It has been reported that the annual output of waste animal hair reaches up to 1.43×10^5 t in the global leather industries.[1] As a major country for leather and fur manufacturing, China produces more than 7×10^7 pieces of bovine hide and 1×10^8 pieces of sheep skin each year. Therefore, a large amount of bovine hair and wool needs to be disposed. At present, although part of waste hair is processed into felt, landfill is still regarded as the main disposal method, resulting in a waste of resources and requiring much soil space.[2] At the same time, there exists a risk of spongiform encephalopathy with this treatment. Hence, the recycling of wastes has become an inevitable trend of industrial development. The extraction of keratin polypeptide from waste hair is deemed an important approach to realize resource utilization.[3-5] The extraction mechanism lies in the destruction of disulfide bonds and amide bonds, which leads to the hydrolyzation of highly crosslinked and water-insoluble keratin into polypeptides with a small molecular weight and good water solubility.

The diversified extraction methods for keratin polypeptide include chemical hydrolysis, biological hydrolysis and physical hydrolysis. Chemical hydrolysis exhibits a high yield and a low requirement for procedure parameters, generally at a temperature of at most 100°C and normal atmospheric pressure. Nevertheless, the product needs to be purified several times to remove residual reagents, which induces breakage of the structural integrity, waste of water and environmental pollution.[6-8] For biological hydrolysis, no or a small number of chemical reagents are adopted under mild conditions. This method entirely depends on the performance of microorganisms or enzymes and requires high control for condition parameters with a low yield. Moreover, most keratinases belong to the excision enzyme, leading to the end product to be composed of free amino acids, with the difficult control of the molecular weight.[4, 9] To date, there are no reports that keratinase hydrolysis can be used to obtain a material with a specific molecular weight or a characteristic property on the premise of guaranteeing the extraction yield. For physical hydrolysis, a highly pure product can be fabricated by means of simple separation, such as filtration or centrifugation, with a low post-treatment cost. Furthermore, the sample is highly water-soluble under neutral conditions (especially superheated water hydrolysis). In contrast, from an environmental point of view, superheated water hydrolysis is more suitable for the recovery of keratin polypeptide from waste hair.[10-12]

Superheated water hydrolysis (SHWH) refers to the process during which the tissue structures of keratin are hydrolyzed under high temperature and high pressure for a certain time. Parag S. Bhavsar et al.[13,14] treated unwashed wool at 170°C for 60-90 min to complete partial hydrolysis by SHWH. The results showed that the molecular weight of the material varied from 600 Da to 1400 Da, the cysteine content decreased by 94.3%, and the C/N ratio declined from 4.26 to 3.55. A wheat germination experiment indicated that wool keratin polypeptide exhibited no toxic side effects and promoted the growth of wheat. M. Zoccola et al.[15] studied the influence of wool keratin polypeptide as a slow-release nitrogen fertilizer on the growth of grass by measuring the variation in the organic element content. The analysis suggested that the utilization of polypeptides reduced fertilizer usage compared to traditional chemical fertilizers in pasture lands and enhanced the carbon sequestration rate, which showed the potential agricultural application value of wool keratin

*Corresponding author email: chenh@scu.edu.cn

Manuscript received March 1, 2022, accepted for publication April 27, 2022.

polypeptide. Parag S. Bhavsar et al.[16] also applied wool keratin polypeptide extracted by SHWH at 170°C to a foaming agent. In the dyeing process of cotton and woolen fabrics with reactive and acid dyes, the sample exhibited a comparable effect to that of conventional dyeing auxiliaries, thus reducing the load on the effluent. However, there is still a lack of insights into the extraction of wool keratin polypeptide by SHWH. As a byproduct of the leather industry, waste hair has significant potential for recycling. Nevertheless, owing to the special physical structure of animal hair and the heterogeneity of the keratin chemical structure, a complete and in-depth performance characterization of the product should be investigated. Therefore, it is extremely urgent to explore multiple approaches to the functional development of keratin polypeptides extracted through environmentally friendly SHWH, which will lay a foundation for the construction of featured functional materials and realize the green high-value conversion of leather waste wool.

Among all the sources of waste animal hair, the waste sheep wool from the shearing factory, tannery and textile mill exhibits a high extraction value for keratin polypeptide due to the absence of pigments and fewer surface impurities. Hence, the raw material in this experiment was obtained from waste sheep wool manually pushed by a sheep leather processing enterprise. In this work, keratin polypeptide was extracted from clean waste sheep wool by using an optimized SHWH scheme. The solubility and the chemical structure of the samples were analyzed, and the ultraviolet absorption and bacteriostatic properties of the degradation product solutions were characterized, which can offer further support for the preparation of natural high-quality biological material from waste wool keratin polypeptide.

Experimental section

Main materials

Staphylococcus aureus *CMCC (B) 26003*, Bacillus subtilis *CMCC (B) 63501*, Pseudomonas aeruginosa *CMCC (B) 10104*, Escherichia coli *CMCC (B) 44102*, Aspergillus niger *CMCC (F) 98003*, Candida albicans *CMCC (F) 98001*, peptone, beef powder, agar, potato powder and glucose were purchased from Zhangzhou Seymour Biotechnology Co., Ltd. (China). All reagents were of biological grade and used as received.

Optimization of PWKP extracted by SHWH

Extraction yield

Approximately 10 g of waste sheep wool crushed to 5-10 mm long segments was degreased by shaking in 50 g of deionized water with 0.1 g of sodium dodecyl benzene sulfonate and 0.2 g of sodium carbonate at 45°C for 1 h. The degreasing fluid was drained, and then 0.5 g of peroxide and 50 g of distilled water were added, followed by stirring at 45°C for 1 h. The liquid was drained and the treated wool was dried to obtain the raw material wool for SHWH.[17] The wool and distilled water were mixed at a certain mass ratio in a 150 mL hydrothermal reaction kettle (Yikai, China) and heated under a specified temperature and time. After that, the hydrolysate was filtered through a microfiltration membrane, and then the filtrate was freeze-dried at -50°C to prepare the pyrohydrolytic wool keratin polypeptide (PWKP). The extraction yield (R) for PWKP was calculated according to Eq. (1).

$$R = \frac{m_2}{m_1} \times 100\% \quad (1)$$

where m_1 is the weight of the wool and m_2 is the weight of PWKP.

Single-factor experiment

During the course of extracting PWKP by SHWH, R is used as a primary evaluation indicator. Therefore, single-factor experiments were conducted to investigate the influence of hydrolysis temperature (T = 150-190°C), wool mass fraction (w = 5-25%) and hydrolysis time (t = 1-5 h) on R and to obtain the optimal factors (T_o, w_o, t_o). Based on previous reports,[14, 18] the basic hydrolysis conditions were set as T = 170°C, w = 10% and t = 2 h. In order of (T, w, t), the optimal temperature was obtained first, followed by dosage, and finally time.

Preparation of PWKP

According to the experimental results (T_o, w_o, t_o) acquired from above, wool was hydrolyzed under three hydrolysis conditions at different temperatures (T_{o1}, w_o, t_o), (T_{o2}, w_o, t_o) and (T_{o3}, w_o, t_o). Subsequently, the hydrolysate was dialyzed with distilled water at 4°C for 8 h to remove inorganic salts. Finally, the dialysate was freeze-dried to prepare PWKP-T_{o1}, PWKP-T_{o2} and PWKP-T_{o3}. All of the above samples were collectively labeled PWKPs.

Characterization

The relative molecular weight parameters of the PWKPs were detected using an RID-20 differential refractive index detector (Shimadzu, Japan) equipped with a TSK-gel GMPWXL aqueous gel permeation chromatography (GPC) column (TOSOH, Japan). The mobile phase consisted of 0.1 mol/L $NaNO_3$ and 0.05% NaN_3 aqueous solution. The flow rate and the column temperature were maintained at 0.6 mL/min and 35°C, respectively. PWKP was added to distilled water and then magnetically stirred at 25°C for 10 min, followed by filtering. Then, the filtrate was freeze-dried at -50°C. The repeated water solubility (R_{re}) of the PWKP was calculated using Eq. (2).

$$R_{re} = \frac{m_2}{m_1} \times 100\% \quad (2)$$

where m_1 is the weight of the PWKP and m_2 is the weight of the water-soluble part of the PWKP. X-ray diffraction (XRD) patterns for wool and PWKPs were characterized using an Empyrean X-ray diffractometer (Panalytical, Holland). The generator voltage and the tube current were 40 kV and 40 mA, respectively. The scanning range was 5-60° and the step size was 0.02°.

Composition characterization

The organic element content of the wool and PWKPs was analyzed using an EL cube elemental analyzer (Elementar, Germany). A total of 0.1 g of the sample was fully dissolved in an ampoule bottle containing 5 mL of HCl solution (6 mol/L), and then N_2 was continuously injected into the bottle for 10 min. Subsequently, the digestion reaction was carried out at 110°C for 24 h. After that, the digestion solution was dried at 60°C, and then the residues were dissolved with 5 mL of a Tris-HCl buffer solution (pH = 7.4), followed by filtering. Finally, the amino acid compositions of the filtrate for the wool and PWKPs were determined using an L-8900 amino acid analyzer (Hitachi, Japan).

The size and temperature of the ion exchange column equipped with a 2622 ion exchange resin (Hitachi, Japan) were 4.6 × 60 mm and 57°C, respectively. The reaction column contained an 855-3523 quartz sand (Hitachi, Japan) with a size of 4.6 × 40 mm and a temperature of 135°C. The flow rates for the ninhydrin and buffer solutions were 0.35 mL/min and 0.4 mL/min, respectively. The injection volume was 20 μL and the detection wavelength was 570 nm. The cycle time and the collection time were 20 min and 10 min, respectively. In addition, based on the amino acid compositions of wool, the reference sample (RS) was prepared with analytical pure amino acids for subsequent experiments.

Absorption characterization

Fourier transform infrared (FT-IR) spectra for the wool, PWKPs and RS were recorded using a Nicolet iS10 Fourier transform infrared spectrometer (Thermo Scientific, USA). Each sample was analyzed from 500 cm^{-1} to 4000 cm^{-1}. Ultraviolet–visible (UV-Vis) absorption characterization for the PWKPs and RS was conducted using a UV-3100 ultraviolet–visible spectrophotometer (Mapada, China). The wavelength range was 250-450 nm and the step size was 1 nm.

Bacteriostasis characterization

Qualitative bacteriostasis characterization

According to the experimental data of R_{re}, the bacteriostatic activity of PWKP, which was observed to be completely water-soluble under neutral conditions, was qualitatively characterized based on the inhibition zone diameter with filter paper. Gram-positive bacteria (Staphylococcus aureus *CMCC (B) 26003*, Bacillus subtilis *CMCC (B) 63501*) and gram-negative bacteria (Pseudomonas aeruginosa *CMCC (B) 10104*, Escherichia coli *CMCC (B) 44102*) were cultured in nutrient agar media, while potato glucose agar media were used for fungi (Aspergillus niger *CMCC (F) 98003*, Candida albicans *CMCC (F) 98001*). The specific experimental procedures are described below.

A certain number of second-generation inclined bacteria were placed into the PBS buffer solution to form the initial bacterial suspension with a concentration of approximately 1 × 10^8 CFU/mL. The suspension concentration was diluted to 1 × 10^6 CFU/mL with buffer solution to prepare the inoculative bacterial suspension. Then, 0.5 mL of the inoculative bacterial suspension was evenly spread over the culture dish containing the culture medium. After 20 min, five standard filter papers with a thickness of 1 mm and a diameter of 6 mm were placed into the dish at intervals of 2.0-2.5 cm. Then, 20 μL of the PWKP solution with different concentrations of 1.0 mg/mL, 3.0 mg/mL, 5.0 mg/mL, 7.0 mg/mL and 10.0 mg/mL was dropped onto the center of each filter paper. Subsequently, the dish was transferred to a 37°C incubator for 24 h to observe the inhibition zone around the filter paper. The inhibition zone diameter (*IZD*) was measured along three directions with a Vernier caliper, and the bacterium on which the PWKP showed the best bacteriostatic effect and the corresponding minimum inhibition concentration (ρ_{min}) were determined for quantitative bacteriostasis characterization.

Quantitative bacteriostasis characterization

Quantitative bacteriostasis characterization of PWKP was performed according to GB/T 39101-2020. Twenty milliliters of the culture medium and 0.2 mL of the inoculative bacterial suspension were homogeneously mixed in a sterilized glass culture dish, followed by solidification at 4°C. After that, five Oxford cups filled with 100 μL of the PWKP solution with different concentrations (ρ_{pwkp}) of $1\rho_{min}$, $2\rho_{min}$, $4\rho_{min}$, $8\rho_{min}$ and $16\rho_{min}$ mg/mL were placed into the dish at intervals. Subsequently, the dish was placed at 4°C for 10 h to ensure the adequate diffusion of PWKP and then transferred to a 37°C incubator for 24 h. The linear fitting curve was established with the negative logarithm of the dilution multiple (n) of ρ_{pwkp} relative to $16\rho_{min}$ as the abscissa and *IZD* as the ordinate. The antibacterial titer (U, AU/mg) of PWKP was calculated using Eq. (3).

$$U = \frac{1}{V \times 10^{X_0} \times 16\rho_{min}} \quad (3)$$

where V is the volume of the PWKP solution and X_0 is the X-intercept of the linear fitting curve.

Results and discussion

Single-factor SHWH experiment analysis

The influence of hydrolysis temperature (T), wool mass fraction (w) and hydrolysis time (t) on R is shown in Table I. It can be found that R markedly increased with increasing T and reached a value of 93.5 ± 1.7% at 170°C. When T exceeded 170°C, R was increased by only 1.4% at 180°C and 2.0% at 190°C. Minor distinctions existed among R in a w range of 5-20%, and R dropped down to 90.9 ± 2.5% when w was raised to 25%. As shown in Table I, R was gradually enhanced with increasing t and reached a value of 95.4 ± 1.9% when wool was hydrolyzed for 3 h, whereas little change occurred after 3 h.

In summary, the single-factor experimental results indicated that the optimal factors were T_o = 170°C, w_o = 20% and t_o = 3 h. On

Table I

The influence of *T*, *w* and *t* on R.

T/°C	150	160	170	180	190
R/%	52.1 ± 1.1	75.4 ± 1.5	93.5 ± 1.7	94.9 ± 1.3	95.5 ± 0.8
w/%	5	10	15	20	25
R/%	95.8 ± 1.2	95.1 ± 1.1	94.9 ± 1.7	95.1 ± 2.1	90.9 ± 2.5
t/h	1	2	3	4	5
R/%	83.2 ± 3.1	91.5 ± 1.5	95.4 ± 1.9	95.5 ± 1.3	95.6 ± 0.9

this basis, raising *T*, reducing *w* and prolonging *t* contributed to improving *R*, but the effects were not evident. Moreover, it was noteworthy that *T* exhibited the most significant influence on *R*. When *T* reached 150°C, *R* was equal to 52.1 ± 1.1%, lower than the data reported for alkaline hydrolysis[19] and higher than that for microwave-assisted SHWH.[11] The *R* value of 75.4 ± 1.5% at 160°C was similar to the result obtained from peracetic acid hydrolysis[8] and greater than that from microwave-assisted SHWH. When *T* was increased to 170°C, *R* reached up to 93.5 ± 1.7%, which was basically the same as that for alkaline hydrolysis. Therefore, the hydrolysis temperatures for further experiments were determined to be T_{o1} = 150°C, T_{o2} = 160°C and T_{o3} = 170°C, and the corresponding products were coded as PWKP-150, PWKP-160 and PWKP-170, respectively.

GPC analysis

As shown in Fig. 1A, the weight average molecular weight (M_w) ranged from 9568 ± 241 Da to 1080 ± 71 Da with much difference. The results indicated that the relative molecular weight of PWKP was highly correlated with *T*, and the macromolecular chain segment dominated PWKP at low hydrolysis temperatures. However, it has been reported that the M_w of alkaline hydrolyzed wool keratin polypeptide was concentrated in the range of 800-1000 Da at the same temperatures,[14] demonstrating the relatively centralized molecular weight distribution and lower number of macromolecular chain segments. The above phenomena revealed that the mechanisms for the two hydrolysis methods were different. In addition, the polydispersion index (*PDI*) can also reflect the distribution characteristic of the molecular weight. The *PDI* values for PWKP-150 and PWKP-160 were determined to be 3.62 ± 0.14 and 2.90 ± 0.14, respectively, which meant that each molecule in the same sample showed a great variation in molecular weight. The *PDI* of PWKP-170 was determined to be 1.55 ± 0.04 with a minor discrepancy between M_w and number average molecular weight (M_n), proving that when *T* was increased to a certain level, the molecular weight distribution of PWKP tended to become uniform, that is, the "equilong chain segments" tendency. Consequently, the molecular weight of wool keratin polypeptide could be concentrated at approximately 1000 Da by SHWH with a hydrolysis temperature of 170°C, which was similar to that obtained in earlier work.[11]

Repeated water solubility analysis

After wool was hydrolyzed with superheated water, the hydrolysate displayed a colloid solution composed of wool keratin polypeptide and water, which belonged to a thermodynamic dispersion system with poor stability. Under certain conditions, the disulfide bonds, which were broken during the hydrolysis process for wool, had the ability to self-heal and thus started aggregating back. Hence, self-aggregation behavior might occur through dynamic covalent interactions of disulfide bonds, inducing the appearance of sediments or suspended particles. Furthermore, during the drying

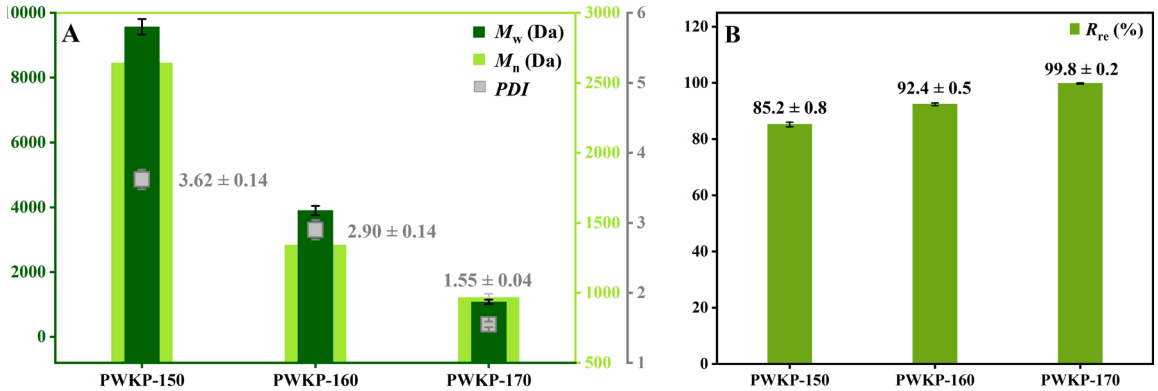

Figure 1. (A) Relative molecular weight parameters and **(B)** repeated water solubilities of PWKPs.

process, molecules contacted each other with the disappearance of hydration layers, leading to a greater likelihood of generating hydrophobic aggregations, and, thus, the formation of a water-insoluble product. Therefore, the repeated water solubility (R_{re}) should be considered to expand the further applications of PWKP. It can be seen in Fig. 1B that the R_{re} values of PWKP-150, PWKP-160 and PWKP-170 were 85.2 ± 0.8%, 92.4 ± 0.5% and 99.8 ± 0.2%, respectively, which meant that only PWKP-170 could be completely dissolved in water under neutral conditions. Apart from that, in combination with the experimental GPC data, the molecular weight of PWKP gradually declined with increasing *T*, giving rise to an increase in R_{re}. The results proved a definite relation between the molecular weight and R_{re} of PWKP. This was because that larger molecular weight meant longer chain length with more hydrophobic region compared to hydrophilic region, which led to PWKP being less water-soluble.

XRD analysis

Fig. 2A displays the XRD patterns for wool and PWKPs. For wool, PWKP-150 and PWKP-160, the two wide diffraction peaks were located at 9.1° and 20°, respectively, which were attributed to the α-helix and β-fold of keratin.[20] Nevertheless, a peak at 9.1° was not detected in PWKP-170. This result indicated that there was no α-helix in PWKP-170, whereas the β-folded structure still existed. It also revealed that when *T* was increased to 170°C, the α-helical structures of wool were completely damaged, which was consistent with other research findings.[11, 14, 18]

Organic element content analysis

Fig. 2B shows the organic element contents of wool and PWKPs. The C, N, H and S content changed before and after hydrolysis. With increasing *T*, *w*(C) and *w*(S) decreased while *w*(N) and *w*(H) increased. Except for S, the fluctuations in the other element contents were not significant. The *w*(S) values decreased from 3.87% to 2.16%, 2.07% and 1.68% as *T* was increased to 150°C, 160°C and 170°C, respectively. This phenomenon could be explained by the fact that the S element in wool principally existed in cystine in the form of a disulfide bond (—S—S—), and the disulfide bonds were broken during the hydrolysis process for wool, leading to a dramatic decrease in *w*(S). With regard to PWKP-170, *w*(S) was reduced by more than 50% compared with wool. The result indicated that the disulfide bonds of wool were adequately hydrolyzed in PWKP-170, inducing a smaller molecular weight, a better repeated water solubility and a lower *w*(S).

Amino acid composition analysis

Table II presents the amino acid compositions of wool and PWKPs. The most evident variation appeared in cysteine (Cys). The Cys content of wool was 10.30%, which was higher than that in the PWKPs. This was because during the acidic treatment process for amino acid composition characterization, many Cys residues were generated owing to the fracture of disulfide bonds, resulting in a greater Cys content in wool. For PWKP-150 and PWKP-160, the Cys contents were determined to be 3.55% and 1.12%, which represented a decrease of 65.5% and 89.1% in comparison with wool, suggesting that there were still some disulfide bonds left in the products. PWKP-170 possessed a lower Cys content of 0.52%, which was reduced by 95.0%, verifying that disulfide bonds were almost fully destroyed.[14] Moreover, the Cys residue could react with dehydroalanine to form lanthionine (Lant) or repolymerize to form cystine (Cya), inducing a dramatic decline in the Cys content and growth in the Lant and Cya contents of PWKPs.[13, 21]

For other amino acid contents, the reasons for the obvious fluctuations were speculated as follows. The hydrolysis of glutamine and asparagine led to the augmentation of the glutamic acid (Glu) and aspartic acid (Asp) contents. The decrease in tyrosine (Tyr) and threonine (Thr) contents resulted from the thermal oxidation of hydroxyl groups in the side chains at high temperatures. The reduction in lysine (Lys) and arginine (Arg) contents was ascribed to the destruction of side-chain alkaline groups at high temperatures. In general, the content of acidic groups (Glu and Asp) increased and that of alkaline groups (Lys and Arg) declined by SHWH. Furthermore, according to the amino acid composition of wool, the reference sample (RS) was prepared with analytical pure amino acids for subsequent characterization.

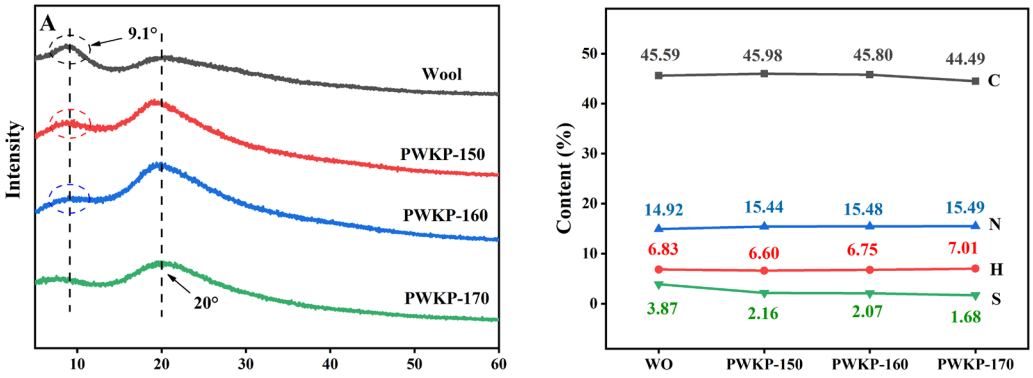

Figure 2. (A) XRD patterns and **(B)** organic element contents of wool and PWKPs.

Table II

Amino acid composition of wool and PWKPs.

Amino acid	Wool/mol%	PWKP-150/mol%	PWKP-160/mol%	PWKP-170/mol%
Cys	10.30	3.55	1.12	0.52
Lant	0.22	0.78	1.34	1.64
Cya	0.09	0.11	0.12	0.12
Glu	13.72	15.92	16.88	18.15
Asp	7.62	7.77	8.22	9.04
Tyr	3.09	2.88	2.55	2.50
Thr	6.03	5.77	5.26	5.09
Lys	3.42	3.35	3.21	3.01
Arg	6.73	6.58	6.16	5.44
Ser	10.39	10.13	9.34	9.12
Gly	7.89	8.46	9.25	9.90
His	0.62	0.63	0.67	0.69
Ala	5.23	5.97	6.77	7.33
Pro	5.71	5.93	6.23	6.44
Val	6.09	6.27	6.59	6.74
Met	0.38	0.39	0.39	0.40
Ile	3.20	3.30	3.36	3.46
Leu	7.15	7.46	7.67	7.88
Phe	2.21	2.11	1.94	1.86

FT-IR and UV-Vis absorption analysis

Fig. 3A displays the FT-IR spectra obtained for wool, PWKPs and RS. The wide absorption peak between 3000-3500 cm^{-1} was attributed to ν(N-H) and ν(O-H) of the amide band A.[22] The three absorption peaks between 2800-3000 cm^{-1} and the two peaks at 1400 cm^{-1} and 1450 cm^{-1} were ascribed to ν(C—H) of —CH_3 and —CH_2.[23] The peaks at 1650 cm^{-1} and 1540 cm^{-1} were assigned to ν(C=O) of amide band I[24] and ν(C—N) and δ(N—H) of amide band II,[21] respectively. The peak at 1240 cm^{-1} belonged to ν(C—N), ν(C—O), δ(N—H) and δ(O=C—H) of amide band III.[22] In addition, the absorption peaks at 1040 cm^{-1} and 1080 cm^{-1} were associated with ν(S-O).[21, 25, 26] Therefore, the absorption of PWKP-170 was not clear in this position. Moreover, it was worth noting that the absorption peak at 2570 cm^{-1} corresponding to ν(S—H) of the side chain of cysteine was visible only in RS,[27] demonstrating that wool and PWKPs contained no free cysteine residues. This was because that the cysteine residues may react with dehydroalanine to generate lanthionine or repolymerize to form cystine and so on.

Due to the conjugated double bond systems of phenylalanine, tryptophan and tyrosine, proteins possess obvious UV-Vis absorption characteristics. In the ultraviolet band, the absorption band can be divided into band R, band K, band B and band E. Among them, band R is formed by the lone pair electron transitions of chromophores, such as —C=O, —N=N— and —NO_2, which is located between 200-400 nm with a weak intensity. As shown in Fig. 3B, a wide absorption peak was located between 280-310 nm for PWKPs and RS. Nevertheless, unlike RS, a shoulder peak between 310-360 nm was detected in PWKPs. Fig. 3C shows the peak fitting curves for the PWKPs. The absorption spectra for the PWKPs were superposed by two curves with peak values of 288 nm and 309 nm. The emergence of a new absorption peak indicated the presence of functional groups capable of producing absorption in band R, such as —N=O and —NO_2. These functional groups were formed by the thermal oxidation of the —NH_2 of the side chains and the end groups in PWKPs. This also induced a solubility change from water-insoluble to water-soluble after oxidation for some keratins, which improved the extraction yield and the water solubility of the product under neutral conditions. In parallel, the absorbance of PWKP was enhanced with increasing *T* at the same wavelength because more chromophores and auxochromes were generated which made the product darker in color.

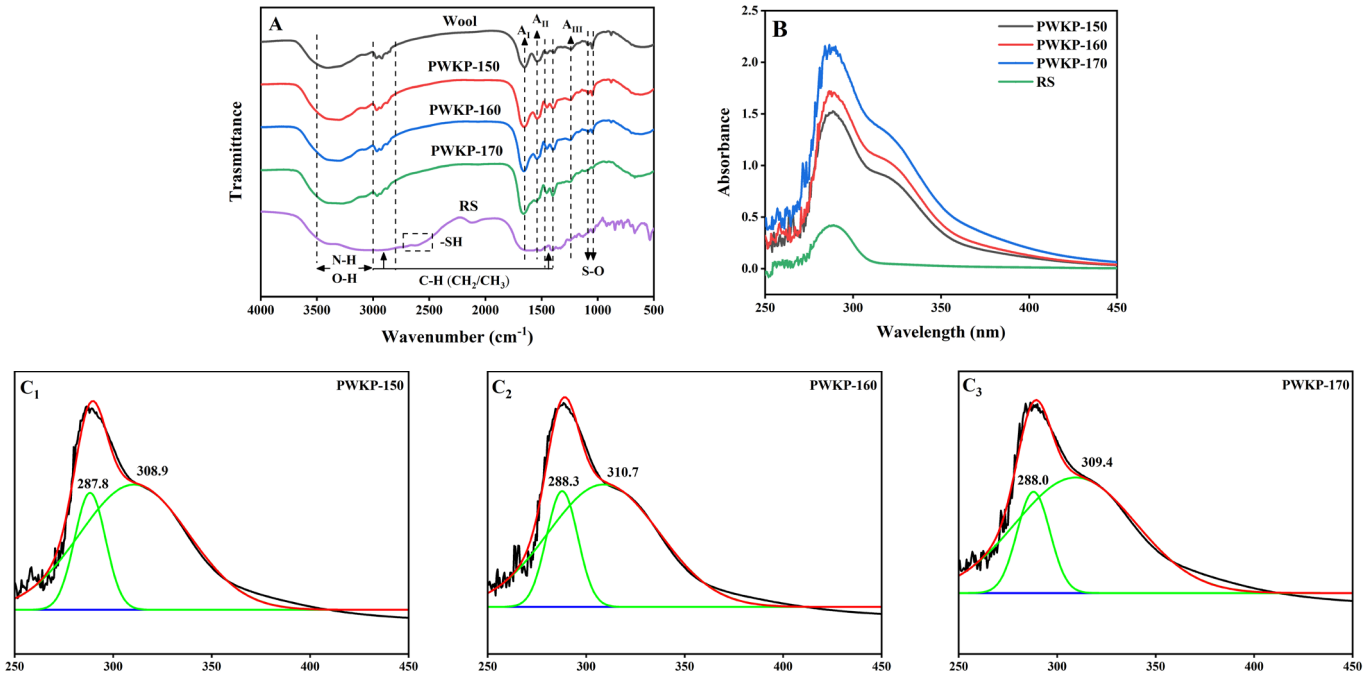

Figure 3. (A) FT-IR spectra for wool, PWKPs and RS; **(B)** UV-Vis spectra for PWKPs and RS; **(C)** Peak fitting curves for the UV-Vis spectra for the PWKPs.

Bacteriostasis analysis

Qualitative bacteriostasis analysis

In recent years, polypeptide compounds with bacteriostatic activity extracted from animals, plants and microorganisms have become a hot topic in the field of bacteriostatic drugs. At present, the widely recognized bacteriostatic mechanism is that polypeptides can bind to lipoteichoic acid in the bacterial cell membrane, leading to the destruction of the cell structure and eventually inhibition of bacterial growth.[28] According to the repeated water solubility acquired from above, only PWKP-170 could be completely dissolved in water under neutral conditions. Therefore, only PWKP-170 was selected for bacteriostasis characterization because of the neutral experimental conditions.

As shown in Fig. 4A, when the PWKP-170 concentration (ρ_{pwkp}) was kept in the range of 1.0-5.0 mg/mL, a clear growth boundary appeared at the edge of the filter paper in *Staphylococcus* aureus medium, whereas *IZD* expansion was not observed owing to the lower concentration. When ρ_{pwk} was increased to 7.0 mg/mL and 10.0 mg/mL, the *IZD* values reached up to 7.84 ± 0.48 mm and 9.98 ± 0.36 mm, respectively. Likewise, for *Bacillus subtilis medium*, *IZD* reached 6.43 ± 0.22 mm and 6.97 ± 0.34 mm when ρ_{pwk} exceeded 5.0 mg/mL. Nevertheless, no inhibition zones were observed around any filter papers in other media. This phenomenon suggested that when ρ_{pwk} grew to over 7.0 mg/mL, PWKP-170 exhibited a significant inhibition effect on the growth of *Staphylococcus aureus*, whereas it had a relatively weak bacteriostatic property for *Bacillus subtilis* and showed no bacteriostasis against *Pseudomonas aeruginosa, Escherichia coli, Aspergillus niger* and *Candida albicans*. Hence, it can be inferred that PWKP-170 possessed bacteriostatic activity against gram-positive bacteria but not against gram-negative bacteria and fungi. This was because of the structural difference between bacteria and fungi. The bacterial cell wall was composed of peptidoglycan,

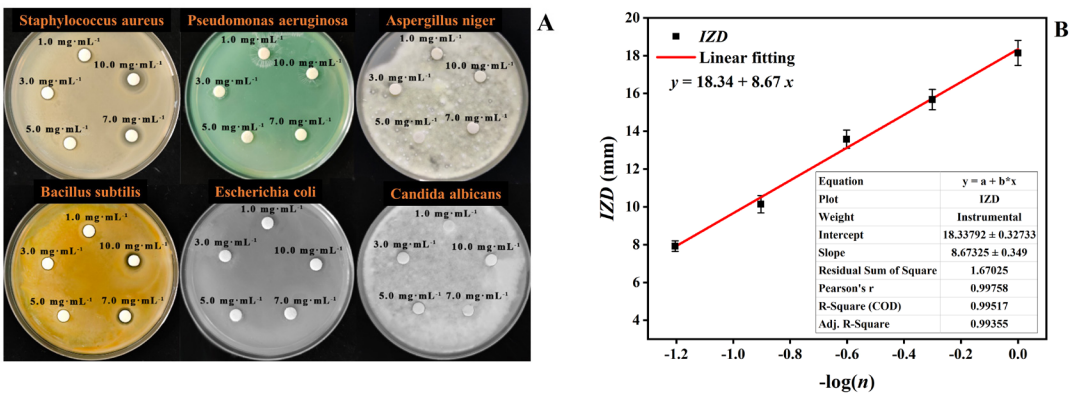

Figure. 4. **(A)** Optical images of the inhibition zones of PWKP-170 in different culture media; **(B)** Linear fitting curve for n and IZD for PWKP-170.

while the fungal cell wall consisted of chitosan. PWKP-170 could penetrate the cell walls of bacteria rather than fungi, rendering it ineffective against fungi. The discrepancy between gram-positive and gram-negative bacteria lied in the presence of lipoteichoic acids in gram-positive bacteria. Consequently, PWKP-170 had a bacteriostatic effect only on gram-positive bacteria.

However, there are different suggestions about the key functional structures and components of antibacterial peptides. Some scholars believe that the antibacterial activity originates from special amino acids, such as tryptophan, proline, arginine and cysteine.[29-31] Other researchers argue that the antibacterial property is derived from the amino acid content (such as hydrophobic amino acid content) and the special molecular structure (such as α-helix or special amino acid sequence fragment).[32] For PWKP-170, the bioactive structure and domain of keratin were destroyed after high-temperature treatment, and XRD analysis proved that no α-helical structure existed. As a consequence, the bioactive molecular structure may not play a contributing role in bacteriostasis. The bacteriostasis of PWKP-170 might be related to the specific amino acid or the amino acid composition ratio.

Quantitative bacteriostasis analysis

Based on the analytical results of 3.8.1, PWKP-170 showed the most evident bacteriostatic effect on *Staphylococcus aureus*, with a minimum inhibition concentration (ρ_{min}) of 7.0 mg/mL. Fig. 4B displays the linear fitting relationship between dilution multiple (*n*) and *IZD*. With a decrease in *n*, that is, with an increase in the PWKP-170 concentration, the *IZD* was gradually increased to 18.14 ± 0.66 mm. The formula of the fitting curve could be expressed as $y = 18.34 + 8.67\,x$ with an X-intercept of -2.11. According to Eq. (3), the antibacterial titer was calculated to be $U = 11.24$ AU/mg.

Conclusion

In this paper, waste sheep wool was hydrolyzed by superheated water, and then the hydrolysate was freeze-dried to prepare pyrohydrolytic wool keratin polypeptide (PWKP). The analytical results for organic element content and amino acid composition indicated that the degree of fracture of disulfide bonds varied with the hydrolysis temperature, which demonstrated a significant effect on the extraction yield, relative molecular weight and repeated water solubility. At 170°C, the product PWKP-170 exhibited excellent performance (R = 93.5 ± 1.7%, M_w = 1080 ± 71 Da, PDI = 1.55 ± 0.04 and R_{re} = 99.8 ± 0.2%). UV-Vis absorption and bacteriostasis experiments revealed that PWKP-170 showed a new UV absorption peak at 309 nm and a significant bacteriostasis to *Staphylococcus aureus*. The minimum inhibition concentration and the antibacterial titer of PWKP-170 were determined to be 7.0 mg/mL and 11.24 AU/mg, respectively, for *Staphylococcus aureus* at a concentration of 1×10^6 CFU/mL.

In summary, superheated water hydrolysis can achieve efficient hydrolysis for keratin and efficient extraction for polypeptide without the need for external chemical reagents, which is fully scalable with the current infrastructures and facilities. Based on the UV-Vis absorption property measured at a wavelength of 309 nm and the good digestibility of wool keratin polypeptide with a low molecular weight, PWKP-170 is intended to be an edible UV-resistant material. Furthermore, the significant bacteriostatic activity of PWKP-170 against *Staphylococcus aureus* indicates its potential application value in the bacteriostatic modification of medical foam. Therefore, it can be confirmed that PWKP-170, the hydrolysis product of waste wool from leather tanning, is a kind of natural intrinsic anti-ultraviolet and bacteriostatic polypeptide material that has potential for high-value applications. This work will provide new ideas for the recovery and utilization of leather waste wool resources.

Credit Authorship Contribution Statement

Ting Wu: Investigation, Methodology, Data curation, Writing-original draft. Min He: Data curation, Formal analysis. Wenhua Yang: Data curation, Formal analysis. Zhihua Shan: Visualization, Writing-review & editing. Hui Chen: Conceptualization, Methodology, Investigation, Writing-review & editing, Supervision.

Declaration of Competing Interest

The authors declare that they have no known competing financial interests or personal relationships that could have appeared to influence the work reported in this paper.

Acknowledgments

The research was supported by the Open Fund of Sichuan Province Cyclic Economy Research Center (No. XHJJ-2009) and the Sichuan University-Dazhou Municipal People's Government Strategic Cooperation Project (2021CDDZ-03).

References

1. Valeika, V., Širvaitytė, J., Bridžiuvienė, D., Švedienė, J.; An Application of Advanced Hair-Save Processes in Leather Industry as the Reason of Formation of Keratinous Waste: Few Peculiarities of its Utilisation. *ESPRI* **26**, 6223-6233, 2019.
2. Guo, J., Dai, R., Chen, H., Liang, Y., Shan, Z.H.; Research on the Composite and Functional Characteristics of Leather Fiber Mixed with Nitrile Rubber. *JLSE* **3**, 1-12, 2021.
3. de Souza, F.d.R., Benvenuti, J., Meyer, M., Wulf, H., Klüver, E., Gutterres, M.; Extraction of Keratin from Unhairing of Bovine Hide. *CEC* **209**, 118-126, 2020.

4. de Medeiros, I.P., Rozental, S., Costa, A.S., Macrae, A., Hagler, A.N., Ribeiro, J.R.A., Vermelho, A.B.; Biodegradation of Keratin by Trichosporum Loubieri RC-S6 Isolated from Tannery/Leather Waste. *IBB* **115**, 199-204, 2016.
5. Hussain, F.S., Memon, N., Khatri, Z., Memon, S.; Solid Waste-Derived Biodegradable Keratin Sponges for Removal of Chromium: A Circular Approach for Waste Management in Leather Industry. *ETI* **20**, 101120(1-13), 2020.
6. Zhang, C.H., Xia, L.J., Zhang, J.J., Liu, X., Xu, W.L.; Utilization of Waste Wool Fibers for Fabrication of Wool Powders and Keratin: A Review. *JLSE* **2**, 2020.
7. Ghosh, A., Clerens, S., Deb-Choudhury, S., Dyer, J.M.; Thermal Effects of Ionic Liquid Dissolution on the Structures and Properties of Regenerated Wool Keratin. *PDS* **108**, 108-115, 2014.
8. Shavandi, A., Carne, A., Bekhit, A.A., Bekhit, A.E-D.A; An Improved Method for Solubilisation of Wool Keratin Using Peracetic Acid. *JECE* **5**, 1977-1984, 2017.
9. Eslahi, N., Dadashian, F., Nejad, N.H.; An Investigation on Keratin Extraction from Wool and Feather Waste by Enzymatic Hydrolysis. *PBB* **43**, 624-648, 2013.
10. Li, Y.C., Guo, R.J., Lu. W.H., Zhu, D.Y.; Research Progress on Resource Utilization of Leather Solid Waste. *JLSE* **1**, 2019.
11. Zoccola, M., Aluigi, A., Patrucco, A., Vineis, C., Forlini, F., Locatelli, P., Sacchi, M.C., Tonin, C.; Microwave-Assisted Chemical-Free Hydrolysis of Wool Keratin. *TRJ* **82**, 2006-2018, 2012.
12. Chen, J.Y., Ding, S.Y., Ji, Y.M., Ding, J.Y., Yang, X.Y., Zou, M.H., Li, Z.L.; Microwave-Enhanced Hydrolysis of Poultry Feather to Produce Amino Acid. *CEPPI* **87**, 104-109, 2015.
13. Bhavsar. P.S., Zoccola, M., Patrucco, A., Montarsolo, A., Mossotti, R., Rovero, G., Giansetti, M., Tonin, C.; Superheated Water Hydrolysis of Waste Wool in a Semi-Industrial Reactor to Obtain Nitrogen Fertilizers. *ACS SCE* **4**, 6722-6731, 2016.
14. Bhavsar, P., Zoccola, M., Patrucco, A., Montarsolo, A., Rovero, G., Tonin, C.; Comparative Study on the Effects of Superheated Water and High Temperature Alkaline Hydrolysis on Wool Keratin. *TRJ* **87**, 1696-1705, 2016.
15. Zoccola, M., Montarsolo, A., Mossotti, R., Patrucco, A., Tonin, C.; Green Hydrolysis as an Emerging Technology to Turn Wool Waste into Organic Nitrogen Fertilizer. *WBV* **6**, 891-897, 2015.
16. Bhavsar, P.S., Zoccola, M., Patrucco, A., Montarsolo, A., Mossotti, R., Giansetti, M., Rovero, G., Maier, S.S., Muresan, A., Tonin, C.; Superheated Water Hydrolyzed Keratin: A New Application as a Foaming Agent in Foam Dyeing of Cotton and Wool Fabrics. *ACS SCE* **5**, 9150-9159, 2017.
17. Shu, C.H., Long, Z.Z., Chen, Z.J., Dai, R., Shan Z.H.; Rapid Improvement of Wool Keratin Fertiliser Efficiency Based on Electrodegradation. *SLTC* **106**, 83-89, 2022.
18. Sweetman, B.J.; The Hydrothermal Degradation of Wool Keratin. *TRJ* 37, 844-851, 1967.
19. Shavandi, A., Bekhit, A.E-D.A., Carne, A., Bekhit, A.; Evaluation of Keratin Extraction from Wool by Chemical Methods for Bio-Polymer Application. *JBCP* **32**, 163-177, 2016.
20. Goodings, A.C.; The Molecular Structure of Wool Keratin. *TRJ* 20, 454-466, 1950.
21. Rajabinejad, H., Zoccola, M., Patrucco, A., Montarsolo, A., Rovero, G., Tonin, C.; Physicochemical Properties of Keratin Extracted from Wool by Various Methods. *TRJ* **88**, 2415-2424, 2017.
22. Idris, A., Vijayaraghavan, R., Rana, U.A., Patti, A.F., MacFarlane, D.R.; Dissolution and Regeneration of Wool Keratin in Ionic Liquids. *GC* **16**, 2857-2864, 2014.
23. McGregor, B.A., Liu, X., Wang, X.G.; Comparisons of the Fourier Transform Infrared Spectra of Cashmere, Guard hair, Wool and other Animal Fibres. *JTI* **109**, 813-822, 2017.
24. Cardamone, J.M.; Investigating the Microstructure of Keratin Extracted from Wool: Peptide Sequence (MALDI-TOF/TOF) and Protein Conformation (FTIR). *JMS* **969**, 97-105, 2010.
25. Călin, M., Constantinescu-Aruxandei, D., Alexandrescu, E., Răut, I., Doni, M.B., Arsene, M-L., Oancea, F., Jecu, L., Lazăr, V.; Degradation of Keratin Substrates by Keratinolytic Fungi. *EJB* **28**, 101-112, 2017.
26. Gaidau, C., Epure, D-G., Enascuta, C.E., Carsote, C., Sendrea, C., Proietti, N., Chen, W.Y., Gu, H.B.; Wool Keratin Total Solubilisation for Recovery and Reintegration - An Ecological Approach. *JCP* **236**, 117586(1-12), 2019.
27. Manivannan, D., Kirubavathi, K., Bakiyaraj, G., Selvaraju, K.; Studies on L-Cystine Hydrobromide Single Crystals for Nonlinear Optical Applications. *JTUS* **12**, 64-68, 2018.
28. Chen, C.H., Lu, T.K.; Development and Challenges of Antimicrobial Peptides for Therapeutic Applications. *A(B)* 9, **24**(1-20), 2020.
29. Shelenkov, A., Slavokhotova, A., Odintsova, T.; Predicting Antimicrobial and Other Cysteine-Rich Peptides in 1267 Plant Transcriptomes. *A(B)* **9**, 60(1-8), 2020.
30. Feng, X.J., Jin, S.J., Wang, M., Pang, Q., Liu, C.L., Liu, R.Q., Wang, Y.J., Yang, H., Liu, F.J., Liu, Y.Y.; The Critical Role of Tryptophan in the Antimicrobial Activity and Cell Toxicity of the Duck Antimicrobial Peptide DCATH. *FM* **11**, 1146(1-14), 2020.
31. Mishra, A.K., Choi, J., Moon, E., Baek, K-H.; Tryptophan-Rich and Proline-Rich Antimicrobial Peptides. *M* 23, **815**(1-23), 2018.
32. Lorenzon, E.N., Piccoli, J.P., Santos-Filho, N.A., Cilli, E.M.; Dimerization of Antimicrobial Peptides: A Promising Strategy to Enhance Antimicrobial Peptide Activity. *PPL* **26**, 98-107, 2019.

Hyperbranched Polyurethanes with Flammability Resistance for Leather Retanning

by
Sheng Ding,[1] Yiban Wu,[2] Jinxing Zhu[1]and Saiqi Tian[1,*]
[1]*College of Education, Wenzhou University,* Wenzhou, 325035, P.R. China
[2]*College of Pharmacy, Jiamusi University,* Jiamusi, 154007, P.R. China

Abstract

In this study, diethyl bis(2-hydroxyethyl) aminomethyl phosphonate was modified by hexamethylene diisocyanate, and then was utilized to partly replace the isocyanates to prepare hyperbranched polyurethanes (HPU-DPAs). The hyperbranched polyurethanes were then employed in the retanning process of wet blue. The shrinkage temperature, average thickness as well as mechanical properties of leather before and after retanning were acquired. The flammability of retanned leather was measured by cone calorimeter test. The morphologies of wet blue and leather after retanning by HPU-DAP were obtained using a scanning electron microscope. Results showed that the average thickness, tensile strength and elongation at break of leather were all improved after retanning. Retanning by HPU-DAPs can effectively increase flame retardancy of final leather.

Introduction

Nowadays, leather products have been widely used in our daily life, such as furniture, clothing, shoes and bag.[1] However, the inflammability of leather greatly limits its further application in more fields. When leather burns, high concentrations of hazardous gases (such as HCN, HNCO, CO, NO, NO_2, etc.) are released,[2, 3] severely causing health problems. As a result, it is crucial to improve the fire resistance of leather. Great efforts have been made to prepare leather with flammability resistance. For instance, Lyu and coworkers[4] utilized zanthoxylum bungeanum seed oil and aqueous miscible organic solvent treatment modified layered double hydroxide to prepare flame retardant leather. The flame retardant property of leather was demonstrated to be improved owing to the formed continuous dense char layer.

The retanning process is considered as one of the important steps in leather manufacturing processing, which can improve the shrinkage temperature, assist the dyeing process, and endow some functional properties to the final leather, such as fire-retardancy, water-proof, antifouling, antimicrobial and so on.[5-7] For example, our group previously prepared a fluorescent waterborne polyurethane retanning agent through chemical incorporation of fluorescer into polyurethane backbone as a chain extender.[8] The resultant leather after retanning exhibited a magic fluorescence effect under a UV lamp.[9] In another research, a chromotropic acid grafted amphoteric polyurethane was synthesized and then applied in the retanning process of aldehyde tanned leather. The reaction between chromotropic acid and formaldehyde occurred between two naphthalene rings, effectively reducing the content of free formaldehyde in leather.

Among the retanning agents, hyperbranched polymers, which are highly branched macromolecules with three-dimensional architecture, have been paid considerable attention because of their novel structures, unique properties, and potential application prospects.[10] On the one hand, hyperbranched polymers have a large number of active groups (such as hydroxyl, carboxylic, amino, etc.), which can not only form hydrogen bonds with hydroxyl, amino and carboxyl groups of leather collagen fibers, but also coordinate with chromium in wet blue.[11] Consequently, the collagen fibers can be cross-linked, thereby increasing the shrinkage temperature, physical and mechanical properties of leather. More specifically, the structure of hyperbranched polyurethane can be tailored during the preparation process, by changing the types and contents of raw materials accordingly, to achieve satisfactory performance.[12] Hence, flame retardant hyperbranched polyurethanes can be achieved by covalently incorporating flame retardant moieties into hyperbranched chains during the synthesis process. Particularly, phosphorus-based flame retardants play an important role in flame retardant additives and change the decomposition as well as combustion characteristics of leather.[13] At elevated temperatures, the chemical interactions in the condensed phase could result in changes in the decomposition pathway of the leather and formation of carbonaceous char residues on the surface of decomposing leather, thus preventing further oxidation. Besides, the volatilized compounds could interact with the combustion intermediates in the gas phase as inhibitors. Such interactions usually cause recombination of the H and OH radicals and prevent oxidation. However, to the best of our knowledge, no research has been done on preparing hyperbranched polyurethane with flammability for leather retanning. Therefore, the flame retardant moieties can be covalently conjugated into the chains of hyperbranched polyurethane.

In this study, hyperbranched polyurethanes were prepared by chemically incorporating phosphorous units into branched chains. Then they were applied as retanning agents in the

*Corresponding author email: tiansaiqi@wzu.edu.cn
Manuscript received December 13, 2021, accepted February 8, 2022.

leather manufacturing process. The microstructure, shrinkage temperature, average thickness and mechanical properties of final leather were measured. Besides, the flammability of leather retanned by hyperbranched polyurethanes with different content of phosphorous units was investigated in detail.

Experimental

Materials

N, *N*-dimethylformamide (DMF), trimethylolpropane (TMP), hexamethylene diisocyanate (HDI), dibutyltin dilaurate (DBTDL), *2*, *2*-bis(hydroxymethyl)propionic acid (DMPA), natrium bicarbonate ($NaHCO_3$) and sodium hydroxide (NaOH) were purchased from Aladdin Industrial Corporation (Shanghai, China). Pyridine was obtained from Sinopharm Chemical Reagent Co., Ltd (Shanghai, China). Phenol phthalein was provided by Shanghai SSS Reagent Co., Ltd (Shanghai, China). Formic acid (HCOOH) was acquired commercially from Shanghai Lingfeng Chemical Reagent Co., Ltd (Shanghai, China). Diethyl bis(2-hydroxyethyl) aminomethylphosphonate (DAP) was supplied by Zhengzhou Alpha Chemical Co., Ltd (Zhengzhou, China).

Synthesis of hyperbranched polyurethane retanning agent (HPU)

Firstly, HDI, TMP (mole ratio of HDI: TMP = 3: 1) and a suitable amount of DMF were added to a three necked flask. The reaction was stirred at room temperature until the molar weight of –NCO group reached the theoretical value.[14] Then, TMP (mole ratio of TMP: initial TMP= 3: 1) was added and stirred for one hour. After that, HDI (mole ratio of HDI: initial TMP= 6: 1) was poured and the polymerization was carried out for a duration of one hour. Subsequently, DMPA (mole ratio of HDI: initial TMP= 6: 1) was put into the three necked flask and the reaction was continued for another one hour. Finally, DMF was evaporated under reduced pressure and then washed by octane to give the transparent product as HPU (Scheme 1(a)).

Synthesis of hyperbranched polyurethane with flammability (HPU-DAP)

DAP and HDI were added into a three necked flask and reacted at room temperature. Until the molar weight of –NCO group reached the theoretical value, the HDI-DAP was obtained. (Scheme 1(b)) HDI-DAP was used to replace part of HDI in Scheme 1(a).

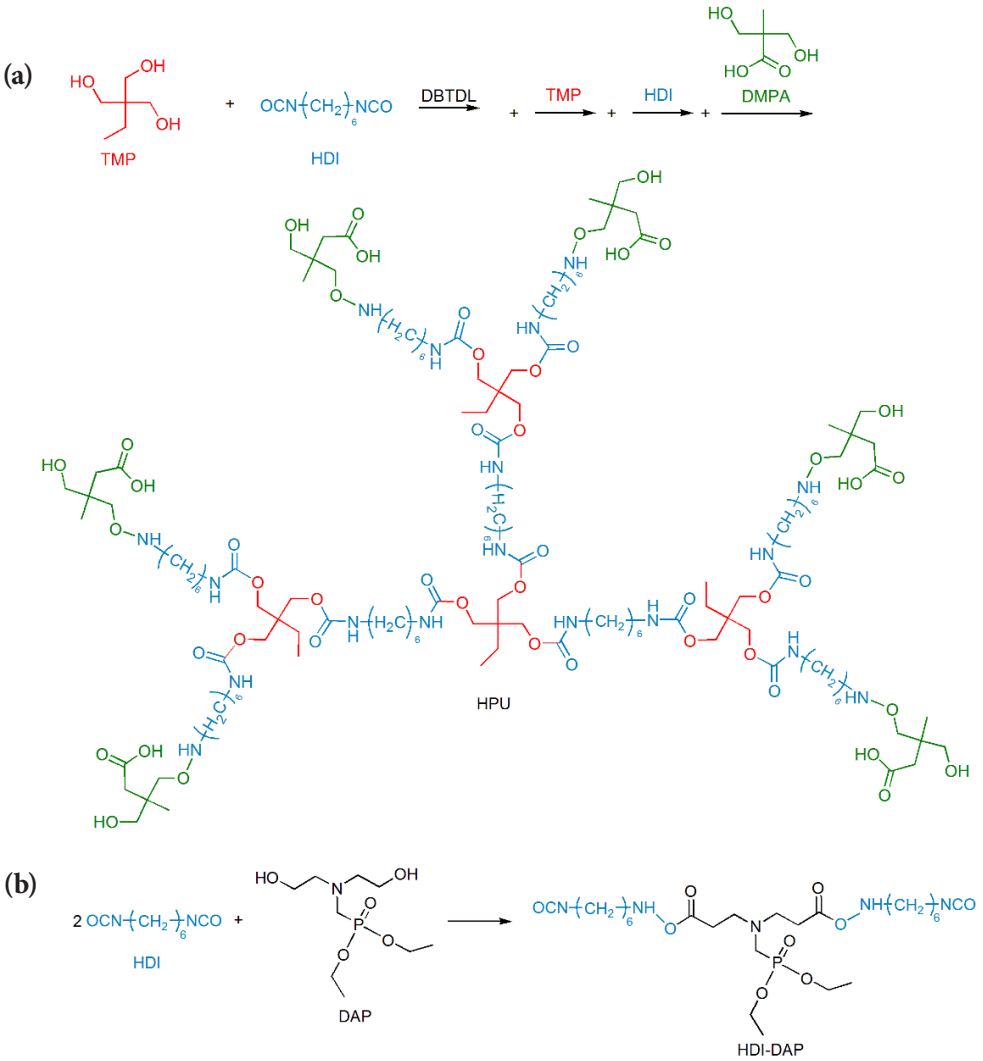

Scheme 1. (a) Synthesis of HPU; **(b)** Synthesis of HDI-DAP

Table I

Retanning process

Process	Chemicals	%	pH	Temp. (°C)	Time (min)
Weighing					
Bleaching	Water	200		35	15
	HCOOH	0.2			
Discharging the solution					
Neutralizing	Water	150		30	40
	HCOONa	1	4.0-4.5		
	$NaHCO_3$	0.4-0.5	5.0-5.5		60
Discharging the solution					
Retanning	Water	100		35	60
	PUH/PUH-DAPs	8			
Horse up					

Samples here are abbreviated as HPU-DAP-x, and the corresponding HDI-DAP weight concentrations in HDI and HDI-DAP of HPU-DAP-3, HPU-DAP-6, HPU-DAP-9, HPU-DAP-12 are 3%, 6%, 9% and 12%, respectively.

Retanning Technology

The wet blue is cattlehide tanned by Cr^{3+} of tanning agents, and was retanned according to the reported process (Table I).[8] In the process of retanning, HPU and HPU-DAPs were simultaneously applied to treat the wet blue with the same technology.

Measurements

Fourier Transform Infrared Spectroscopy (FTIR, Thermo Fisher Nicolet Is5, USA) was utilized to ascertain the functional groups present in DAP, HPU and HPU-DAP. The FTIR spectra were taken in the range of 400 cm^{-1}-4000 cm^{-1} with 32 scans, 2 cm^{-1} resolution, at room temperature. Molecular weights of HPU and HPU-DAPs were determined by gel permeation chromatography (GPC) using a Waters-Breeze GPC apparatus equipped with four TSK HXL series polystyrene divinylbenzene gel columns (300 9 7.8 mm, particle size about 5 - 6 mm) and a differential refractometer (DMF as eluent at a flow rate of 1.0 mL min^{-1}) at 35°C. Hydroxyl value was measured using the acetic anhydride/pyridine refluxing method.[15] Particle sizes were obtained by laser particle size analyser (Mastersizer 3000E). The shrinkage temperature of leather samples was acquired through a MSW-YD4 shrinkage meter (Yangguang Research Institute of Shanxi University of Science Technology, China) according to Chinese Industrial Standard (QB/T 2713-2005). A universal material testing machine ((Woodstock, model tensiTECH, USA) was used to measure the mechanical properties of leather samples. Each sample was cut as dumbbell shaped leather specimens of 50-mm length and 10-mm neck width and was measured five times to get the average values. Cone calorimetry experiments were conducted using an FTT Dual Cone Calorimeter (icone plus FTT0402) according to ISO 5660-1 standard. Each sample (10×10×0.2 cm^3) was placed in an aluminum foil pan and exposed horizontally to an external heat flux of 35 kW/m^2. Vertical burning test of samples (130 mm×13 mm) was conducted by FTT0082 instrument (Fire Testing Technology, UK) according to ASTM D3801. Scanning electron microscopy (SEM) images of leather after burning were obtained using scanning electron microscope (FEI, QUANTA250/QUANTA430, USA). Before the test, the wet blue was dried at room temperature.

Results and Discussion

Structure characterization

The FTIR spectra of DAP, HPU and HPU-DPA are presented in Figure 1. As for the spectra of HPU and HPU-DAP, the peak at 3324 cm^{-1} was assigned to the N-H stretching mode. The absorbance peaks around 2931 cm^{-1} were the characteristic stretching vibration peak of $-CH_3$ and $-CH_2-$. The stretching vibration peak at 1705cm^{-1} was related to C=O groups in the urethane bond. These are all the characteristic groups of polyurethane. In the spectrum of DAP, the peak at 1018 cm^{-1} and 540 cm^{-1} were assigned to P-O-C and P-C, respectively. The two peaks were also observed in the spectrum of HPU-DPA rather that of HPU, which confirmed the successful introduction of DPA into HPU.

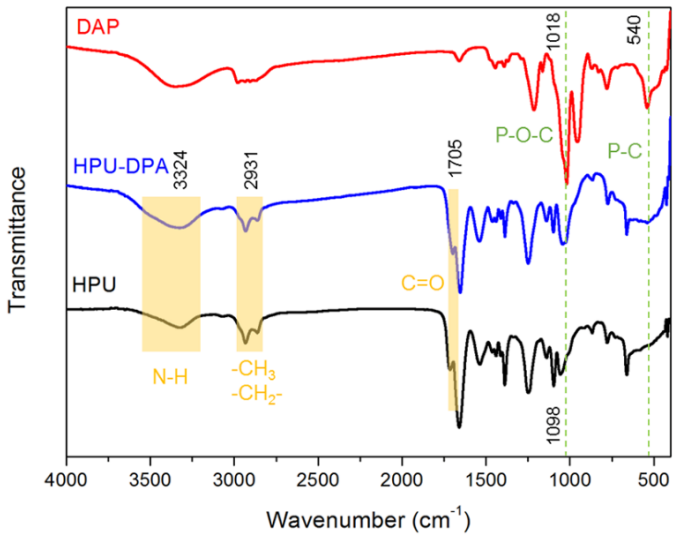

Figure 1. FTIR spectra of DAP, HPU-DPA and HPU.

The GPC data, hydroxyl value as well as particle size of HPU and HPU-DPAs were summarized in Table II. With the content of DAP increased, both the Mw and Mn of HPU-DAPs gradually increased. Because of the covalent conjugation of DAP into hyperbranched chains, the molecular weight inevitably grew larger. However, the polydispersity was not distinctly affected after the incorporation of DAP moieties. The hydroxyl value decreased when the molecular weights of the polyurethane increased. With the increase of molecular weights, the number of terminal hydroxyl groups increased concurrently. Besides, the increasing content of DPA, the particle size accordingly increased.

Application of FWPRA in retanning process

The Shrinkage temperature (T_s), average thickness and mechanical properties of leather before and after retanned by HPU were measured (Table III). T_s is an indicative parameter to evaluate the

Table II

GPC data, hydroxyl value as well as particle size of HPU and HPU-DPAs

Sample	M_w (g/ mol)	M_n (g/ mol)	M_w/ M_n	[OH]m (mg KOH g^{-1})	d (nm)
HPU	1793	2080	1.16	169.14	33
HPU-DPA-3	1860	2288	1.23	143.96	39
HPU-DPA-6	1932	2415	1.25	141.03	41
HPU-DPA-9	2003	2424	1.21	136.87	44
HPU-DPA-12	2096	2599	1.24	135.34	45

Table III

T_S, average thickness and mechanical properties of leather

Samples	T_S (°C)	Average thickness (mm)	Tensile strength (MPa)	Elongation at break (%)
Wet blue	94.3	0.714	14.79	38.912
Leather retanned by HPU	97.9	1.249	16.59	69.423
Leather retanned by HPU-DAP-3	98.2	1.253	16.68	64.236
Leather retanned by HPU-DAP-6	97.7	1.248	16.53	69.687
Leather retanned by HPU-DPA-9	98.1	1.252	16.62	66.549
Leather retanned by HPU-DAP-12	97.4	1.247	16.51	68.165

efficiency of tanning process.[8] The T_s of the wet blue was 94.3°C. After retanned by HPU, it increased to 97.7°C. On the one hand, numerous –COOH groups in HPU chains are able to form coordination bonds with Cr^{3+}. On the other hand, a great number of –OH groups in HPU can be hydrogen bonded with $–NH_2$ in collagen.[5] This ensures the stability of the interaction between retanning agents and collagen fibers. Compared with wet blue before retanning, the average thickness of leather after retanning increased by 0.535mm, showing the good filling performance of HPU. The tear strength of leather after HPU retanning was similar to that before retanning, but slightly increased. the final leather was endowed with better tensile strength after retanning. The elongation at break of leather before retanning was only 38.912%, but increased to 69.42% after retanning. Because the outstanding lubricating and filling of polyurethane between collagen fibers, the elongation of leather was significantly increased.

Flammability of retanned leather

Cone calorimeter test (CCT) can predict the combustion behavior of materials in an actual fire, and thus has been widely used in the study of flame retardant properties of materials.[16-18] Data obtained from CCT included heat release rate(HRR), total heat release(THR), smoke production rate(SPR) as well as total smoke releases(TSR). The results are plotted in Figure 2 and corresponding data are recorded in Table IV. PHRR is the peak of heat release rate. TPHRR is time to peak of heat release rate. PTSR is the perk of total smoke release. TTI is time to Ignition. With the increasing content of DAP content in retanning agent, PHRR, TPHRR, THR, SPR, PTSR and TTI decreased and the TPHRR was advanced. Both PHRR and THR were the foremost parameter to indicate the size and growth rate of the fire.[19] It is well known that most fire deaths result from oxygen deprivation, toxic gases, and smoke containing lots of heat.[20] Typically, smoke particles that are generated during combustion could influence the sight of survivors, reduce the visibility, and seriously affect the evacuation and rescue.[2] From Figure 2 (c), compared with HPU, the SPR of leather retanned by HPU-DAPs dramatically decreased. In Figure 2 (d), The TSR of all leather retanned by HPU-DAP was much lower than that of leather retanned by HPU and was positively correlated with the change of DAP content. The phosphorus compounds and some of their decomposition products are regarded to volatilize from the leather when heated. Reactive phosphorus species were released by the further decomposition of these phosphorus species and then interacted with the combustion intermediates in the gas phase as

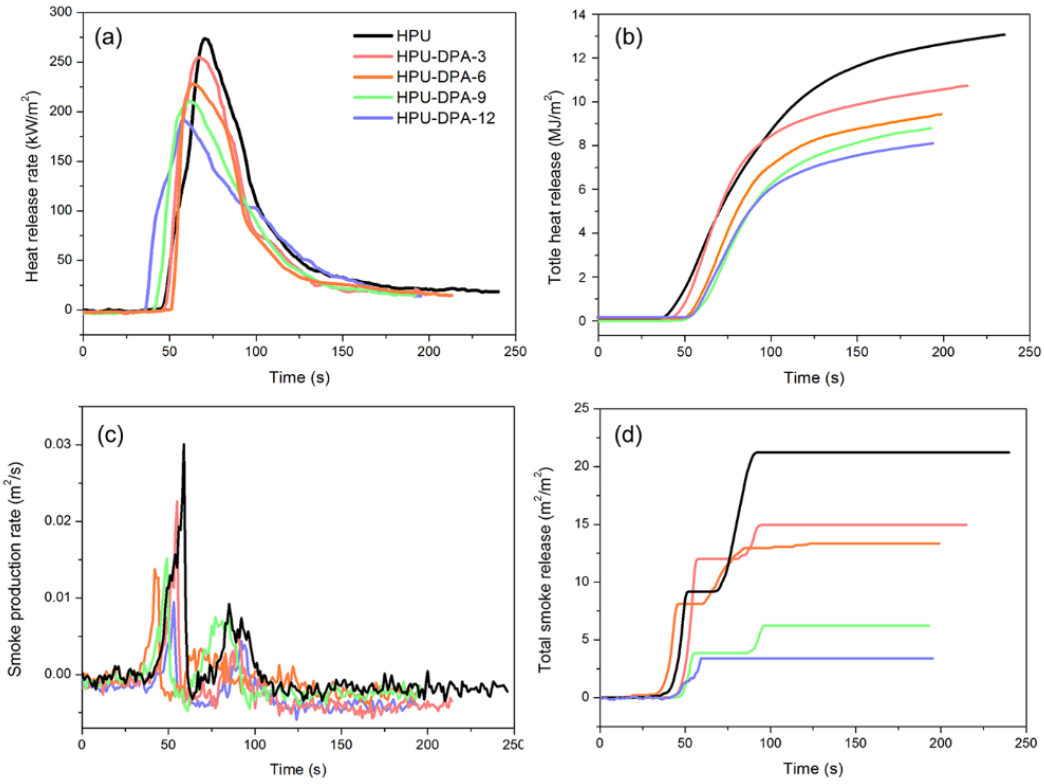

Figure 2. **(a)** Heat release rates of leather retanned by HPU and HPU-DPAs; **(b)** Total heat release of leather retanned by HPU and HPU-DPAs; **(c)** Smoke production rates of leather retanned by HPU and HPU-DPAs; **(d)** Total smoke releases of leather retanned by HPU and HPU-DAPs;

Table IV

Main parameters from cone calorimeter test and vertical burning test

Sample	PHRR (kW/m²)	TPHRR (s)	THR (MJ/m²)	SPR (m²/s)	PTSR ((m²)/m²)	TTI (s)	TFC (s)	TGC (s)	LC (cm)
HPU	276.04	70	13.06	0.0301	13.20	60	75	163	7.0
HPU-DPA-3	255.24	67	11.41	0.0227	12.08	56	64	64	2.6
HPU-DPA-6	228.45	64	9.37	0.0152	5.310	55	61	39	2.4
HPU-DPA-9	210.81	62	8.82	0.0138	3.190	51	60	29	2.2
HPU-DPA-12	194.26	58	8.16	0.0095	2.389	46	55	26	2.1

inhibitors. These interactions resulted in recombination of the H and OH radicals, consequently preventing their oxidation.[21] Vertical burning tests are also employed to evaluate the flammability of leather, and the corresponding results are presented in Table IV, including flaming combustion time (TFC), glowing combustion time (TGC) and length of carbonization (LC). Leather retanned by HPU was ignitable and burned out quickly according to the results of vertical burning tests. After retanning by HPU-DAP, the flame combustion time, flameless combustion time and length of carbonization were all decreased. All these results provided supporting evidence that retanning by HPU-DAP can increase flame retardancy of final leather.

Leather retanned by HPU -DAP-6 was selected as a representative sample to measure the morphology after burn. Figure 3 presents the SEM micrographs of wet blue after burn and leather retanned

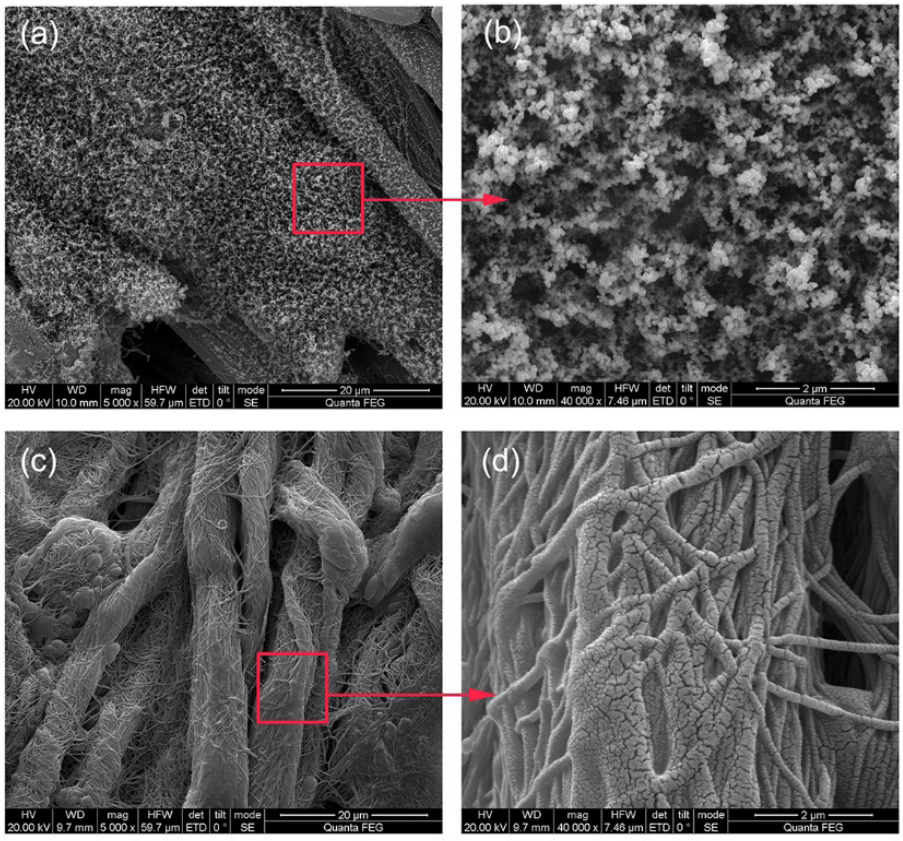

Figure 3. (a) and **(b)** SEM images of wet blue after burn; **(c)** and **(d)** SEM of leather retanned by HPU-DPA-6 after burn.

by HPU -DAP-6 after burn. For the wet blue, the fiber structures were heavily damaged, and the surface was covered by powder after combustion. On the contrary, although small cracks were found on the surface of the fiber, the fiber structure of leather retanned by HPU-DPA-6 was clearly retained.

Conclusion

In this study, hyperbranched polyurethane leather retanning agents with flammability were synthesized. A phosphorous compound was modified by hexamethylene diisocyanate, and then was used to partly replace the isocyanates to prepare hyperbranched polyurethanes. After retanning, the average thickness, tensile strength and elongation at break of leather were all improved. When the content of DAP increased, PHRR, TPHRR, THR, SPR, PTSR and TTI of leather retanned by HPU-DAPs decreased and the TPHRR was advanced. For the wet blue, the fiber structures were heavily damaged after combustion. On the contrary, the fiber structure of leather retanned by HPU-DPA was clearly retained. All these results suggested the potential application of HPU-DAPs as flame retarded retanning agents for leather manufacturing.

Acknowledgments

The authors acknowledge the support from Department of Education of Zhejiang Province (Y202043348). National College Students Innovation and Entrepreneurship Training Program (202110351008) and College Students Innovative Entrepreneurial Training of Wenzhou University (JWSC2020020).

Reference

1. Zhong, A. H.; Wang, J.; Ling, Y. L. Comparative Study of Moisture Permeability of Three Natural Leathers, *Journal of the Society of Leather Technologists and Chemists* **2020**, 104, 271-274.
2. Lu, S. L.; Feng, Y. C.; Zhang, P. K.; Hong, W.; Chen, Y.; Fan, H. J.; Yu, D. S.; Chen, X. D. Preparation of Flame-Retardant Polyurethane and Its Applications in the Leather Industry, *Polymers* **2021**, 13.
3. Jiang, Y. P.; Li, J. X.; Li, B.; Liu, H. Y.; Li, Z. J.; Li, L. X. Study on a novel multifunctional nanocomposite as flame retardant of leather, *Polymer Degradation and Stability* **2015**, 115, 110-116.
4. Lyu, B.; Luo, K.; Gao, D. G.; Wang, Y. F.; Ma, J. Z. Modified layered double hydroxide/zanthoxylum bungeanum seed oil composites to improve the flame retardant of leather, *Polymer Degradation and Stability* **2021**, 183.
5. Xu, W.; Chai, X. Y.; Zhao, G. H.; Li, J.; Wang, X. C. Preparation of reactive amphoteric polyurethane with multialdehyde groups and its use as a retanning agent for chrome-free tanned leather, *Journal of Applied Polymer Science* **2019**, 136.
6. Liu, X. H.; Yue, O.; Wang, X. C.; Hou, M. D.; Zheng, M. H.; Jiang, H. Preparation and application of a novel biomass-based amphoteric retanning agent with the function of reducing free formaldehyde in leather, *Journal of Cleaner Production* **2020**, 265.
7. Huang, W.; Song, Y.; Yu, Y.; Wang, Y.-n.; Shi, B. Interaction between retanning agents and wet white tanned by a novel bimetal complex tanning agent, *Journal of Leather Science and Engineering* **2020**, 2, 8.
8. Tian, S. Q.; Zhang, P. K.; Fan, H. J.; Chen, Y.; Yan, J.; Shi, B. A Polyurethane-Based Retannıng Agent wıth Fluorescent Effect, *JALCA* **2016**, 111, 148-154.
9. Wang, X. C.; Yan, Z.; Liu, X. H.; Qiang, T. T.; Chen, L.; Guo, P. Y.; Yue, O. An environmental polyurethane retanning agent with the function of reducing free formaldehyde in leather, *Journal of Cleaner Production* **2019**, 207, 679-688.
10. He, B. Z.; Zhang, J.; Wang, J.; Wu, Y. W.; Qin, A. J.; Tang, B. Z. Preparation of Multifunctional Hyperbranched Poly(beta-aminoacrylate)s by Spontaneous Amino-yne Click Polymerization, *Macromolecules* **2020**, 53, 5248-5254.
11. Ren, L. F.; Zhao, Y. X.; Zhang, H. Synthesis and Properties of Hydroxyl-terminated Hyperbranched Poly Isocyanurate-ester Retanning Agents, *JALCA* **2017**, 112, 240-249.
12. Zhang, J.; Ren, H. J.; Chen, P. P.; Zhang, Z.; Hu, C. P. Preparation and properties of waterborne polyurethane with star-shaped hyperbranched structure, *Polymer* **2019**, 180.
13. Salmeia, K. A.; Gaan, S.; Malucelli, G. Recent Advances for Flame Retardancy of Textiles Based on Phosphorus Chemistry, *Polymers* **2016**, 8.
14. Ji, W. J.; Song, W.; Zheng, Y. Y.; He, X. Z. Improvement of Method for Determination of Isocyanate Group Content in Polyurethane Prepolymer, *Applied Mechanics & Materials* **2013**, 303-306, 2533-2536.
15. Fritz, J. S.; Schenk, G. H. Acid-Catalyzed Acetylation of Organic Hydroxyl Groups, *Analytical Chemistry* **1959**, 31, 1808-1812.
16. Xu, Q.; Jin, C.; Jiang, Y. Compare the flammability of two extruded polystyrene foams with micro-scale combustion calorimeter and cone calorimeter tests, *Journal of Thermal Analysis and Calorimetry* **2017**, 127, 2359-2366.
17. Mastori, H.; Sonnier, R.; Ferry, L.; Coutin, M. Fire behavior of lead-containing PMMA based Kyowaglas, *Polymer Degradation and Stability* **2021**, 190.
18. Xu, Q.; Jin, C.; Majlingova, A.; Zachar, M.; Restas, A. Evaluate the flammability of a PU foam with double-scale analysis, *Journal of Thermal Analysis and Calorimetry* **2019**, 135, 3329-3337.
19. Duan, B. R.; Wang, Q. J.; Wang, X.; Li, Y.; Zhang, M. M.; Diao, S. Flame retardance of leather with flame retardant added in retanning process, *Results in Physics* **2019**, 15.
20. Chen, X. L.; Zhuo, J. L.; Jiao, C. M. Thermal degradation characteristics of flame retardant polylactide using TG-IR, *Polymer Degradation and Stability* **2012**, 97, 2143-2147.
21. Schartel, B. Phosphorus-based Flame Retardancy Mechanisms—Old Hat or a Starting Point for Future Development?, *Materials* **2010**, 3, 4710-4745.

UNITED STATES POSTAL SERVICE®

Statement of Ownership, Management, and Circulation (All Periodicals Publications Except Requester Publications)

1. Publication Title	2. Publication Number	3. Filing Date
The Journal of The American Leather Chemists Association	019334	09/15/2022
4. Issue Frequency	**5. Number of Issues Published Annually**	**6. Annual Subscription Price**
monthly	12	$185

7. Complete Mailing Address of Known Office of Publication *(Not printer) (Street, city, county, state, and ZIP+4®)*
1314 50th Street, Suite 103
Lubbock, Lubbock County, Texas 79412-2940

Contact Person: Carol Adcock
Telephone *(Include area code)*: (806) 744-1798

8. Complete Mailing Address of Headquarters or General Business Office of Publisher *(Not printer)*
same as Item 7

9. Full Names and Complete Mailing Addresses of Publisher, Editor, and Managing Editor *(Do not leave blank)*

Publisher *(Name and complete mailing address)*
Carol Adcock, ALCA Executive Secretary
1314 50th Street, Suite 103
Lubbock, TX 79412-2940

Editor *(Name and complete mailing address)*
Steven D. Lange, ALCA Editor
1314 50th Street, Suite 103
Lubbock, TX 79412-2940

Managing Editor *(Name and complete mailing address)*
None

10. Owner *(Do not leave blank. If the publication is owned by a corporation, give the name and address of the corporation immediately followed by the names and addresses of all stockholders owning or holding 1 percent or more of the total amount of stock. If not owned by a corporation, give the names and addresses of the individual owners. If owned by a partnership or other unincorporated firm, give its name and address as well as those of each individual owner. If the publication is published by a nonprofit organization, give its name and address.)*

Full Name	Complete Mailing Address
The American Leather Chemists Association	1314 50th Street, Suite 103, Lubbock, TX 79412-2940

11. Known Bondholders, Mortgagees, and Other Security Holders Owning or Holding 1 Percent or More of Total Amount of Bonds, Mortgages, or Other Securities. If none, check box → ☑ None

Full Name	Complete Mailing Address

12. Tax Status *(For completion by nonprofit organizations authorized to mail at nonprofit rates) (Check one)*
The purpose, function, and nonprofit status of this organization and the exempt status for federal income tax purposes:
☑ Has Not Changed During Preceding 12 Months
☐ Has Changed During Preceding 12 Months *(Publisher must submit explanation of change with this statement)*

PS Form **3526,** July 2014 *[Page 1 of 4 (see instructions page 4)]* PSN: 7530-01-000-9931 **PRIVACY NOTICE:** See our privacy policy on *www.usps.com.*

13. Publication Title The Journal of The American Leather Chemists Association			14. Issue Date for Circulation Data Below 09/01/2022	
15. Extent and Nature of Circulation			**Average No. Copies Each Issue During Preceding 12 Months**	**No. Copies of Single Issue Published Nearest to Filing Date**
a. Total Number of Copies *(Net press run)*				
b. Paid Circulation *(By Mail and Outside the Mail)*	(1)	Mailed Outside-County Paid Subscriptions Stated on PS Form 3541 (Include paid distribution above nominal rate, advertiser's proof copies, and exchange copies)	46	46
	(2)	Mailed In-County Paid Subscriptions Stated on PS Form 3541 *(Include paid distribution above nominal rate, advertiser's proof copies, and exchange copies)*	0	0
	(3)	Paid Distribution Outside the Mails Including Sales Through Dealers and Carriers, Street Vendors, Counter Sales, and Other Paid Distribution Outside USPS®	0	0
	(4)	Paid Distribution by Other Classes of Mail Through the USPS (e.g., First-Class Mail®)	51	48
c. Total Paid Distribution *[Sum of 15b (1), (2), (3), and (4)]* ▶			97	94
d. Free or Nominal Rate Distribution *(By Mail and Outside the Mail)*	(1)	Free or Nominal Rate Outside-County Copies included on PS Form 3541	0	0
	(2)	Free or Nominal Rate In-County Copies Included on PS Form 3541	0	0
	(3)	Free or Nominal Rate Copies Mailed at Other Classes Through the USPS (e.g., First-Class Mail)	0	0
	(4)	Free or Nominal Rate Distribution Outside the Mail *(Carriers or other means)*	0	0
e. Total Free or Nominal Rate Distribution *(Sum of 15d (1), (2), (3) and (4))*			0	0
f. Total Distribution *(Sum of 15c and 15e)* ▶			97	94
g. Copies not Distributed *(See Instructions to Publishers #4 (page #3))* ▶			37	37
h. Total *(Sum of 15f and g)*			134	131
i. Percent Paid *(15c divided by 15f times 100)* ▶			100	100

* If you are claiming electronic copies, go to line 16 on page 3. If you are not claiming electronic copies, skip to line 17 on page 3.

16. Electronic Copy Circulation	**Average No. Copies Each Issue During Preceding 12 Months**	**No. Copies of Single Issue Published Nearest to Filing Date**
a. Paid Electronic Copies ▶		
b. Total Paid Print Copies (Line 15c) + Paid Electronic Copies (Line 16a) ▶	0	0
c. Total Print Distribution (Line 15f) + Paid Electronic Copies (Line 16a) ▶	0	0
d. Percent Paid (Both Print & Electronic Copies) (16b divided by 16c × 100) ▶		

☐ **I certify that 50% of all my distributed copies (electronic and print) are paid above a nominal price.**

17. Publication of Statement of Ownership

☑ If the publication is a general publication, publication of this statement is required. Will be printed in the 10/1/22 issue of this publication. ☐ Publication not required.

18. Signature and Title of Editor, Publisher, Business Manager, or Owner	Date
Carol Adcock, Executive Secretary	09/15/2022

I certify that all information furnished on this form is true and complete. I understand that anyone who furnishes false or misleading information on this form or who omits material or information requested on the form may be subject to criminal sanctions (including fines and imprisonment) and/or civil sanctions (including civil penalties).

LEATHER

AVELLISYNCO

Selected Dyestuffs

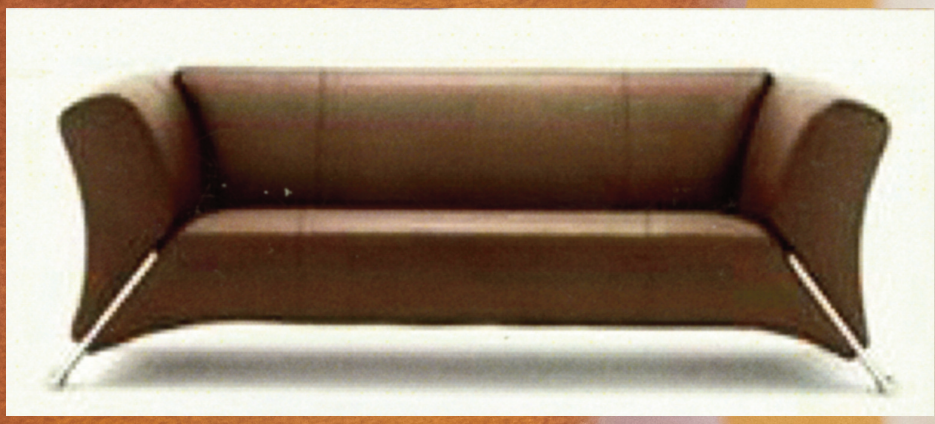

CHEMTAN

17 Noble Farm Drive • Lee, NH 03861 (Office)
57 Hampton Road • Exeter, NH 03833 (Manufacturing)
Tel: (603) 772-3741 • Fax: (603) 772-0796
www.CHEMTAN.com

Lifelines

GC Jayakumar is currently working as a scientist at Centre for Academic and Research Excellence, CSIR-Central Leather Research Institute, Chennai, India. His research interests include cleaner leather processing technologies and utilization of tannery wastes for developing products.

C Niklesh is currently a Post Graduate Student of Footwear Engineering and Management at the Department of Leather Technology, A. C. Tech of Anna University housed at CSIR-Central Leather Research Institute, Chennai, India. His research interests include Computer Numeric Control (CNC) and 3D printing.

S Jeyas Kandhan is currently a Post Graduate Student of Leather Technology at the Department of Leather Technology, A. C. Tech of Anna University housed at CSIR-Central Leather Research Institute, Chennai, India. His research interests include biotechnological aspects of leather processing and waste management system in the leather industry.

K Phebe Aaron is presently the Senior Principal Scientist working in the area of Leather Apparel & Products. She has involved in benchmarking of functional properties of leathers for apparel manufacturing and has made significant contributions in exploring replenishable natural plant based fabrics for combination products with leather

K Krishnaraj is currently working as Chief scientist. His research interest include comfort studies on leather apparel, drape studies on garment leathers including FEM, Computer Aided Design for Leather Products, New materials development and evaluation etc. He is author of more than twenty publications in peer reviewed international journals and holds three copyrights to his credit.

Shuangfeng Xu received her master's degree in School of Chemical Engineering at Sichuan University in 2019. Now she is studying for her doctorate in Biomass Chemistry and Engineering at Sichuan University. Her research focuses on clean technology of leather manufacture.

Ya-nan Wang, see *JALCA* **116**, 299, 2021.

Bi Shi, see *JALCA* **99**, 220, 2004.

Lili Yan is a postgraduate student at Sichuan University, China. Her research work focuses on resource utilization of animal skins/hides solid waste. She is under the guidance of Pro. Biyu Peng.

Sadaqat Ali Chattha is a Ph. D. student at Sichuan University, China. He is working at clean technology of leather-making and resource utilization of chrome-containing leather solid waste. He is under the guidance of Prof. Biyu Peng.

Xu Zhang obtained a Ph. D. in fermentation engineering from Sichuan University, China, in 2022. He is working at clean technology of leather-making, mainly the performance, mechanism and application of enzymes for leather manufacture. He is under the guidance of Prof. Biyu Peng.

Mengchu Gao is a Ph. D. student at Sichuan University, China. She is working at separation science and the application of enzyme in the leather manufacture. She is under the guidance of Prof. Biyu Peng.

Chunxiao Zhang obtained a Ph. D. in leather science and engineering from Sichuan University, China, in 2016. He is working in the Department of Biomass and Leather Engineering, Sichuan University from July 2016 up to now. After an additional associate Prof. position, he is working primarily with cleaner production technology of leather manufacture, biotechnology of leather making, tanning chemistry and greener leather chemicals.

Biyu Peng see *JALCA* **109**, 207, 2014

Ting Wu studied Light Industry Technology and Engineering at the College of Biomass Science and Engineering, Sichuan University. Her main interests are biomaterial application.

Min He studied Light Chemical Engineering at the College of Biomass Science and Engineering, Sichuan University. Her main research interests are gelatin and starch.

Wenhua Yang studied Leather Chemistry and Engineering at the College of Biomass Science and Engineering, Sichuan University, where he earned his PhD. His research thesis was on the high-value conversion and utilization of leather waste.

Industry News

IULTCS Asks EU Legislators to Reconsider Proposed Restrictions

Members of IULTCS have collaborated with industry scientists from FILK, Stahl and TFL to prepare a document that was submitted to DG Grow (the European Commission Directorate-General department responsible for EU policy on the single market, industry, entrepreneurship and small businesses) and DG ENV (The Directorate-General for Environment department responsible for EU policy on the environment).

The purpose of preparing the document was to address proposed EU restrictions on the presence of Chrome VI and Bisphenols in leather. It is considered that the new proposed REACH restrictions could seriously impact the leather industry, particularly in the European Union.

The IULTCS document asks the EU for a proper assessment of the impact of these measures on the environment, people and leather manufacture. IULTCS President Jean-Pierre Gualino and Executive Secretary Dr Luis Zugno stated "Our call is for a more detailed study of data and testing methodology relating to Chrome VI and more time to implement the proposed Bisphenol restrictions".

WARDROBE MALFUNCTION

LEATHER. IF WE DON'T USE IT, WE DO MORE THAN JUST LOSE IT.

From food to fashion, a burger and shake is just the start of the story of waste and recklessness. We live in a world where the cheap and easy option is to throw away the byproducts of our society. Instead we crop new land, drill or frack for short lived replacements. Isn't it time to shake things up, to think slow instead of fast. To think of our future and that of the planet?

300M HIDES COME FROM THE MEAT & DAIRY INDUSTRIES EVERY YEAR

60% IS USED FOR LEATHER. THE REST IS JUST TROWN AWAY

THAT IS **120M** 3M TONNES OF LANDFILL & 2.7M TONNES OF GREENHOUSE GASES. EVERY YEAR.

THE FASHION INDUSTRY PRODUCES

144 BILLION ITEMS OF CLOTHING EVERY YEAR

WE NEED 3.5M ACRES OF FOREST, JUST TO RE-CAPTURE THE CARBON CREATED BY THIS WASTE.

65% OF ALL OUR CLOTHES ARE PLASTIC, SOURCED THROUGH DRILLING & FRACKING

EACH HIDE COVERS **4 SQM**

WE WASTE NEARLY **480 MILLION SQM**

OF MATERIAL EACH YEAR, ENOUGH TO COVER

78,000 FOOTBALL PITCHES

OR TO PUT SHOES ON THE FEET OF

EVERY MAN, WOMAN & CHILD IN AFRICA

AND ONE LEATHER ITEM CAN LAST A LIFETIME

TO JOIN THE DISCUSSION FIND US AT: CHOOSEREALLEATHER.COM

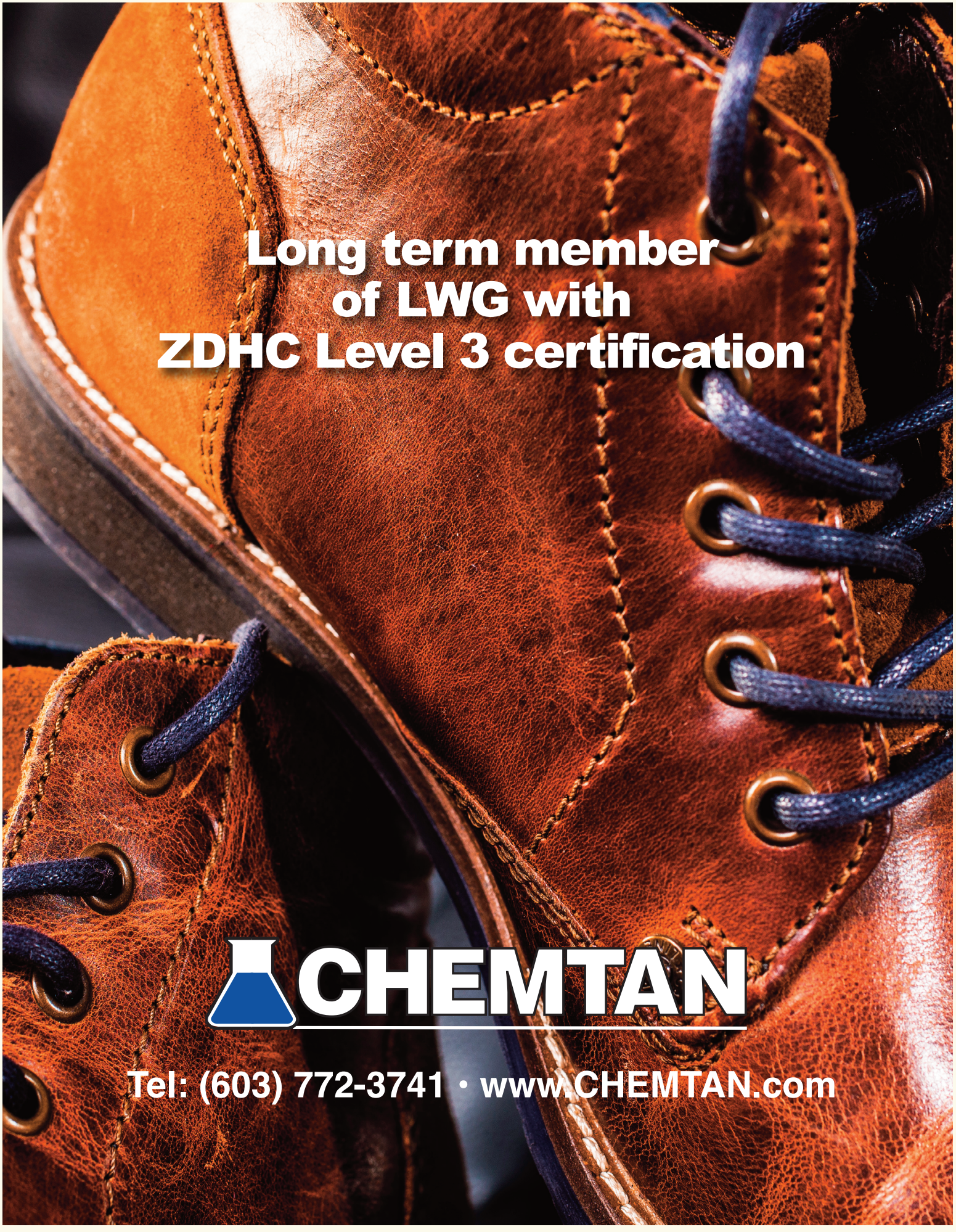
Long term member
of LWG with
ZDHC Level 3 certification
CHEMTAN
Tel: (603) 772-3741 • www.CHEMTAN.com